

Physicochemical Studies of the Membrane Disrupting Action of Antimicrobial Peptides

Submitted by

Sara Pandidan

Bachelor of Science (Chemistry), 2010 Alzahra University
Master of Analytical Chemistry, 2013 Shahid Beheshti University

This thesis is submitted in total fulfilment of the
requirements for the degree

Doctor of Philosophy

Department of Chemistry and Physics
School of Molecular Sciences
College of Science, Health and Engineering

La Trobe University
Victoria, Australia
April 2020

Statement of Authorship

Except where reference is made in the text of the thesis, this thesis contains no material published elsewhere or extracted in whole or in part from a thesis accepted for the award of any other degree or diploma. No other person's work has been used without due acknowledgement in the main text of the thesis. This thesis has not been submitted for the award of any degree or diploma in any other tertiary institution.

This thesis contains two journal articles as detailed below, as well as three co-authored manuscripts. In each of these works, I have performed all experiments (with the exception of the AFM images included in Chapter four), analysed the data and prepared the manuscripts following advice from my supervisor and, in case of neutron reflectometry data, from Dr Stephen Holt, the beamline scientist at the ANSTO neutron source.

Sara Pandidan

29, April 2020

Peer reviewed publications

1. Pandidan S, Mechler A. *Nano-viscosimetry analysis of the membrane disrupting action of the bee venom peptide melittin*. Scientific Reports 2019;**9**:10841.

DOI : 10.1038/s41598-019-47325-y

2. Pandidan S, Mechler A. *Membrane morphology effects in quartz crystal microbalance characterization of antimicrobial peptide*. Biophysical Chemistry: in press.

Acknowledgement

First and foremost, I would like to express my sincere gratitude to my supervisor, associate professor Adam Mechler for his guidance, patience, constant support and for generously sharing his knowledge during my study. Thanks for giving me this opportunity and always encouraging me with your heart-warming comments.

I also would like to thank all my colleagues and friends in Dr Mechler's group especially PhD candidate Zelun Zhi for his help and companionship, thanks for being such a good coffee mate.

I wish to acknowledge La Trobe University for providing La Trobe University Postgraduate Research Scholarship and La Trobe University Full Fee Research Scholarship that gave me this exceptional opportunity.

I want to acknowledge the support of the Australian Nuclear Science and Technology Organisation (ANSTO) in providing the facility used in this work.

Most importantly, I would like to acknowledge my wonderful family especially my brother, Ali for always being there for me and guiding me through my life.

And my deepest appreciation to my incredible parents for their boundless love and support and always believing in me.

Last but not least I would like to thank my beloved husband, Hossein, for his support and patience during these years, who always stood by me, in my happiness and sadness.

Dedication

I would like to dedicate this dissertation to my wonderful family whom are my endless source of energy and especially my beloved parents who had unwavering faith in me.

Your unconditional love and support and constant encouragement are the reasons for who I am today.

I could never ask for a better family.

این بحر وجود آمده بیرون ز نهفت

کس ندانست که این گوهر تحقیق بفت

هر کس سخنی از سر سودا گفتند

ز آن روی که هست کس نمی داند گفت

عمر خیام

The sea of life from secret well has sprung,

This pearl of inquiry no one has strung;

And fancies are the thoughts learned men expound

Unheard is yet the truth from any tongue.

Omar Khayyam (1048-1131)

Abstract

The infections caused by antibiotic resistant bacteria are harder and, in many cases, impossible to treat. This raises the spectre that common infections and minor injuries may start killing people, like they did just a century ago. Antibiotic resistant strains of bacteria are spreading at dangerously high pace, turning to a global health threat that requires urgent global action. Other than the trivial response of strict restriction of the application of antibiotic medicine to only the critical cases would be to develop new antibiotic agents that bacteria could not develop resistance toward, if new drug targets were identified. However, the development of new antibiotic drugs following traditional drug development principles has stalled. Antimicrobial peptides (AMPs) may offer a feasible answer to this demand. AMPs offer the first line of innate immune defence in all complex organisms.

AMPs are specific and selective to bacterial targets in their host. However, most small AMPs that are feasible to develop into drugs originate from insects or amphibians, and thus the specificity and selectivity is lost in humans. In order to serve as an alternative to antibiotics human cytotoxicity has to be addressed. For this the mechanism of action of AMPs should be clearly understood, preferable at the residue level, to allow for the design of artificial AMPs adopt to human therapeutics. The most interesting class of AMPs for pharmaceutical purpose are membrane disrupting AMPs. This category follows two main pathways of mechanism of action, both resulting in cell lysis: transmembrane and surface action. In this thesis the focus will be on mechanism and distinct molecular stages of interaction of transmembrane acting AMPs with model membranes. Chapter one introduces general properties and proposed mechanisms of AMPs, as well as the membranes that the peptides target. Chapter two outlines the methodology and techniques used to achieve the goal of my work.

The focus of Chapter three is the mechanism of action of one of the best-known membrane disruptor AMPs, melittin, the main component of honeybee (*Apis mellifera*) venom. In this chapter by using quartz crystal microbalance “with dissipation monitoring” (QCM) nano viscosimetry measurements were performed, supported by dye leakage experiments. I outline the membrane-specific action of melittin and propose two distinct new pathways for melittin-membrane interaction based on the model membrane used. The fissure pathway is described for saturated zwitterionic lipid membrane and the asymmetric tension pathway for phosphatidylglycerol lipids. In the second part of

Chapter three I investigated the effect of membrane morphology on the observable QCM fingerprints. In this section I also found that melittin shows higher binding and disrupting tendency to curved membrane.

In Chapter four I describe my studies of the action mechanism of magainin 2, a pore former AMP of 23 amino acids secreted by African clawed frog (*Xenopus laevis*). In this chapter I could also identify different stages in magainin 2-membrane interaction and confirm the well-accepted model for the mechanism of action.

In chapter five focus is on finding novel, independent ways of confirming the mechanisms proposed in the previous two chapters. In the first part I introduce a method to identify membrane bound states of the peptides from phase transition temperature changes, measured via viscosity changes as the function of temperature changes. This method reveals the presence of distinct thermodynamic states in the mechanistic pathway of the action of melittin and magainin 2. The presence of four and three distinct domains, respectively, correlated well to hypothetical model mechanism described in the previous chapters for melittin and magainin 2.

In the second part of chapter five I report on the use of neutron reflectometry to find and compare the orientation of AMPs in model membranes. For this purpose, melittin and, as a reference surface acting peptide, aurein 1.2 (from Australian tree frog *Litoria aurea*) were selected, with DMPC membrane. NR analysis shows that in lower concentration, peptides are mainly on the top leaflet bound to the head group region. However, by increasing concentration specific processes commence: in the case on aurein 1.2 results show the disruption of outer leaflet consisting with carpet mechanism. On the other hand, for melittin it was shown that at higher concentration, peptide can insert first into the top leaflet and then the bottom leaflet. This neutron reflectometry model fitting confirms the previous proposed models for both peptides.

Thus, in this thesis work I succeeded in obtaining data on the stages and thermodynamic states of the membrane disrupting actions of melittin and magainin 2, while I have also developed a new method suitable for the characterization of AMP-membrane interactions.

Abbreviations

Name	Abbreviation	
Alanine	Ala	A
Arginine	Arg	R
Asparagine	Asn	N
Aspartate	Asp	D
Cysteine	Cys	C
Glutamine	Gln	Q
Glycine	Gly	G
Glutamate	Glu	E
Histidine	His	H
Isoleucine	Ile	I
Leucine	Leu	L
Lysine	Lys	K
Methionine	Met	M
Phenylalanine	Phe	F
Proline	Pro	P
Serine	Ser	S
Threonine	Thr	T
Tryptophan	Trp	W
Tyrosine	Tyr	Y
Valine	Val	V
Antimicrobial peptide	AMP	
Intensive care unit	ICU	
1,2-dimyristoyl-sn-glycero-3-phosphocholine	DMPC	
1,2-dipalmitoyl-sn-glycero-3-phosphocholine	DPPC	
1,2-dioleoyl-sn-glycero-3-phosphocholine	DOPC	
1,2-Dimyristoyl-sn-glycero-3-phosphorylglycerol (sodium salt)	DMPG	
1,2-dioleoyl-sn-glycero-3-phospho-(1'-rac-glycerol) (sodium salt)	DOPG	
1-palmitoyl-2-oleoyl-sn-glycero-3-phosphocholine	POPC	
1-palmitoyl-2-oleoyl-sn-glycero-3-phosphocholine	POPG	
Superlattice model	SM	
Condensed complex model	CCM	
Carboxylfluorescein	CF	
Differential scanning calorimetry	DSC	
Isothermal titration calorimetry	ITC	
Crystalline dehydrated phase	L_c	
Disordered gel phase	L_β	
Ripple phase	P_β	

Main transition	T_m
Liquid phase	L_α
Nuclear magnetic resonance	NMR
Circular dichroism	CD
Atomic force microscopy	AFM
Infrared	IR
Transmission electron microscopy	TEM
Quartz crystal microbalance	QCM
Frequency	f
Energy dissipation	D
Frequency change	Δf
Dissipation energy change	ΔD
Self-assembled monolayer	SAM
Mercaptopropionic acid	MPA
Dynamic light scattering	DLS
Supported lipid bilayers	SLB
Phosphate buffered saline	PBS
Sum frequency generation	SFG
Solid-state nuclear magnetic resonance	ss-NMR
Ditetradecyl glycerol phosphocholine	DPTC
Neutron reflectometry	NR
Scattering length density	SLD
Resonance energy transfer	RET
Giant unilamellar vesicle	GUV
Analog digital converter	ADC

List of figures

Chapter 1/ Figure 1/ Schematic presentation of cell membrane	5
Chapter 1/ Figure 2/ The basic structure of bacterial peptidoglycan and the cell wall structures of Gram-positive and Gram-negative bacteria	6
Chapter 1/ Figure 3/ Schematic representation of bilayer formation	7
Chapter 1/ Figure 4/ Phosphoacylglycerol structure	7
Chapter 1/ Figure 5/ Cholesterol chemical structure	9
Chapter 1/ Figure 6/ Representation of the different phases one in a lipid membrane: crystal phase (L_c), gel phase (L_β), and liquid phase (L_α). Certain types of lipid can be found in the ripple phase (P_β), which is a transitional phase between the gel and liquid phase	12
Chapter 1/ Figure 7/ AMPs structure: a) α -helical b) β -sheet c) Extended	14
Chapter 1/ Figure 8/ β -sheets peptides: a) anti-parallel hydrogen bonding b) parallel hydrogen bonding	15
Chapter 1/ Figure 9/ Barrel-stave pore formation model	19
Chapter 1/ Figure 10/ Toroidal pore formation model	20
Chapter 1/ Figure 11/ Carpet model	21
Chapter 2/ Figure 1/ QCM-D principles. (a) Schematic representation of the QCM-D principle. The spheres resemble unruptured vesicles and blue balls resemble attached solvent. (b) A monolayer of unruptured vesicles formed on substrates e.g., gold and titanium oxide. (c) A supported lipid bilayer	41
Chapter 2/ Figure 2/ The simple schematic representation of dialysis process	43
Chapter 2/ Figure 3/ Schematic figure of dye leakage process	44
Chapter 2/ Figure 4/ Block diagram of DLS	45
Chapter 2/ Figure 5/ The schematic figure of AFM	46
Chapter 2/ Figure 6/ Schematic figure of different modes of AFM	47
Chapter 2/ Figure 7/ Reflection on an infinite planar surface	48
Chapter 3/ Part 1/ Figure 1/ Results of dye leakage experiments. Normalized intensity of dye release shown as a function of time for a range of membrane mixtures and peptide concentrations as indicated. (a) DMPC; (b) DMPC:cholesterol (9:1); (c) DMPC:Cholesterol (8:2); (d) DOPC; (e) DMPC:DMPG (3:2); (f) DMPC:DMPG (4:1). The fluorescence intensity of dye loaded liposomes before the addition of the peptide was set as unity	61
Chapter 3/ Part 1/ Figure 2/ Viscoelastic fingerprints of interactions of melittin at varied concentrations with neutral membranes as follows. (a–d) 1 μ M melittin, (a) DMPC, (b) DMPC:cholesterol (9:1), (c) DMPC:cholesterol (8:2), (d) DOPC (e–h) 3 μ M melittin, (e) DMPC, (f) DMPC:cholesterol (9:1), (g) DMPC:cholesterol (8:2), (h) DOPC. (i–l) 5 μ M melittin, (i) DMPC, (j) DMPC:cholesterol (9:1), (k) DMPC:cholesterol (8:2), (l) DOPC. (m–p) 7 μ M melittin, (m) DMPC, (n) DMPC:cholesterol (9:1), (o) DMPC:cholesterol (8:2), (p) DOPC. (q–t) 10 μ M melittin, (q) DMPC, (r) DMPC:cholesterol (9:1), (s)	62

DMPC:cholesterol (8:2), (t) DOPC

Chapter 3/ Part 1/ Figure 3/ Viscoelastic fingerprints of melittin interactions with anionic membranes at different concentrations as follows. 3 μ M melittin: (a) DMPC/DMPG (4:1), (b) DMPC/DMPG (3:2). 5 μ M melittin: (c) DMPC/DMPG (4:1), (d) DMPC/DMPG (3:2). 7 μ M melittin: (e) DMPC/DMPG (4:1), (f) DMPC/DMPG (3:2). 10 μ M melittin: (g) DMPC/DMPG (4:1), (h) DMPC/DMPG (3:2). The arrows in panel (b) indicate stages of the interaction with Roman numerals

Chapter 3/ Part 1/ Figure 4/ Hypothetic pathways of melittin pore forming mechanism. In the schematic representation of the lipid headgroups, red are ester, orange are phosphate and blue are choline moieties. The peptides are shown fully helical according to melittin crystal structure; it is likely that under physiological conditions the C-terminal segment is unstructured and in that form, it directly associates to the lipid headgroups

Chapter 3/ Part 2/ Figure 1/ Comparison of viscoelastic fingerprints of the interaction of melittin with different DMPC membrane morphologies. (a-d) multiple bilayer stacks, (e-h) single bilayer membrane. (i-l) liposome containing deposit with 3 μ M, 5 μ M, 7 μ M, and 10 μ M melittin as indicated. Temperature 19°C, pH 7.2

Chapter 3/ Part 2/ Figure 2/ Comparison of viscoelastic fingerprints of interaction of melittin with different DMPC:DMPG (4:1) membrane morphologies as follows. (a-d) multiple bilayer stacks, (e-h) single bilayer, (i-l) liposome containing deposit with 3 μ M, 5 μ M, 7 μ M, and 10 μ M melittin as indicated. Temperature 19°C, pH 7.2

Chapter 3/ Part 2/ Figure 3/ Viscoelastic fingerprints of the interaction of 10 μ M melittin with DMPC membrane as a) liposome-containing deposit, b) multiple bilayer stacks. Temperature 19°C, pH 7.2

Chapter 3/ Part 2/ Figure 4/ Schematic representation of the stages appearing in viscoelastic fingerprints of liposome containing and multilayer DMPC deposits. The schematics are not intended to represent a particular thermodynamic membrane state

Chapter 4/ Figure 1/ Fluorescence intensity after adding after adding different concentration of magainin2 on a) DMPC, b) DMPC:chol (9:1), c) DMPC:chol (8:2), d) DOPC, e) DOPC:DOPG (4:1), f) DMPC:DMPG (4:1), g) DMPC:DMPG (3:2)

Chapter 4/ Figure 2/ From top to bottom 3, 5, 7, 10 μ M magainin2 added on a) DMPC b) DMPC:chol (9:1) c) DMPC:chol (8:2) d) DOPC

Chapter 4/ Figure 3/ Viscoelastic fingerprint of 3, 5, 7, 10 μ M magainin 2 on; DMP:DMPG (4:1), DMPC:DMPG (3:2), DOPC:DOPG (4:1)

Chapter 4/ Figure 4/ AFM images of DMPC:DMPG (4:1) membrane: (A), before the addition of magainin 2; (B), after the addition of magainin 2; C) a high resolution zoom at the collapsed membrane area. Images are 3D rendered. Image sizes: 1.14 μ m (A, B) and 400 nm (C). The colour bar for the height scale (total height: 4.3 nm for all frames) is provided in (D)

Chapter 5/ Part 1/ Figure 1/ Heating and cooling versus temperature for third loop of temperature ramping after adding 15 μ M a) melittin b) magainin 2

Chapter 5/ Part 1/ Figure 2/ Gaussian fitting of dD/dT vs temperature for the heating cycle in the third loop of temperature sweeping after adding a) 15 μ M melittin b) 15 μ M magainin 2 respectively

Chapter 5/ Part 1/ Figure 3/ Average temperature achieved for each domain on different concentration of a) melittin and, b) magainin 2	117
Chapter 5/ Part 2/ Figure 1/ SLD graph and reflectivity graph for the fitted lipid on three contrasts as D ₂ O amber, CMSI blue and H ₂ O green	132
Chapter 5/ Part 2/ Figure 2/ SLD graph of fitted 10 μ M melittin on fitted lipid data for the same position	133
Chapter 5/ Part 2/ Figure 3/ Membrane thickness changes in each layer by adding different concentrations of melittin	134
Chapter 5/ Part 2/ Figure 4/ Membrane thickness changes in each layer by adding different concentrations of aurein 1.2	134

Table of contents

Chapter One: Introduction	1-38
1. 1. Antimicrobial peptides	2
1. 2. Chemical structure of AMPs	4
1. 3. The target of AMPs: the biological membrane	5
1. 4. The main structural elements of biological membranes: phospholipids	7
1. 5. Cholesterol	9
1. 6. Biomimetic membrane	10
1. 7. Thermodynamic phase behavior of phospholipids	11
1. 8. Structural categories of AMPs	13
1. 8. 1. α -helical AMPs	13
1. 8. 2. β -Sheet AMPs	15
1. 8. 3. Extended AMPs	15
1. 9. Target Specificity and Selective Toxicity	16
1. 10. Proposed mechanisms of α -helical peptide-membrane interaction	18
1. 10. 1. Barrel-stave pore formation	18
1. 10. 2. Toroidal-pore formation	20
1. 10. 3. Carpet model	21
1. 11. Overcoming the limitations of methodology	22
1. 12. Aims of the work	24
References	25
Chapter Two: Methodology	39-52
2. 1. Quartz Crystal Microbalance (QCM)	40
2. 1. 1. Biomimetic membrane formation on QCM sensor surface	42
2. 1. 2. Viscoelastic fingerprinting analysis	42
2. 2. Dye leakage experiments	43
2. 3. Dynamic light scattering (DLS)	44
2. 4. Atomic Force Microscopy (AFM)	46
2. 5. Neutron reflectometry (NR)	48
References	50
Chapter Three: Mechanism of action of melittin	53-84
Preamble	54
Part one: Nano-viscosimetry analysis of the membrane disrupting action of the bee venom peptide melittin	57
Part Two: Membrane morphology effects in quartz crystal microbalance characterization of antimicrobial peptide activity	70

Chapter Four: Mechanism of action of magainin 2	85-105
Preamble	86
References	87
Nano-viscosimetry analysis of antimicrobial peptide magainin 2 interactions with model membranes	89
Chapter Five: Further biophysical characteristics of AMP-membrane interactions	106-139
Preamble	107
References	108
Part One: Membrane disrupting antimicrobial peptides form distinct domains in single bilayer membranes: a nano-viscosimetry study	109
Part Two: Neutron reflectometry study of the mechanism of membrane disrupting antimicrobial peptide action	128
Conclusions	140
Appendix	143

Chapter One

Introduction

1. 1. Antimicrobial peptides

Following the discovery of penicillin in 1928 medical practice changed forever, expanding to hitherto unimaginable areas, curing conditions impossible to treat before [1]. Antibiotics provided a vital tool not only for the treatment of infections, but also to allow a range of new medical procedures, as they could be used to avoid infections during transplantation, chemotherapy, Intensive care unit (ICU) interventions and to conduct safe surgeries [2, 3]. Without effective antibiotics to control infection these therapies would be impossible. During 1940s and 1950s, antibiotics were extremely effective [4]. However, as early as 1946 scientists including Fleming himself in his Nobel prize lecture [5] warned about the danger of antibiotic resistant bacteria [6, 7].

Soon those predictions were proven correct in everyday practice. It was discovered that microorganisms evolve to withstand those medications that are used to kill them, so infections persist and standard treatments become ineffective [8]. Once resistance occurs, it will spread rapidly because the resistant bacteria would multiply rapidly, producing a big population of bacteria with the resistant genes [9]. Although antibiotic resistance is a natural phenomenon, inappropriate and over use of antibiotics are its major driving factors [10, 11]. In theory the situation could be managed by expanding and diversifying the number of available drugs; however few new antibiotics have been developed in recent years and most of the current antibiotics in use were developed before the 1970s [12, 13].

The emergence of bacterial resistance to conventional antibiotics is one of the most significant international health issue of our time that requires an urgent solution [14, 15]. Probably the first and foremost thing to do would be minimising unnecessary antibiotic prescriptions to preserve what we have, but obviously new antibiotics are also urgently required [15, 16]. These new antimicrobial agents supposed to kill or inhibit growth of pathogens quickly before allowing them to mutate and develop resistance. Previously, pharmaceutical industry had exacting requirements towards new drugs that focused attention on synthetic small molecules. However, the looming emergency broadened the scope: any working solution is acceptable when our modern way of life is under threat.

One of the potential alternatives to traditional antibiotics is the use of antimicrobial peptides (AMPs), as they can work quickly, efficiently, and have wide ranging

activity [17]. These naturally occurring AMPs represent one of the initial and most effective forms of innate chemical defence in all living creatures, including e.g. insects, octopus and star fish, against bacteria, parasite, fungi, and viruses, which are released at the time of hazardous situations such as facing the risk of hunter's attack [18-21]. Generally, AMPs contain 12 to 50 amino acids however with substantial differences in their sequence [18]. Most AMPs can kill both Gram-positive and Gram-negative bacteria, while some of them show anticancer and antiviral activities as well [22, 23]. Hence, since their discovery, they were seen as a potential solution for global health threat of antibiotic resistance [24, 25]. Since they are naturally occurring, they are less likely to be toxic to host cells and give rise to AMP-resistant bacterial strains because their mechanism of action fundamentally differs from conventional antibiotics [26-28].

AMPs have a broad range of activity against pathogenic bacteria, fungi, viruses, and even cancerous cells and parasites [29]. By the late-90s it was believed that all AMPs share two common physical features: cationic charge and a hydrophobic region. The then-popular view was that the former feature promotes selectivity for negatively charged microbial membranes over zwitterionic mammalian membranes, while the second one facilitates interaction and disruption of lipid membranes [30, 31]. However, later in 1997 with the discovery of negatively charged AMPs the concept that AMPs need to be cationic was changed [32]. Anionic peptides found to be rich in glutamic and aspartic acids [33, 34], usually need a metal cation such as potassium ion as a co-factor, and some of them undergo post-translational modifications to show antimicrobial activity [35, 36]. As the number of known AMPs expanded, distinct subclasses were identified based on their structure and/or way of action.

Perhaps the most intensively studied subclass of AMPs is the membrane disrupting peptides as they mostly seem to exhibit common fundamental characteristics, being cationic, α -helical and amphiphilic [37, 38]. Membrane disruption is suggested to proceed either through a detergent-like carpet mechanism [39-41], or discrete pore formation [42-45], either of which subsequently lead to cell death [46]. However, the exact molecular mechanism of the membrane disrupting action is still debated [47].

1. 2. Chemical structure of AMPs

AMPs as all naturally occurring peptides are chemically defined by a specific sequence of amino acids, containing various combinations of the 20 natural proteinogenic amino acids (Table 1) that differ from each other with respect to their side chains [48]. The codes defined in Table 1 will be used in this thesis. It should be mentioned that occasionally other amino acids are also included in the AMP sequence, especially for peptides of bacterial origin.

Table 1.1. Properties and Letter Codes for 20 natural amino acids [48]

Amino acid	3 Letter code	1 Letter code	Properties
Alanine	Ala	A	Hydrophobic
Arginine	Arg	R	Basic, charged
Asparagine	Asn	N	Neutral-polar
Aspartate	Asp	D	Acidic, charged
Cysteine	Cys	C	Neutral-polar
Glutamine	Gln	Q	Neutral-polar
Glycine	Gly	G	Hydrophobic
Glutamate	Glu	E	Acidic, charged
Histidine	His	H	Basic
Isoleucine	Ile	I	Hydrophobic
Leucine	Leu	L	Hydrophobic
Lysine	Lys	K	Basic, charged
Methionine	Met	M	Neutral-polar
Phenylalanine	Phe	F	Hydrophobic
Proline	Pro	P	Conformational, cyclic
Serine	Ser	S	Neutral-polar
Threonine	Thr	T	Neutral-polar
Tryptophan	Trp	W	Aromatic
Tyrosine	Tyr	Y	Aromatic
Valine	Val	V	Aliphatic, hydrophobic

1.3. The target of AMPs: the biological membrane

The biological membrane is a vital component of the cell, for enclosing the living part of cell from the surrounding environment and serving as a selectively permeable barrier [49]. Studying the structure and understanding the role of each part of the membrane was for a while one of the most appealing issues in science [50, 51]. Already in 1925, the first hypothesized model for biological membranes was proposed to be a lipid bilayer [52]. Follow up studies led to finding more details about the membrane culminating in the “Fluid mosaic model” by Singer–Nicolson in 1972 [53]. Based on this model, protein molecules, carbohydrates and all components are freely diffusing in a sea of lipid bilayer, giving fluidity and elasticity to the membrane.

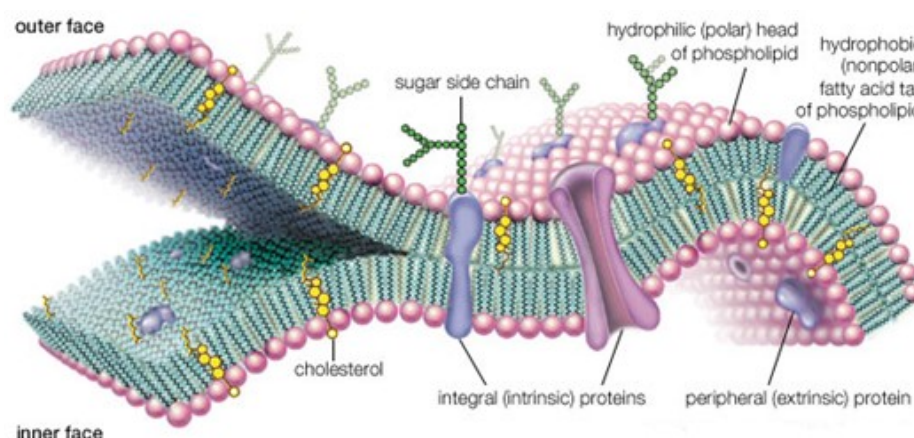


Figure 1.1. Schematic presentation of cell membrane. Image was adapted with the permission from Encyclopaedia Britannica, Inc. c 2007 [59]

The fundamental structure of the cell membrane is common in both prokaryotic and eukaryotic cells but with significant differences in configuration [54, 55]. The membrane platform is provided by the phospholipid molecules that are amphipathic, leading to an arrangement where a hydrophobic core region separates hydrophilic domains, providing a semipermeable barrier that controls the passage of different molecules into and out of the cell; the latter function is mostly performed by special transport proteins [56, 57]. If the integrity of the membrane is lost, uncontrolled passing of molecules leads to cell death; such a mechanism was suggested for the functioning of antimicrobial peptides (AMPs) [18]. Specificity and selectivity of AMPs is mainly based on the differences between microbial and host cell membrane structures [58]. The fundamental distinction between prokaryotic and eukaryotic cell membranes is found in the configuration of

phospholipid bilayer components and presence or absence of cholesterol [59]. Bacterial (prokaryote) exterior membrane surface is covered by anionic phospholipids (such as phosphatidylglycerol “PG”, cardiolipin “CL”), while the outer cell surface in eukaryotes is mostly composed of zwitterionic phospholipids, (such as; sphingomyelin “SM” and phosphatidylcholine “PC”) with neutral net charge [60]. Another significant distinction is the presence of sterols such as cholesterol in the mammalian cell membrane (20-40 mole%) [61, 62], which will usually reduce the activity of antimicrobial peptides [63-65]. In contrast, bacterial cells lack cholesterol [66].

Even among bacteria there are substantial differences in their cell membrane compositions. This is the basis of the Gram stain test that divides them into two different types: Gram-positive and Gram-negative bacteria [67]. Gram positive bacteria have a single cell membrane protected by a thick network of peptidoglycan and teichoic acid [68]. It is believed that cationic peptides are more active against Gram-positive bacteria [69]. Gram negative bacteria have plant-like cell walls with a thin layer of peptidoglycan and an outer membrane with a lipopolysaccharide component which is not found in Gram positive bacteria [70]

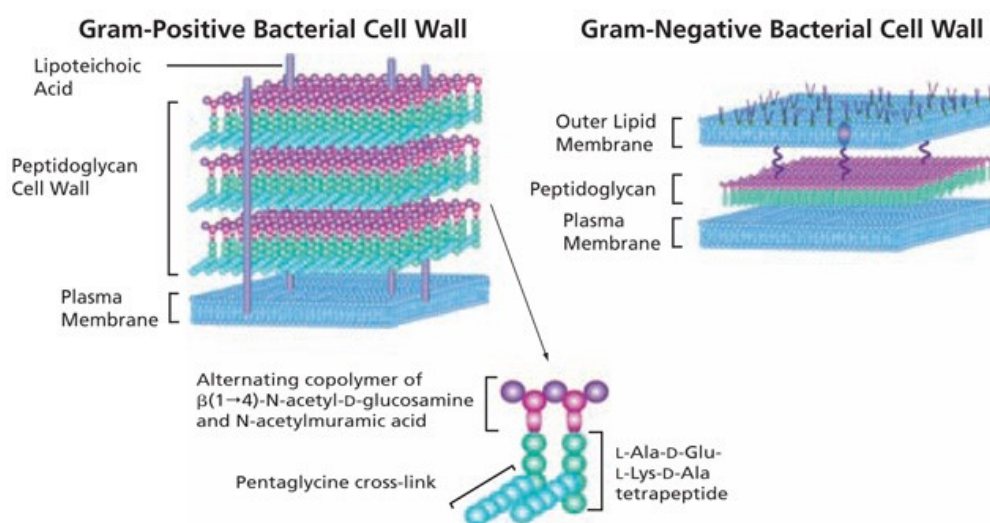


Figure 1.2. The basic structure of bacterial peptidoglycan and the cell wall structures of Gram-positive and Gram-negative bacteria [68]

Live bacteria cells with the protein-containing membrane and many different lipid and non-lipid components is a complex structure for study [71]. Therefore, biomimetic membranes consisting of different phospholipid structures are used for physicochemical studies to reduce the complexity of biological membranes [72].

1.4. The main structural elements of biological membranes: phospholipids

Lipids are a large and diverse group of naturally occurring organic compounds that are related by their amphiphilic character and weak solubility in water. There is great structural variety among the lipids that include fatty acids, phospholipids, alkyl glycerides, sterols, sphingolipids, glycolipids, glycerophospholipids, prenol lipids, saccharolipids, and polyketides [73]. Phospholipids are the main membrane forming lipids and the most important group of lipids for supporting life.

As shown in figure 1.3, phospholipids are amphiphiles: the polar moiety of the head group is a phosphodiester which in glycerophospholipids attach to hydrophobic aliphatic acyl chains by a glycerol backbone [74-76]. The hydrophilic head group also contains a terminal group such as a glycerol, choline or ethanolamine moiety [77].

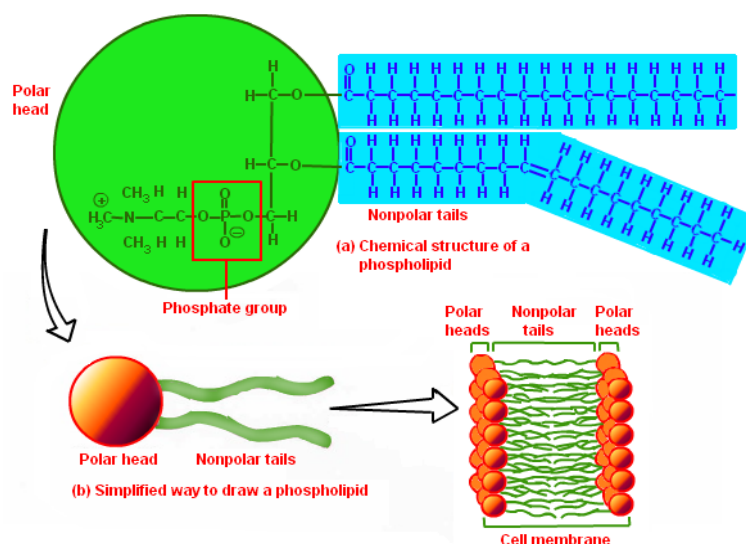


Figure 1.3. Schematic representation of bilayer formation [76]

There are two classes of phospholipids based on the backbone structure: glycerophospholipids and sphingophospholipids with glycerol and amide backbone, respectively [78]. The general structure of phosphoacylglycerol as the main physiological phospholipid in nature is shown in figure 1.4.

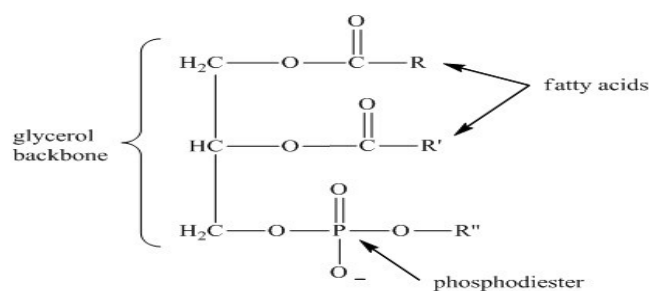
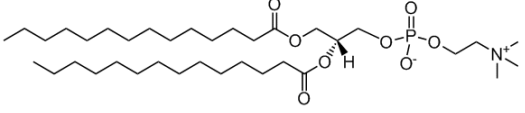
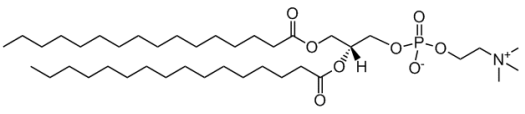
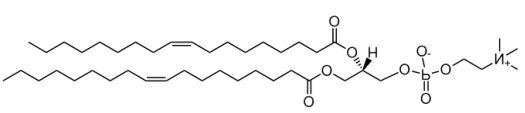
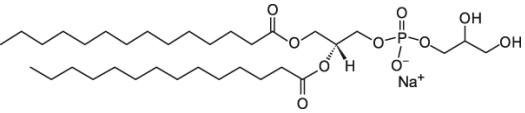
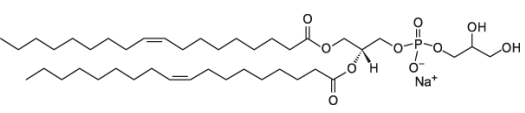
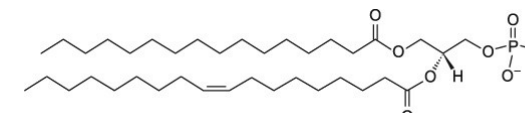
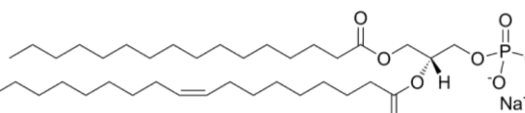


Figure 1.4. Phosphoacylglycerol structure

Depending on the identity of R'' of head group region and R and R' in the hydrophobic tail region different types of phosphoacylglycerol lipids can be distinguished. Table 1.2 shows the structure and abbreviated names of widely used natural phosphoacylglycerol lipids.

The amphiphilic structure makes phospholipid molecules able to aggregate spontaneously to bury their hydrophobic “tails” in the interior and expose their hydrophilic heads to water; this self-assembly process leads to lipid bilayer formation [79, 80]. Figure 1.3 shows the schematic representation of a phospholipid bilayer. In biomimetic membranes, DMPC is frequently used as a saturated zwitterionic lipid and DOPC as the unsaturated counterpart; these lipids yield “neutral” mammalian-mimetic membranes. For bacterial mimetic membrane DMPG or DOPG were added to the mixture, respectively.

Table 1.2. Widely used phospholipids and their molecular structures

Lipid name	Abbreviated name	Molecular structure
1,2-dimyristoyl-sn-glycero-3-phosphocholine	DMPC	
1,2-dipalmitoyl-sn-glycero-3-phosphocholine	DPPC	
1,2-dioleoyl-sn-glycero-3-phosphocholine	DOPC	
1,2-Dimyristoyl-sn-glycero-3-phosphorylglycerol (sodium salt)	DMPG	
1,2-dioleoyl-sn-glycero-3-phospho-(1'-rac-glycerol) (sodium salt)	DOPG	
1-palmitoyl-2-oleoyl-sn-glycero-3-phosphocholine	POPC	
1-palmitoyl-2-oleoyl-sn-glycero-3-phospho-(1'-rac-glycerol) (sodium salt)	POPG	

1.5. Cholesterol

Sterols, also known as steroid alcohols, are a subgroup of one of the most important class of organic molecules known as steroids, a class of natural lipids in plants, animals and fungi [81]. Cholesterol is the most common type of animal sterol, which is a vital component of cell membrane structure and also the basis of some specific hormone synthesis pathways [82-84]. The sterols found in plants and fungi are phytosterols and ergosterol, respectively [61]. The proposed model for the role of cholesterol in lipid membranes postulates that it interacts with lipid head group through its small hydrophilic OH region and can insert into half leaflet of membrane and reorder the lipid core region [61]. Presence of cholesterol in mammalian plasma membrane modulates the fluidity of membrane structure and controls the membrane permeability [85-88]. Figure 1.5 shows the chemical structure of cholesterol.

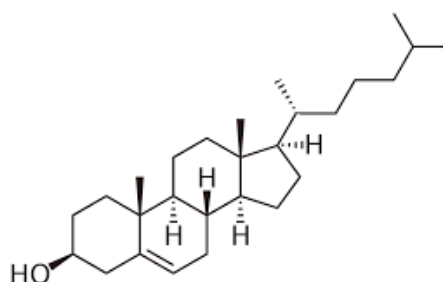


Figure 1.5. Cholesterol chemical structure

To explain the molecular-level interaction of cholesterol with neighbouring lipids different models were proposed, namely condensed complex model (CCM) [89, 90], the superlattice model (SM) [91] and the umbrella model [92, 93]. It should be noted that all of these models are based on in vitro studies and assume that cholesterol-cholesterol interaction is repulsive, however, in 2005 it was suggested that the interaction might be attractive [94]. In the CCM, it was hypothesized that cholesterol will preferably associate with saturated acyl chains by hydrogen bond and forms condensed complexes [89, 95]. The Superlattice Model assumes that presence of cholesterol among other lipid molecules may cause a long-range repulsive force and subsequent formation of regular superlattice distributions [91, 96]. The small polar “head group” of cholesterol cannot provide the shielding for its hydrophobic sterol region in aqueous environment, thus in the Umbrella model

cholesterol shows higher tendency to interact with larger headgroup lipids, such as PC or sphingomyelin [92, 97]. Based on the Umbrella model, beneath the phospholipid headgroup the hydrophobic cholesterol region shares the space with the phospholipid acyl chains causing the “cholesterol condensing effect” [98]. Consequently, cholesterol shows higher preference for saturated acyl chain lipids than unsaturated lipids because of higher packing order [98]. It was proposed that cholesterol may not distribute uniformly throughout the membrane and instead will condense leading to the so called raft formation [99]. Differential scanning calorimetry (DSC) experiments shows that presence of cholesterol may alter the main transition temperatures of lipid membranes [100-103]. It was shown that at low concentration of cholesterol there are two separate domains, one cholesterol-rich and one cholesterol-poor and by increasing cholesterol content the cholesterol-poor domain will shrink [104].

Studies on cholesterol enriched membrane mostly focus on the regions known as rafts or liquid ordered domains; the existence of these regions is one of the initial differences between eukaryote and bacterial membranes [105]. Furthermore, knowing that physical membrane properties are the main factors affecting peptide-membrane interaction, therefore, existence of cholesterol rich/poor domains may lead to different peptide behaviour toward the membrane [106]. Several studies proposed that the presence of cholesterol in eukaryote membrane would reduce or inhibit the disruption activity of AMPs, by increasing membrane cohesion and stiffness [60, 107-116]. Despite all these findings the effect of cholesterol on AMP-membrane interaction is still not clearly understood.

1. 6. Biomimetic membrane

Different techniques can be used for supported lipid membrane formation including spin coating [117], micro contact printing [118], solvent-exchange deposition [119], Langmuir Blodgett deposition [120], lipid-surfactant micelle deposition [121], evaporation induced assembly [122], bubble collapse deposition [123], lipid dip-pen nanolithography [124], and vesicle fusion [125, 126]. The main problem of using supported bilayer membrane platforms for studying the interaction between transmembrane peptides and proteins with membrane is not so much the formation of such membrane platforms, rather the lack of enough space between the

supporting surface and membrane [127]. Attempts to address the issue introduced various spacers, such as, soft polymer cushions [128, 129], tethers [130-132] and polar peptides [133, 134] to lift the membrane a few nanometres above the surface. However soon it was revealed that the anchor molecules potentially hinder protein diffusion [135, 136]. Potentially the best biomimetic model of plasma membrane structure is the partially suspended bilayer which uses the roughness of the surface to include a liquid reservoir underneath the membrane [137-139]. Liposome deposition is the simplest technique for membrane formation for the study of peptide-membrane interaction [105], lipid domain formation [140, 141], membrane cytoskeleton interactions [142] and protein self-assembly [143-145]. It involves addition of lipid vesicles to a hydrophilic surface following liposomes rupture to form a continuous bilayer on the surface [137, 138, 146-151]. The liposome deposition is the main technique used in this thesis.

1. 7. Thermodynamic phase behaviour of phospholipids

Homogeneous matter can be found in one of three fundamental thermodynamic phases: solid, liquid, or gas [152]. At a specific combination of temperature and pressure depending on the intermolecular forces homogeneous matter can transition from one phase to another that is known as phase transition [153]. Lipid membranes also exhibit phase transitions, however can not be considered homogeneous matter given the stabilizing role of the environment (water surface tension) in the formation of a bilayer, and the amphiphilic nature of the lipid molecules that create two distinct interaction zones, one van der Waals/hydrophobic and the other polar/hydrophilic, in the cross section of the bilayer. Phospholipid bilayers undergo multiple phase transitions while remaining in two dimensional condensed state [154].

In very low temperature, lipids are in the most ordered phase, the individual phospholipids are closely packed and fully extended, described as a crystalline dehydrated phase (L_c) [155-157]. By increasing the temperature, the polar headgroups become hydrated and the tightly packed lipids gain more freedom of motion leaving some gaps between them until the formation of gel phase (L_β) at the sub-transition temperature [158]. PC lipids with 14 carbon atoms show only two phase transitions, known as main transition and pre-transition [159]. Most of

saturated phospholipids with more than 15 hydrocarbons in their acyl chains and depending on their head groups have three phase transitions by having another phase between L_β and L_α known as ripple phase (P_β) [160]. Phospholipids with 10 hydrocarbon long acyl chains have only one phase transition and shorter than 9 hydrocarbons do not have any phase transition [161, 162]. In the literature, the “main transition” (T_m) of lipids is the gel to fluid transition resulting from melting or disordering of the hydrocarbon chains.

Different phospholipids may have different phase transition temperatures [160, 163]. Factors affecting the phase transition are acyl chain length and structure, state of hydration, pH and presence/ absence of ions influencing the head group configuration [164-167]. Presence of unsaturated acyl chains, by weakening the van der Waals interactions between hydrocarbon tails will decrease T_m , directly depending on the number of double bonds [168, 169]. Likewise by increasing hydrocarbon chain length, van der Waals interaction become stronger requires more energy to disrupt the ordered packing, thus the T_m increases [170]. It was also shown that increasing hydration of head groups may decrease in hydrocarbon packing and

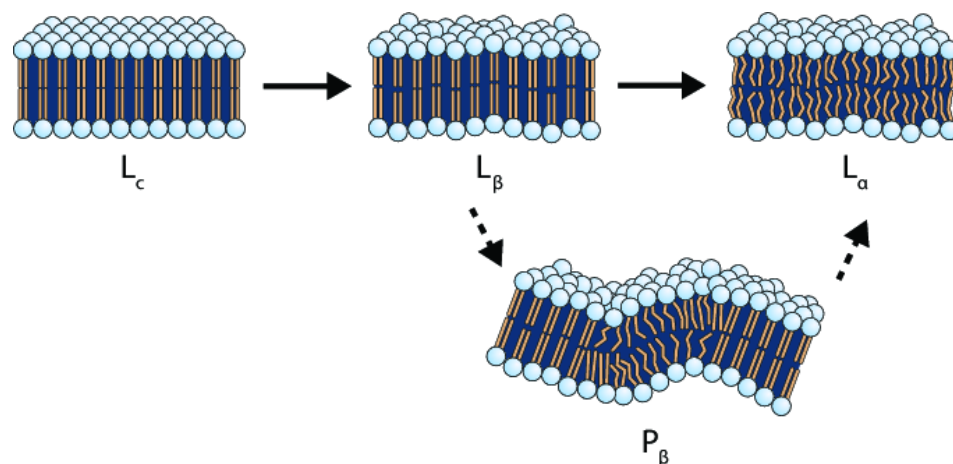


Figure 1.6. Representation of the different phases one in a lipid membrane: crystal phase (L_c), gel phase (L_β), and liquid phase (L_α). Certain types of lipid can be found in the ripple phase (P_β), which is a transitional phase between the gel and liquid phase [172]

subsequently decrease the main phase transition temperature [171].

Figure 1.6 shows the simple schematic presentation of different phases in the lipid membrane [172]. Furthermore, it was reported that presence of cholesterol in the membrane inhibits the lipid gel phase formation by disrupting the lipid packing [100, 173].

1. 8. Structural categories of AMPs

According to APD database only 13% of AMPs have a known 3D structure, as determined by solution nuclear magnetic resonance (NMR) spectroscopy or X-ray diffraction [174]. However it is known that many linear AMPs that are unstructured in aqueous solution such as magainin [175], and melittin [176], adopt at least partially folded conformation as they interact with the biological membrane [177].

The highly environment-dependent conformation of the peptides lead to circular dichroism (CD) becoming the method of choice to characterize, indirectly, the folded state of the peptides [178]. Thus the three dominant structural groups for AMPs were identified: α -helical, β -sheet and extended peptides (figure 1.7) [179, 180].

1. 8. 1. α -helical AMPs

α -helical AMPs form the most broadly studied category of AMPs. More than 100 AMPs have been identified to have α -helical structure, consisting 12 to 40 residues and may have a central “hinge” region, like the one in e.g. dermaseptins [181] and caerin [182]. α -helix is formed by establishing hydrogen bonds between the amide moieties, C=O in one loop and N-H in the other. This regular pattern repeats precisely every 4 amino acid residues through the helix which gives the α -helix definite rise and diameter [183].

Usually, the amphipathicity of the peptides manifests along the axis of the α -helix, so it can lie parallel on the membrane surface with the hydrophobic parts sinking into the hydrophobic core of the membrane during the lipid interactions [184]. The length of the helical segment differs, in some cases long enough to span the membrane bilayer and disrupt the hydrophobic region of cell membrane [185, 186] while shorter α -helical peptides such as aurein1.2 usually may act on the surface, dissolving the membrane once a threshold concentration is reached [187].

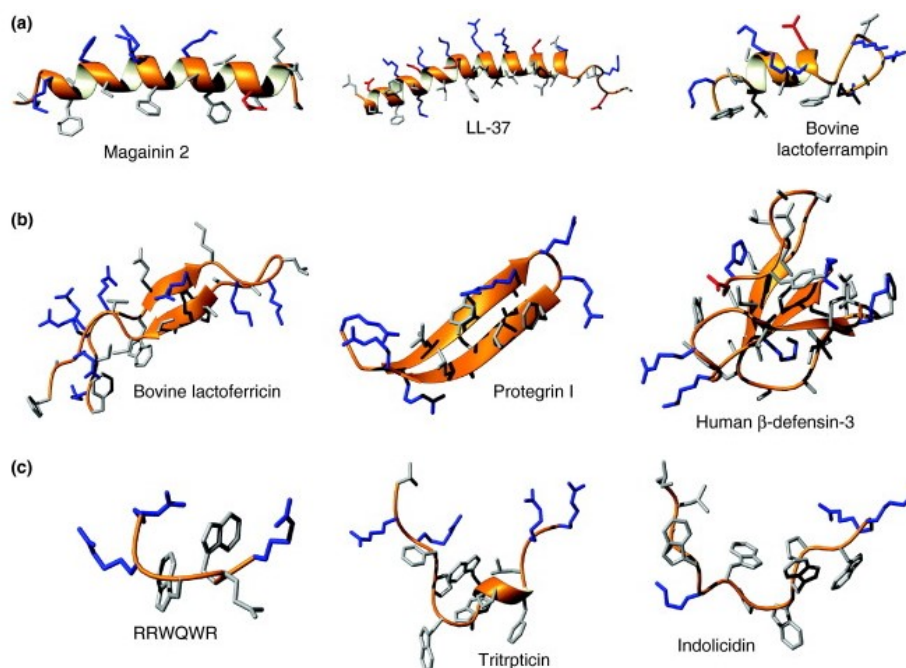


Figure 1. 7. AMPs structure: a) α -helical b) β -sheet c) Extended [176]

The properties of the α -helix would affect the depth of membrane insertion and consequently the antimicrobial activity of the AMPs [188]. The length of an α -helix may also affect its cytotoxicity [189]. By decreasing peptide length, the tendency to form secondary structure and subsequently membrane binding would decrease as the result of increasing entropic penalty, per amino acid on adsorption [190]. Therefore, antimicrobial activity and membrane lysis usually decrease with decreasing peptide length [191, 192]. For example it was found that a shortened derivative of melittin and HP showed at least 300 times less toxicity to rat and human erythrocytes, respectively [193].

1. 8 .2. β -Sheet AMPs

The β -sheet, β -pleated sheet or β -form structure was first suggested in 1930s by William Astbury [194]. The structure is formed when two or more polypeptide chains overlap and form a row of hydrogen bonds. This can happen in a parallel or anti-parallel arrangement [195].

In anti-parallel arrangement, the C-terminus end of one piece and the N-terminus end of the other one is on the same side. In parallel arrangement, the C-terminus end and the N-terminus end of both segments are on the same sides. Hence, the hydrogen bonds form at an angle, which makes the bond longer and thus less stable. Furthermore, in the anti-parallel arrangement as the nitrogen and oxygen

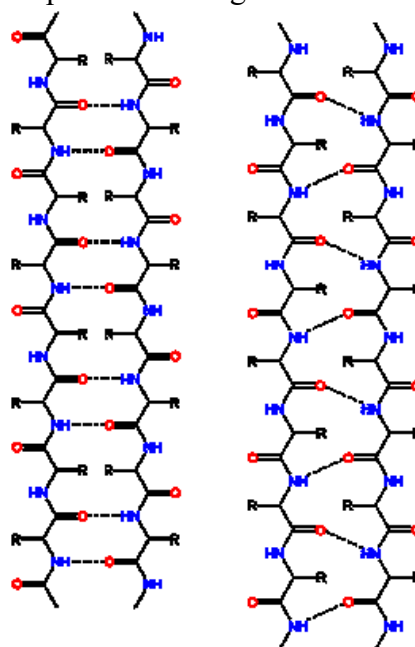


Figure 1.8. β -sheets peptides: a) anti-parallel hydrogen bonding b) parallel hydrogen bonding

components are directly opposite to each other, they can form stronger and more stable bonds [196]. Disulphide bridges between conserved cysteine residues often stabilize this conformation however this covalent bond doesn't contribute to antimicrobial activity [197, 198].

1. 8. 3. Extended AMPs

There are many examples of AMPs that do not fold into classical secondary structures, and they are usually small and contain high proportions of specific amino acids, typically Arg, Trp, Cys or Pro residues that impose particular constraints to their structure [63]. Many of them are not membrane active, and they exert their activity by penetrating the membrane and interacting with intracellular proteins [179]. It is believed that these peptides will insert into the membrane with the hydrophobic core making contacts in the interfacial regions while the flanking parts interact more prominently with the lipid headgroups [199]. Extended peptides show a boat-like conformation when bound to the membrane [199]. Although a number

of studies argue about the mechanism of extended peptides [199-202], their mechanism of action with short and unique sequences yet wide-range of activities is still under debate [203].

1. 9. Target Specificity and Selective Toxicity

As described above, AMPs form the first line of defence against infections in most organisms. The essential consideration about the potential pharmaceutical application of each AMP is the degree to which it can differentiate between the pathogens and the host cells. The selective toxicity of an AMP, or the lack thereof, is based on different physicochemical parameters of peptide (including charge, hydrophobicity, conformation, amphipathicity) and complex interactions of the peptide and target cells [204]. As noted earlier all biological membranes are composed of amphipathic phospholipids but there are some significant differences between microbial membranes and AMPs secreted organisms (from here on host membranes) [205, 206]. There can be significant differences between different host membranes as well, as membrane lipid composition has marked differences between amphibians, insects, plants and mammals [18, 21, 25, 207, 208]. Bacterial pathogens have highly anionic membranes, composed mostly of PG or CL lipids [18, 209]. On the other hand, mammalian membranes are composed of zwitterionic phospholipids such as PE, PC, or SM [210]. The presence of sterols in mammalian membrane is the other difference between these cells and bacterial [111, 211]. Thus, the main driving force of the selectivity of AMPs towards bacterial membrane is believed to be the electrostatic interaction between cationic AMP and anionic bacterial membrane [212-215]. However, empirical evidence shows that higher positive charge does not necessarily result in higher antimicrobial activity, it was found that in peptides with higher than +5 charge the antimicrobial activity is reduced, as it can interfere with peptide conformation [115, 216, 217]. Different studies on the peptide helicity show that stability of peptide helical structure and dynamic conformations may result in higher antimicrobial activity, however unfortunately there is a parallel increase in haemolytic activity as well [46, 218-221].

Studies on the interaction of linear and cyclic variants of melittin and magainin showed that peptide conformational dynamics have a significant effect on peptides

initial binding to the membrane and their disrupting ability [222]. It was found that cyclic melittin analogues were less efficient in the initial binding but show overall higher antimicrobial activity. On the other hand, the magainin cyclic analogue is less efficient in both disruptive action and the initial binding [222]. Hydrophobicity and α -helicity are believed to be crucial factors in antimicrobial activity of cationic membrane disrupting peptides [223]. It was revealed that increasing the peptide hydrophobicity may lead to increased antimicrobial activity that has also increased haemolytic effect of the peptide [220, 224-229]. However, it was found that further hydrophobicity increasing beyond a certain threshold result in a decrease of antimicrobial activity probably due to higher self-association and dimerization which inhibits peptide reaching to the membrane [224].

In other studies it was shown that peptide amphipathicity has a positive correlation with antimicrobial but also haemolytic activity of peptide [230]. Many studies have shown that the hydrophobic moment or amphipathic structure distribution is more important in antimicrobial activity than overall hydrophobicity [231-233]. Amphiphilicity is not simply the presence of hydrophobic/ hydrophilic moieties in the sequence but also the distance between them which is known as amphipathicity [234-236]. In some helical AMPs (such as human peptide LL-37) amphipathicity is distributed along the longitudinal centreline with hydrophobic residues on one side and hydrophilic ones on the other side. A peptide like that is typically oriented parallel to the membrane surface on the interface between the hydrophobic membrane core and hydrophilic headgroup region, leading to surface acting mechanism [231, 237]. This type of amphipathic structure distribution found to be effective against Gram-negative bacteria [231]. Another more contractive amphiphilicity forms by separating the hydrophilic section with a hydrophobic intermediate by a transverse line perpendicular to the longitudinal axis of peptide; peptides exhibiting this unique motif found to be effective against both Gram-positive and Gram-negative bacteria and act by transmembrane mechanism [231, 236, 238]. The details of these mechanism of actions will be explained in the following section.

1. 10. Proposed mechanisms of α -helical peptide-membrane interaction

While the exact mechanism of action of an AMP is rarely known, and in many cases still debated [198, 239], two distinct membrane permeabilization mechanisms have been proposed and widely accepted based on available data and the structure of AMPs. Transmembrane pore formation that is divided into two different pore geometries known as barrel-stave and toroidal pores, and surface acting “carpet” mechanism.

The distinction between these mechanisms is mostly empirical with a weak correlation to the peptide length [240]. It is believed that both shorter peptides (<3 nm helical length) and longer ones (>7nm) have difficulty forming pores through the membrane. 4nm peptides (approximately 20-30 amino acid residues in the α -helix) are optimal to span a lipid membrane by forming pores [241].

An important general characteristic of membrane disrupting AMPs is the existence of an activity threshold. Often, but not always, at low concentration peptides are inactive and only after reaching a critical concentration can they exert their activity [219].

1. 10. 1. Barrel-stave pore formation

Barrel-stave mechanism was first proposed in 1974 to explain alamethicin activity in black lipid membranes [242, 243]. In this hypothetical mechanism first the peptide monomers bind to the membrane and form an α -helical structure. Then the peptide as monomer or oligomer aggregate on the surface to form a bundle or an ion-channel in the core region of membrane, without significant perturbation of the lipid molecules in the way that their hydrophobic surfaces interact with the lipid core and their hydrophilic surfaces form the interior region of an aqueous pore [100,

243-248]. So, the logic of the model necessitates that hydrophobic interaction is the main driving force in this model [244].

A more generic model of the barrel-stave mechanism involves four main stages: (a) initial electrostatic binding of the helical peptide monomers to the membrane

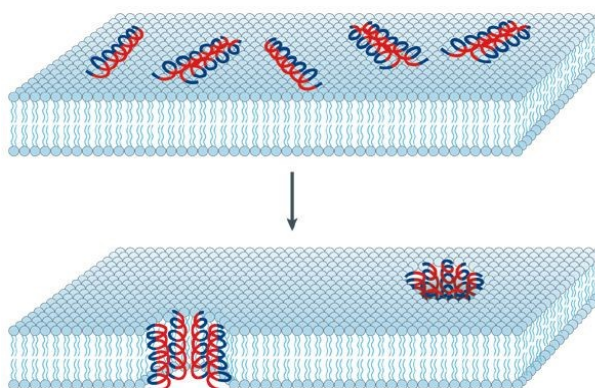


Figure 1.9. Barrel-stave pore formation model [254]

Hydrophobic peptide region coloured blue and hydrophilic region are red

surface (b) membrane-bound monomers start assembly even at low surface density of bound peptide (c) at least two assembled monomers insert into the membrane to start the pore formation (d) increase the pore size by progressive insertion of further monomers [244].

It has been concluded that the barrel-stave pore formation model is only feasible for very weakly charged peptides, which can be tightly packed [44, 45, 249]. This unique pore formation in alamethicin is well studied and reported; it is the only confirmed peptide following this model [45, 241]. Based on the mechanism it was believed that alamethicin pore would be formed by a fixed number of monomers[250], however some argued that the pore size formed from this aggregation will increase with the number of monomers in the aggregate, and subsequently increasing the conductance [251, 252].

1. 10. 2. Toroidal-pore formation

Toroidal pore or wormhole mechanism was first proposed in 1996 to describe magainin-induced pores [44]. In the toroidal pore mechanism, AMPs insertion into the membrane lead to forming pores at critical threshold concentration by induced surface bending in membrane leaflets, bridging the two leaflets so the water core is lined by both the inserted peptides and the lipid head groups [44, 204]. By disruption of the bilayer curvature and forming a torus, the inserted peptides would cause permeabilization, or disintegration of the membrane [253, 254]. The main

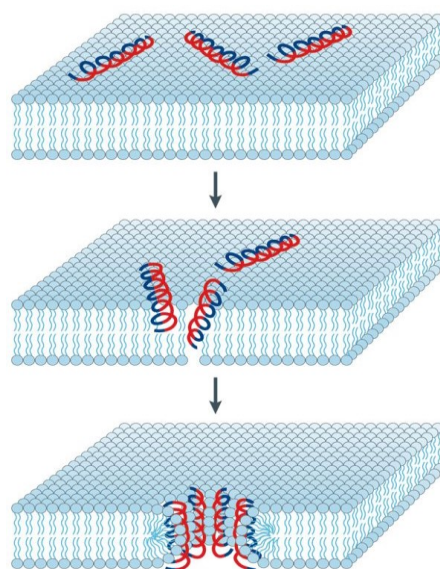


Figure 1.10. Toroidal pore formation model [254]

Hydrophobic peptide region coloured blue and hydrophilic region are red

difference between barrel-stave and toroidal model is that in the toroidal pore model, peptides are always associated with the lipid head groups even when they are vertically inserted in the lipid bilayer [45, 255].

It was predicted based on the model that the formation of stable toroidal pore highly depends on a critical peptide-lipid ratio, and increasing peptide concentration would lessen the pore stability because of higher electrostatic repulsion between the positive charged monomers [56].

Recent studies suggested the toroidal pore formation by various peptides, such as mellitin from bee venom [45], and magainins from amphibian [256, 257].

1. 10. 3. Carpet model

The so called carpet model is the most commonly cited model, and was first suggested by Pouny et al. in 1992 for explaining the mechanism of action of dermaseptin [258]. Carpet mechanism is described in four steps: a) peptides bind

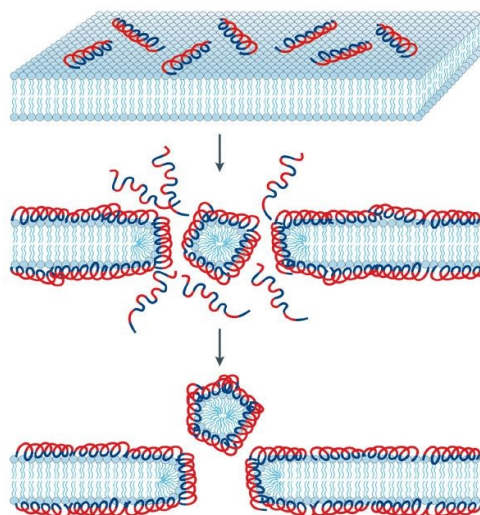


Figure 1.11. Carpet model [254]

Hydrophilic peptide region coloured blue and hydrophobic region is red

parallel to the surface through their hydrophilic surface, it is assumed that main force in this mechanism is electrostatic forces between the negative charge of bacteria surface and positively charged peptides, however, the exact role of peptide charge is not fully known [187, 259]. (b) laying of peptide helical monomers on the surface of the membrane in the way that the positive charges of amino acids interact with the negatively charged lipid headgroups or water molecules, covering the membrane surface in a carpet-like fashion. c) reorientation of the hydrophobic peptide residues toward the hydrophobic core region and (d) finally breaking down the membrane by disrupting the bilayer curvature [244]. The parallel orientation of the peptide on the membrane head group during the whole process would change the membrane fluidity by displacement of phospholipids by peptides and destabilizes the phospholipids packing [37, 260]. It should be noted that in this mechanism the membrane cannot be permeated before reaching a critical peptide threshold concentration [64, 260, 261], which could be described as causing imbalance between surface tension of two membrane leaflets that at a specific concentration leads to membrane disintegration [262]. There are some examples of

AMPs reported to disrupt the membrane via carpet mechanism including, cecropin P1 [39] and aurein 1.2 [138, 262] and citropin 1.1 [263].

All these models predict that the cell killing activity of AMPs happens via perturbation of membrane integrity [264]. Recent NMR studies proposed that by passing sufficient time all AMPs may fragment the membrane bilayer to form micelle structures, which leads to cell death, regardless of their preferred mechanism [204]. However, all these mechanisms are only hypothesis based on the final stage of peptide-membrane interaction and none of the known AMPs would exactly match any of these models [18, 265, 266]. In order to understand the exact mechanism of AMPs action we need to find a way to study the entire pathway leading to the final disruption.

1. 11. Overcoming the limitations of methodology

As noted, a persistent problem in this field is how to confirm the mechanism of peptide-membrane activity directly. The exact cell killing mechanism of AMPs is not completely understood in most cases, particularly the role of specific peptide residues and their interactions with specific membrane components in the mechanism of action [267]. It was confirmed for most peptides in this family that their mechanism of action involves membrane permeabilization; for this reason it is acknowledged that their interaction with specific membrane components is an important feature of their behaviour [267, 268]. However, in reality this interaction is more complex than any of the proposed models [269, 270].

To identify the underlying molecular processes a wide variety of biophysical techniques have been used to evaluate the secondary or tertiary structure of the peptide, and its orientation, or the thermodynamic states associated with the binding to membrane. Those biophysical techniques were used to clarify the mechanism of action of AMP lysing of phospholipid membranes which provides most of our knowledge of the molecular details. However, each method provides a slightly different aspect of peptide activity and none of them found to be capable of effectively determining the mechanism of AMP action individually [271].

Studying the interaction of AMPs with model membranes can be the best way to gain insights into the mechanisms of their activities [56]. For this purpose, different

techniques applied, with different strength and limitations [272, 273]. Namely: atomic force microscopy (AFM) can provide a good approximation of surface topography of the membrane and probable restructuring or destabilization happening with peptide in real time, under physiological condition with slight sample preparation [272, 274]. However, it lacks chemical specificity and unable to study situation without enough topographical contrast (such as inserted peptide in the membrane) [275, 276]. Generally, spectroscopic techniques (fluorescence, nuclear magnetic resonance (NMR), circular dichroism (CD), infrared (IR) and etc) are non-invasive fast techniques based on the changes of electronic and spectroscopic energy levels by the peptide binding with the advantage of application in solution, providing a better understanding of binding process and help insight into the three-dimensional peptide structural and conformational findings [277], while having the disadvantage of lack of sensitivity and ability to study multiple equilibria processes [278, 279]. Fluorescence and NMR spectroscopy are providing structural and dynamic information of the binding and indicating which group or part of peptide involve in the binding, respectively [280, 281]. NMR is very accurate but expensive and requiring large amount of peptides [282, 283]. IR and CD are particularly useful to study the peptide secondary structure and three-dimensional structure of binding sites but less accurate than NMR, respectively [284-286].

One of the calorimetry technique used is differential scanning calorimetry (DSC) with the ability to offer a direct and complete thermodynamic view of the interaction but with the disadvantage of large sample required and low throughput [287, 288]. Another calorimetry method used as a fast method for localizing membrane transitions of AMPs is isothermal titration calorimetry (ITC) [289, 290]. The quartz crystal microbalance-with dissipation monitoring (QCM-D) is an attractive real-time and insitu technique for measuring the dynamic behaviours of a layer on the quartz crystal surface, and providing information of the mass and structural changes happening on the surface [262, 291]. Therefore, it found as a useful method to study the dynamic process of peptide adsorption and desorption on the surface [292, 293]. Particularly to study the molecular-level interactions between a supported membrane and AMPs in order to find their mechanism of action [262, 293, 294]. Transmission electron microscopy (TEM) helps to directly observe the changes in membrane morphology before and after peptide treatment [295, 296]. Another useful microscopic technique is confocal microscopy which the source of light

imaged through a pinhole for increasing optical resolution and improved signal-to-noise ratio [297, 298].

The continuous progress in biophysical methods ranging from structural analysis to live imaging opens new prospective and may challenge former findings. Despite thousands of studies and findings, there are still unclear and debated issues in the field.

1. 11. Aims of the work

AMPs, as an effective innate defence found to have the potential to battle the growing threat of antibiotic resistant bacterial strains. However, despite all the efforts spent on developing AMP drugs and describing their mechanism of action, there is still controversy and uncertainty in the understanding of mechanism. The lytic action of most AMPs is well proven however, for a prospective antibiotic, the hemolytic activity in humans needs to be eliminated, which has not been successful thus far, due to persistent uncertainties about their mechanism of action, and the basis of their specificity and selectivity in their natural host. In this thesis I aim to resolve some of those unclear aspects of AMP action.

The specific aims of my thesis are to

1. Identify the molecular mechanism of action of well-known membrane disruptor peptides melittin and magainin 2 on different model membranes mimicking fundamental mammalian and bacteria-like membrane properties.
2. Describe the effect of basic membrane properties, such as charge, alkyl chain saturation, cholesterol content and morphology on the mechanism of action of these peptides.
3. Explore the feasibility of using lipid phase transition temperature measurements to detect distinct thermodynamic states of membrane bound peptides, manifesting as domains. Develop this as a method, in reference to the mechanisms of melittin and magainin 2 action defined in Aims 1 and 2.
4. Study the means of determining the location and orientation of the AMPs in model membranes in support of the proposed mechanisms developed in Aims 1 and 2.

References

- [1] Diggins FW. The true history of the discovery of penicillin, with refutation of the misinformation in the literature. *Br J Biomed Sci* 1999;56:83.
- [2] Dent CD, Olson JW, Farish SE, Bellome J, Casino AJ, Morris HF, et al. The influence of preoperative antibiotics on success of endosseous implants up to and including stage II surgery: a study of 2,641 implants. *J Oral Maxillofac Surg* 1997;55:19-24.
- [3] Kass EH. Chemotherapeutic and antibiotic drugs in the management of infections of the urinary tract. *Am J Med* 1955;18:764-81.
- [4] Macfarlane JT, Worboys M. The changing management of acute bronchitis in Britain, 1940–1970: the impact of antibiotics. *Medical History* 2008;52:47-72.
- [5] Nobelstiftelsen. Nobel Lectures: Physiology Or Medicine 1942-1962: Elsevier; 1964.
- [6] Powers J. Antimicrobial drug development—the past, the present, and the future. *Clin Microbiol Infect* 2004;10:23-31.
- [7] Moellering Jr RC. Past, present, and future of antimicrobial agents. *Am J Med* 1995;99:11s-8s.
- [8] Laxminarayan R, Duse A, Wattal C, Zaidi AK, Wertheim HF, Sumpradit N, et al. Antibiotic resistance—the need for global solutions. *Lancet Infect Dis* 2013;13:1057-98.
- [9] Klein E. Antimalarial drug resistance: a review of the biology and strategies to delay emergence and spread. *Int J Antimicrob Agents* 2013;41:311-7.
- [10] Laxminarayan R, Malani A. Extending the cure: policy responses to the growing threat of antibiotic resistance: Earthscan; 2007.
- [11] Högberg LD, Heddini A, Cars O. The global need for effective antibiotics: challenges and recent advances. *Trends Pharmacol Sci* 2010;31:509-15.
- [12] Spellberg B, Powers JH, Brass EP, Miller LG, Edwards Jr JE. Trends in antimicrobial drug development: implications for the future. *Arch Clin Infect Dis* 2004;38:1279-86.
- [13] Fischbach MA, Walsh CT. Antibiotics for emerging pathogens. *Science* 2009;325:1089-93.
- [14] Cohen ML. Epidemiology of drug resistance: implications for a post—antimicrobial era. *Science* 1992;257:1050-5.
- [15] Livermore D. The need for new antibiotics. *Clin Microbiol Infect* 2004;10:1-9.
- [16] Zumla A, Grange JM. Multidrug-resistant tuberculosis—can the tide be turned? *Lancet Infect Dis* 2001;1:199-202.
- [17] Hancock RE, Sahl H-G. Antimicrobial and host-defense peptides as new anti-infective therapeutic strategies. *Nat Biotechnol* 2006;24:1551-7.
- [18] Zasloff M. Antimicrobial peptides of multicellular organisms. *Nature* 2002;415:389-95.
- [19] Conlon JM, Sonnevend A. Antimicrobial peptides in frog skin secretions. *Antimicrobial Peptides*: Springer; 2010. p. 3-14.
- [20] Steiner H, Hultmark D, Engström Å, Bennich H, Boman H. Sequence and specificity of two antibacterial proteins involved in insect immunity. *Nature* 1981;292:246.
- [21] Zasloff M. Magainins, a class of antimicrobial peptides from *Xenopus* skin: isolation, characterization of two active forms, and partial cDNA sequence of a precursor. *PNAS* 1987;84:5449-53.
- [22] Hancock RE, Diamond G. The role of cationic antimicrobial peptides in innate host defences. *Trends Microbiol* 2000;8:402-10.
- [23] Mangoni ML, Shai Y. Temporins and their synergism against Gram-negative bacteria and in lipopolysaccharide detoxification. *BBA-Biomembranes* 2009;1788:1610-9.
- [24] Dubos RJ. Studies on a bactericidal agent extracted from a soil bacillus: I. Preparation of the agent. Its activity in vitro. *J Exp Med* 1939;70:1.
- [25] Steiner H, Hultmark D, Engström Å, Bennich H, Boman HG. Sequence and specificity of two antibacterial proteins involved in insect immunity. *Nature* 1981;292:246.
- [26] Parisien A, Allain B, Zhang J, Mandeville R, Lan C. Novel alternatives to antibiotics: bacteriophages, bacterial cell wall hydrolases, and antimicrobial peptides. *J Appl Microbiol* 2008;104:1-13.

- [27] Klotman ME, Chang TL. Defensins in innate antiviral immunity. *Nat Rev Immunol* 2006;6:447.
- [28] Hoskin DW, Ramamoorthy A. Studies on anticancer activities of antimicrobial peptides. *BBA-Biomembranes* 2008;1778:357-75.
- [29] Ebbensgaard A, Mordhorst H, Overgaard MT, Nielsen CG, Aarestrup FM, Hansen EB. Comparative evaluation of the antimicrobial activity of different antimicrobial peptides against a range of pathogenic bacteria. *PLoS One* 2015;10:e0144611.
- [30] Lohner K. Development of novel antimicrobial agents: emerging strategies: Horizon Scientific Press; 2001.
- [31] Lohner K. The role of membrane lipid composition in cell targeting and their mechanism of action. *Development of Novel Antimicrobial Agents: Emerging Strategies*, Horizon Scientific Press, Wymondham, Norfolk, UK 2001:149-65.
- [32] Brogden KA, Ackermann M, Huttner KM. Small, anionic, and charge-neutralizing propeptide fragments of zymogens are antimicrobial. *Antimicrob Agents Chemother* 1997;41:1615-7.
- [33] Lai R, Liu H, Lee WH, Zhang Y. An anionic antimicrobial peptide from toad *Bombina maxima*. *Biochem Biophys Res Commun* 2002;295:796-9.
- [34] Steffen H, Rieg S, Wiedemann I, Kalbacher H, Deeg M, Sahl H-G, et al. Naturally processed dermcidin-derived peptides do not permeabilize bacterial membranes and kill microorganisms irrespective of their charge. *Antimicrob Agents Chemother* 2006;50:2608-20.
- [35] Laverty G, Gorman SP, Gilmore BF. The potential of antimicrobial peptides as biocides. *Int J Mol Sci* 2011;12:6566-96.
- [36] Harris F, Dennison SR, Phoenix DA. Anionic antimicrobial peptides from eukaryotic organisms. *Curr Protein Pept Sc* 2009;10:585-606.
- [37] Powers J-PS, Hancock RE. The relationship between peptide structure and antibacterial activity. *Peptides* 2003;24:1681-91.
- [38] Sato H, Feix JB. Peptide-membrane interactions and mechanisms of membrane destruction by amphipathic α -helical antimicrobial peptides. *BBA-Biomembranes* 2006;1758:1245-56.
- [39] Gazit E, Miller IR, Biggin PC, Sansom MS, Shai Y. Structure and orientation of the mammalian antibacterial peptide cecropin P1 within phospholipid membranes. *J Mol Biol* 1996;258:860-70.
- [40] Shai Y. Mode of action of membrane active antimicrobial peptides. *J Pept Sci* 2002;66:236-48.
- [41] Steiner H, Andreu D, Merrifield RB. Binding and action of cecropin and cecropin analogues: antibacterial peptides from insects. *BBA-Biomembranes* 1988;939:260-6.
- [42] Huang HW. Action of antimicrobial peptides: two-state model. *Biochemistry* 2000;39:8347-52.
- [43] Matsuzaki K, Sugishita K-i, Ishibe N, Ueha M, Nakata S, Miyajima K, et al. Relationship of membrane curvature to the formation of pores by magainin 2. *Biochemistry* 1998;37:11856-63.
- [44] Ludtke SJ, He K, Heller WT, Harroun TA, Yang L, Huang HW. Membrane pores induced by magainin. *Biochemistry* 1996;35:13723-8.
- [45] Yang L, Harroun TA, Weiss TM, Ding L, Huang HW. Barrel-stave model or toroidal model? A case study on melittin pores. *Biophys J* 2001;81:1475-85.
- [46] Huang Y, Huang J, Chen Y. Alpha-helical cationic antimicrobial peptides: relationships of structure and function. *Protein Cell* 2010;1:143-52.
- [47] Fuertes G, Giménez D, Esteban-Martín S, Sánchez-Munoz OL, Salgado J. A lipocentric view of peptide-induced pores. *Eur Biophys J* 2011;40:399-415.
- [48] Cooper GM, Hausman RE. *The cell: Molecular approach*: Medicinska naklada; 2004.
- [49] Boal D, Boal DH. *Mechanics of the Cell*: Cambridge University Press; 2012.
- [50] Zwolinski BJ, Eyring H, Reese CE. Diffusion and Membrane Permeability. *J Phys Chem* 1949;53:1426-53.
- [51] Bangham AD, Hill MW, Miller N. Preparation and use of liposomes as models of biological membranes. *Methods Mem Biol*: Springer; 1974. p. 1-68.
- [52] Bagatolli LA, Ipsen JH, Simonsen AC, Mouritsen OG. An outlook on organization of lipids in membranes: searching for a realistic connection with the organization of biological membranes. *Prog Lipid Res* 2010;49:378-89.

- [53] Singer SJ, Nicolson GL. The fluid mosaic model of the structure of cell membranes. *Science* 1972;175:720-31.
- [54] Vellai T, Vida G. The origin of eukaryotes: the difference between prokaryotic and eukaryotic cells. *P Roy Soc B-Biol Sc* 1999;266:1571-7.
- [55] Kaiser CA, Krieger M, Lodish H, Berk A. *Molecular cell biology*: WH Freeman; 2007.
- [56] Brogden KA. Antimicrobial peptides: pore formers or metabolic inhibitors in bacteria? *Nat Rev Microbiol* 2005;3:238-50.
- [57] Higgins CF. ABC transporters: from microorganisms to man. *Annu Rev Cell Biol* 1992;8:67-113.
- [58] Kabelka I, Vacha R. Optimal conditions for opening of membrane pore by amphiphilic peptides. *J Chem Phys* 2015;143:243115.
- [59] Encyclopedia Britannica I. molecular view of the cell membrane.
- [60] Glukhov E, Stark M, Burrows LL, Deber CM. Basis for selectivity of cationic antimicrobial peptides for bacterial versus mammalian membranes. *J Biol Chem* 2005;280:33960-7.
- [61] Mouritsen OG, Zuckermann MJ. What's so special about cholesterol? *Lipids* 2004;39:1101-13.
- [62] Raffy S, Teissie J. Control of lipid membrane stability by cholesterol content. *Biophys J* 1999;76:2072-80.
- [63] Yeaman MR, Yount NY. Mechanisms of antimicrobial peptide action and resistance. *Pharmacol Rev* 2003;55:27-55.
- [64] Shai Y. Mechanism of the binding, insertion and destabilization of phospholipid bilayer membranes by α -helical antimicrobial and cell non-selective membrane-lytic peptides. *BBA-Biomembranes* 1999;1462:55-70.
- [65] Brender JR, McHenry AJ, Ramamoorthy A. Does cholesterol play a role in the bacterial selectivity of antimicrobial peptides? *Front Immunol* 2012;3:195.
- [66] Cavalier-Smith T. The origin of eukaryote and archaebacterial cells. *Ann N Y Acad Sci* 1987;503:17-54.
- [67] Ratledge C, Wilkinson SG. *Microbial lipids*: Academic Pr; 1988.
- [68] Merck. The basic structure of bacterial peptidoglycan and the cell wall structures of Gram-positive and Gram-negative bacteria. *Peptidoglycans*;2nd Edition.
- [69] Ouardien S, Brul S, Zaat SA. Antimicrobial activity of cationic antimicrobial peptides against gram-positives: current progress made in understanding the mode of action and the response of bacteria. *Front Cell Dev Biol* 2016;4:111.
- [70] Murray PR, Rosenthal KS, Pfaller MA. *Medical microbiology*: Elsevier Health Sciences; 2015.
- [71] Strömstedt AA, Ringstad L, Schmidtchen A, Malmsten M. Interaction between amphiphilic peptides and phospholipid membranes. *Curr Opin Colloid Interface Sci* 2010;15:467-78.
- [72] Shen Y-x, Saboe PO, Sines IT, Erbakan M, Kumar M. Biomimetic membranes: A review. *J Membr Sci* 2014;454:359-81.
- [73] Vermuri S, Rhodes C. Preparation and characterization of liposomes as therapeutic delivery system: a review. *Pharm acta Helv* 1995;10:95-111.
- [74] Tresset G. The multiple faces of self-assembled lipidic systems. *PMC Biophysics* 2009;2:3.
- [75] Griffith O, Dehlinger P, Van S. Shape of the hydrophobic barrier of phospholipid bilayers (evidence for water penetration in biological membranes). *J Membr Biol* 1974;15:159-92.
- [76] Lindsay M. Biga SD, Amy Harwell, Robin Hopkins, Joel Kaufmann, Mike LeMaster, Philip Matern, Katie Morrison-Graham, Devon Quick & Jon Runyeon. *Anatomy & Physiology*. Oregon State University.
- [77] Yeagle PL. Phospholipid headgroup behavior in biological assemblies. *Acc Chem Res* 1978;11:321-7.
- [78] Yamada T, Uchikata T, Sakamoto S, Yokoi Y, Fukusaki E, Bamba T. Development of a lipid profiling system using reverse-phase liquid chromatography coupled to high-resolution mass spectrometry with rapid polarity switching and an automated lipid identification software. *J Chromatogr A* 2013;1292:211-8.
- [79] Krishnamurthy S, Stefanov M, Mineva T, Bégu S, Devoisselle J-M, Goursot A, et al. Density functional theory-based conformational analysis of a phospholipid molecule (dimyristoyl phosphatidylcholine). 2008;112:13433-42.

- [80] Tanford C. The hydrophobic effect: formation of micelles and biological membranes 2d ed: J. Wiley.; 1980.
- [81] Wei JH, Yin X, Welander PV. Sterol Synthesis in Diverse Bacteria. 2016;7.
- [82] Qiao X, Zhang X, Tian Y, Meng Y. Progresses on the theory and application of quartz crystal microbalance. *Appl Phys Rev* 2016;3:031106.
- [83] Incardona JP, Eaton S. Cholesterol in signal transduction. *Curr Opin Cell Biol* 2000;12:193-203.
- [84] Finegold LX. Cholesterol in membrane models: CRC Press; 1992.
- [85] Ikonen E. Cellular cholesterol trafficking and compartmentalization. *Nat Rev Mol Cell Biol* 2008;9:125.
- [86] Haines TH. Do sterols reduce proton and sodium leaks through lipid bilayers? *Prog Lipid Res* 2001;40:299-324.
- [87] Jain MK, Toussaint DG, Cordes E. Kinetics of water penetration into unsonicated liposomes effects ofn-alkanols and cholesterol. *J Membr Biol* 1973;14:1-16.
- [88] Simons K, Vaz WL. Model systems, lipid rafts, and cell membranes. *Annu Rev Biophys* 2004;33:269-95.
- [89] Radhakrishnan A, McConnell HM. Condensed complexes of cholesterol and phospholipids. *Biophys J* 1999;77:1507-17.
- [90] Chong PL. Evidence for regular distribution of sterols in liquid crystalline phosphatidylcholine bilayers. 1994;91:10069-73.
- [91] Somerharju P, Virtanen JA, Cheng KH, Hermansson M. The superlattice model of lateral organization of membranes and its implications on membrane lipid homeostasis. *BBA-Biomembranes* 2009;1788:12-23.
- [92] Huang J, Feigenson GW. A microscopic interaction model of maximum solubility of cholesterol in lipid bilayers. *Biophys J* 1999;76:2142-57.
- [93] Huang JI. Model membrane thermodynamics and lateral distribution of cholesterol: from experimental data to Monte Carlo simulation. *Method Enzymol* 2009;455:329-64.
- [94] Pata V, Dan N. Effect of membrane characteristics on phase separation and domain formation in cholesterol-lipid mixtures. *Biophys J* 2005;88:916-24.
- [95] Radhakrishnan A, McConnell HM. Chemical activity of cholesterol in membranes. *Biochemistry* 2000;39:8119-24.
- [96] Chong P. Evidence for regular distribution of sterols in liquid crystalline phosphatidylcholine bilayers. *PNAS* 1994;91:10069-73.
- [97] Parker A, Miles K, Cheng KH, Huang J. Lateral distribution of cholesterol in dioleoylphosphatidylcholine lipid bilayers: cholesterol-phospholipid interactions at high cholesterol limit. *Biophys J* 2004;86:1532-44.
- [98] Dai J, Alwarawrah M, Huang J. Instability of cholesterol clusters in lipid bilayers and the cholesterol's umbrella effect. *J Phys Chem B* 2009;114:840-8.
- [99] Goluszko P, Nowicki B. Membrane cholesterol: a crucial molecule affecting interactions of microbial pathogens with mammalian cells. *Infect Immun* 2005;73:7791-6.
- [100] Estep T, Mountcastle D, Biltonen R, Thompson T. Studies on the anomalous thermotropic behavior of aqueous dispersions of dipalmitoylphosphatidylcholine-cholesterol mixtures. *Biochemistry* 1978;17:1984-9.
- [101] Genz A, Holzwarth J, Tsong T. The influence of cholesterol on the main phase transition of unilamellar dipalmytoylphosphatidylcholine vesicles. A differential scanning calorimetry and iodine laser T-jump study. *Biophys J* 1986;50:1043-51.
- [102] Mabrey S, Mateo PL, Sturtevant JM. High-sensitivity scanning calorimetric study of mixtures of cholesterol with dimyristoyl- and dipalmitoylphosphatidylcholines. *Biochemistry* 1978;17:2464-8.
- [103] Vist MR, Davis JH. Phase equilibria of cholesterol/dipalmitoylphosphatidylcholine mixtures: deuterium nuclear magnetic resonance and differential scanning calorimetry. *Biochemistry* 1990;29:451-64.
- [104] Hasan IY, Mechler A. Cholesterol Rich Domains Identified in Unilamellar Supported Biomimetic Membranes via Nano-Viscosity Measurements. *Anal Chem* 2016;88:5037-41.

- [105] Samuel BU, Mohandas N, Harrison T, McManus H, Rosse W, Reid M, et al. The role of cholesterol and glycosylphosphatidylinositol-anchored proteins of erythrocyte rafts in regulating raft protein content and malarial infection. *J Biol Chem* 2001;276:29319-29.
- [106] Arsov Z, Nemec M, Schara M, Johansson H, Langel Ü, Zorko M. Cholesterol prevents interaction of the cell-penetrating peptide transportan with model lipid membranes. *J Pept Sci* 2008;14:1303-8.
- [107] Raghuraman H, Chattopadhyay A. Cholesterol inhibits the lytic activity of melittin in erythrocytes. *Chem Phys Lipids* 2005;134:183-9.
- [108] Matsuzaki K, Murase O, Fujii N, Miyajima K. Translocation of a channel-forming antimicrobial peptide, magainin 2, across lipid bilayers by forming a pore. *Biochemistry* 1995;34:6521-6.
- [109] Matsuzaki K, Sugishita K, Fujii N, Miyajima K. Molecular basis for membrane selectivity of an antimicrobial peptide, magainin 2. *Biochemistry* 1995;34:3423-9.
- [110] Ramamoorthy A, Lee D-K, Narasimhaswamy T, Nanga RP. Cholesterol reduces pardaxin's dynamics—a barrel-stave mechanism of membrane disruption investigated by solid-state NMR. *BBA-Biomembranes* 2010;1798:223-7.
- [111] Tytler EM, Anantharamaiah G, Walker DE, Mishra VK, Palgunachari M, Segrest JP. Molecular basis for prokaryotic specificity of magainin-induced lysis. *Biochemistry* 1995;34:4393-401.
- [112] Verly RM, Rodrigues MA, Daghestanli KRP, Denadai AML, Cuccovia IM, Bloch Jr C, et al. Effect of cholesterol on the interaction of the amphibian antimicrobial peptide DD K with liposomes. *Peptides* 2008;29:15-24.
- [113] Feigin AM, Teeter JH, Brand JG. The influence of sterols on the sensitivity of lipid bilayers to melittin. *Biochem Biophys Res Commun* 1995;211:312-7.
- [114] Allende D, Simon S, McIntosh TJ. Melittin-induced bilayer leakage depends on lipid material properties: evidence for toroidal pores. *Biophys J* 2005;88:1828-37.
- [115] Henzler Wildman KA, Lee D-K, Ramamoorthy A. Mechanism of lipid bilayer disruption by the human antimicrobial peptide, LL-37. *Biochemistry* 2003;42:6545-58.
- [116] Wu G, Wu H, Fan X, Zhao R, Li X, Wang S, et al. Selective toxicity of antimicrobial peptide S-thanatin on bacteria. *Peptides* 2010;31:1669-73.
- [117] Dols-Perez A, Fumagalli L, Simonsen AC, Gomila G. Ultrathin spin-coated dioleoylphosphatidylcholine lipid layers in dry conditions: a combined atomic force microscopy and nanomechanical study. *Langmuir* 2011;27:13165-72.
- [118] Chalmeau J, Salomé L, Thibault C, Severac C, Vieu CJMe. Elaboration of micro-domains of supported bilayer membranes using micro-contact printing. *Microelectron Eng* 2007;84:1754-7.
- [119] Hohner AO, David MPC, Rädler JO. Controlled solvent-exchange deposition of phospholipid membranes onto solid surfaces. *Biointerphases* 2010;5:1-8.
- [120] Nye JA, Groves JT. Kinetic control of histidine-tagged protein surface density on supported lipid bilayers. *Langmuir* 2008;24:4145-9.
- [121] Roth Y, Opatowski E, Lichtenberg D, Kozlov M. Phase behavior of dilute aqueous solutions of lipid-surfactant mixtures: Effects of finite size of micelles. *Langmuir* 2000;16:2052-61.
- [122] Dunphy DR, Sheth PH, Garcia FL, Brinker CJ. Enlarged pore size in mesoporous silica films templated by pluronic F127: Use of poloxamer mixtures and increased template/SiO₂ ratios in materials synthesized by evaporation-induced self-assembly. *Chem Mater* 2014;27:75-84.
- [123] Mager MD, Melosh NA. Lipid bilayer deposition and patterning via air bubble collapse. *Langmuir* 2007;23:9369-77.
- [124] Sekula-Neuner S, Maier J, Oppong E, Cato AC, Hirtz M, Fuchs HJS. Allergen Arrays for Antibody Screening and Immune Cell Activation Profiling Generated by Parallel Lipid Dip-Pen Nanolithography. 2012;8:585-91.
- [125] Kalb E, Frey S, Tamm LK. Formation of supported planar bilayers by fusion of vesicles to supported phospholipid monolayers. *BBA -Biomembranes* 1992;1103:307-16.
- [126] Leonenko Z, Carnini A, Cramb D. Supported planar bilayer formation by vesicle fusion: the interaction of phospholipid vesicles with surfaces and the effect of gramicidin on bilayer properties using atomic force microscopy. *BBA-Biomembranes* 2000;1509:131-47.

- [127] Tanaka M, Sackmann E. Polymer-supported membranes as models of the cell surface. *Nature* 2005;437:656.
- [128] Dorrer C, Rühe Jr. Mimicking the Stenocara Beetle • Dewetting of Drops from a Patterned Superhydrophobic Surface. *Langmuir* 2008;24:6154-8.
- [129] Sackmann E, Tanaka M. Supported membranes on soft polymer cushions: fabrication, characterization and applications. *Trends Biotechnol* 2000;18:58-64.
- [130] Basit H, Van der Heyden A, Gondran C, Nysten B, Dumy P, Labbé P. Tethered bilayer lipid membranes on mixed self-assembled monolayers of a novel anchoring thiol: impact of the anchoring thiol density on bilayer formation. *Langmuir* 2011;27:14317-28.
- [131] Wagner ML, Tamm LK. Tethered polymer-supported planar lipid bilayers for reconstitution of integral membrane proteins: silane-polyethyleneglycol-lipid as a cushion and covalent linker. *Biophys J* 2000;79:1400-14.
- [132] Krishna G, Schulte J, Cornell BA, Pace RJ, Osman PD. Tethered bilayer membranes containing ionic reservoirs: selectivity and conductance. *Langmuir* 2003;19:2294-305.
- [133] Song H, Sinner E-K, Knoll W. Peptid-tethered bilayer lipid membranes and their interaction with Amyloid β -peptide. *Biointerphases* 2007;2:151-8.
- [134] Naumann R, Baumgart T, Gräber P, Jonczyk A, Offenhäusser A, Knoll W. Proton transport through a peptide-tethered bilayer lipid membrane by the H⁺-ATP synthase from chloroplasts measured by impedance spectroscopy. *Biosens Bioelectron* 2002;17:25-34.
- [135] Naumann R, Jonczyk A, Kopp R, van Esch J, Ringsdorf H, Knoll W, et al. Incorporation of membrane proteins in solid-supported lipid layers. 1995;34:2056-8.
- [136] Rebaud S, Maniti O, Girard-Egrot AP. Tethered bilayer lipid membranes (tBLMs): interest and applications for biological membrane investigations. *Biochimie* 2014;107:135-42.
- [137] Hasan IY, Mechler A. Viscoelastic changes measured in partially suspended single bilayer membranes. *Soft Matter* 2015;11:5571-9.
- [138] Shahmiri M, Enciso M, Mechler A. Controls and constraints of the membrane disrupting action of Aurein 1.2. *Sci Rep* 2015;5:16378.
- [139] Hasan IY, Mechler A. Analytical approaches to study domain formation in biomimetic membranes. *Analyst* 2017;142:3062-78.
- [140] El Kirat K, Morandat S, Dufrêne YF. Nanoscale analysis of supported lipid bilayers using atomic force microscopy. *BBA -Biomembranes* 2010;1798:750-65.
- [141] Giocondi M-C, Milhiet PE, Dosset P, Le Grimmellec C. Use of cyclodextrin for AFM monitoring of model raft formation. *Biophys J* 2004;86:861-9.
- [142] Loose M, Schwille P. Biomimetic membrane systems to study cellular organization. *J Struct Biol* 2009;168:143-51.
- [143] Zasadzinski JA, Viswanathan R, Madsen L, Garnaes J, Schwartz D. Langmuir-blodgett films. *Science* 1994;263:1726-33.
- [144] Hardy GJ, Nayak R, Zauscher S, science i. Model cell membranes: Techniques to form complex biomimetic supported lipid bilayers via vesicle fusion. *Curr Opin Colloid Interface Sci* 2013;18:448-58.
- [145] Carton I, Brisson AR, Richter RP. Label-free detection of clustering of membrane-bound proteins. *Anal Chem* 2010;82:9275-81.
- [146] Watts TH, Brian AA, Kappler JW, Marrack P, McConnell HM. Antigen presentation by supported planar membranes containing affinity-purified I-Ad. *PNAS* 1984;81:7564-8.
- [147] Watts TH, Gaub HE, McConnell HM. T-cell-mediated association of peptide antigen and major histocompatibility complex protein detected by energy transfer in an evanescent wave-field. *Nature* 1986;320:179.
- [148] Hain N, Gallego M, Reviakine I. Unraveling supported lipid bilayer formation kinetics: osmotic effects. *Langmuir* 2013;29:2282-8.
- [149] Zhu T, Xu F, Yuan B, Ren C, Jiang Z, Ma YJC, et al. Effect of calcium cation on lipid vesicle deposition on silicon dioxide surface under various thermal conditions. *Colloid Surface B* 2012;89:228-33.

- [150] Mechler A, Praporski S, Piantavigna S, Heaton SM, Hall KN, Aguilar M-I, et al. Structure and homogeneity of pseudo-physiological phospholipid bilayers and their deposition characteristics on carboxylic acid terminated self-assembled monolayers. *Biomaterials* 2009;30:682-9.
- [151] Hasan IY, Mechler A. Formation of planar unilamellar phospholipid membranes on oxidized gold substrate. *Biointerphases* 2016;11:031017.
- [152] Olander D. General thermodynamics: CRC Press; 2007.
- [153] Oxtoby DW, Gillis HP, Butler LJ. Principles of modern chemistry: Cengage learning; 2015.
- [154] Baret JF. Phase transitions in two-dimensional amphiphilic systems. *Progress in Surface and Membrane Science: Elsevier*; 1981. p. 291-351.
- [155] Kinnunen PK. On the principles of functional ordering in biological membranes. *Chem Phys Lipids* 1991;57:375-99.
- [156] Noothalapati H, Iwasaki K, Yoshimoto C, Yoshikiyo K, Nishikawa T, Ando M, et al. Imaging phospholipid conformational disorder and packing in giant multilamellar liposome by confocal Raman microspectroscopy. *Spectrochim Acta A* 2017;187:186-90.
- [157] Engelman DM. Lipid bilayer structure in the membrane of *Mycoplasma laidlawii*. *J Mol Biol* 1971;58:153-65.
- [158] Oh E, Jackman JA, Yorulmaz S, Zhdanov VP, Lee H, Cho N-J. Contribution of temperature to deformation of adsorbed vesicles studied by nanoplasmonic biosensing. *Langmuir* 2015;31:771-81.
- [159] Caffrey M, Hogan J. LIPIDAT: A database of lipid phase transition temperatures and enthalpy changes. DMPC data subset analysis. *Chem Phys Lipids* 1992;61:1-109.
- [160] Ruocco MJ, Shipley GG. Characterization of the sub-transition of hydrated dipalmitoylphosphatidylcholine bilayers. Kinetic, hydration and structural study. *BBA-Biomembranes* 1982;691:309-20.
- [161] Lewis RN, Mak N, McElhaney RN. A differential scanning calorimetric study of the thermotropic phase behavior of model membranes composed of phosphatidylcholines containing linear saturated fatty acyl chains. *Biochemistry* 1987;26:6118-26.
- [162] Huang C-h. Empirical estimation of the gel to liquid-crystalline phase transition temperatures for fully hydrated saturated phosphatidylcholines. *Biochemistry* 1991;30:26-30.
- [163] Tardieu A, Luzzati V, Reman F. Structure and polymorphism of the hydrocarbon chains of lipids: a study of lecithin-water phases. *J Mol Biol* 1973;75:711-33.
- [164] Chapman D. Biological membranes; physical fact and function. 1968.
- [165] Ladbroke B, Williams RM, Chapman D. Studies on lecithin-cholesterol-water interactions by differential scanning calorimetry and X-ray diffraction. *BBA-Biomembranes* 1968;150:333-40.
- [166] Chapman D, Williams RM, Ladbroke BD. Physical studies of phospholipids. VI. Thermotropic and lyotropic mesomorphism of some 1, 2-diacyl-phosphatidylcholines (lecithins). *Chem Phys Lipids* 1967;1:445-75.
- [167] Kranenburg M, Smit B. Phase behavior of model lipid bilayers. *J Phys Chem B* 2005;109:6553-63.
- [168] Koynova R, Caffrey M. Phases and phase transitions of the phosphatidylcholines. *Biochim Biophys Acta, Rev Biomembr* 1998;1376:91-145.
- [169] Lewis R, McElhaney RN. The mesomorphic phase behavior of lipid bilayers. *The Structure of Biological Membranes* 1992;2.
- [170] Akbarzadeh A, Rezaei-Sadabady R, Davaran S, Joo SW, Zarghami N, Hanifehpour Y, et al. Liposome: classification, preparation, and applications. *Nanoscale Res Lett* 2013;8:102.
- [171] Ulrich AS, Watts A. Molecular response of the lipid headgroup to bilayer hydration monitored by ²H-NMR. *Biophys J* 1994;66:1441-9.
- [172] phase M. Representation of the different phases one can observe in a lipid membrane: crystal phase (Lc), gel phase (LB), and liquid phase (La). Certain types of lipid can be found in the ripple phase (PB), which is a transitional phase between the gel and liquid phase.
- [173] Yeagle PL, Frye J. Effects of unsaturation on ²H-NMR quadrupole splittings and ¹³C-NMR relaxation in phospholipid bilayers. *BBA-Biomembranes* 1987;899:137-42.

- [174] Wang Z, Wang G. APD: the antimicrobial peptide database. *Nucleic Acids Res* 2004;32:D590-D2.
- [175] Marion D, Zasloff M, Bax A. A two-dimensional NMR study of the antimicrobial peptide magainin 2. *FEBS Lett* 1988;227:21-6.
- [176] Hristova K, Dempsey CE, White SH. Structure, location, and lipid perturbations of melittin at the membrane interface. *Biophys J* 2001;80:801-11.
- [177] Hwang PM, Vogel HJ. Structure-function relationships of antimicrobial peptides. *Biochem Cell Biol* 1998;76:235-46.
- [178] Rydberg HA, Kunze A, Carlsson N, Altgarde N, Svedhem S, Norden B. Peptide-membrane interactions of arginine-tryptophan peptides probed using quartz crystal microbalance with dissipation monitoring. *Eur Biophys J* 2014;43:241-53.
- [179] Nguyen LT, Haney EF, Vogel HJ. The expanding scope of antimicrobial peptide structures and their modes of action. *Trends Biotechnol* 2011;29:464-72.
- [180] Bhattacharjya S, Ramamoorthy A. Multifunctional host defense peptides: functional and mechanistic insights from NMR structures of potent antimicrobial peptides. *FEBS J* 2009;276:6465-73.
- [181] Vouille V, Amiche M, Nicolas P. Structure of genes for dermaseptins B, antimicrobial peptides from frog skin: Exon 1-encoded prepropeptide is conserved in genes for peptides of highly different structures and activities. *FEBS Lett* 1997;414:27-32.
- [182] Pukala TL, Brinkworth CS, Carver JA, Bowie JH. Investigating the importance of the flexible hinge in caerin 1.1: solution structures and activity of two synthetically modified caerin peptides. *Biochemistry* 2004;43:937-44.
- [183] Kilosanidze GT, Kutsenko AS, Esipova NG, Tumanyan VG. Analysis of forces that determine helix formation in α -proteins. *Protein Sci* 2004;13:351-7.
- [184] Smith R, Separovic F, Milne T, Whittaker A, Bennett F, Cornell B, et al. Structure and orientation of the pore-forming peptide melittin, in lipid bilayers. *J Mol Biol* 1994;241:456-66.
- [185] Holt A, Killian JA. Orientation and dynamics of transmembrane peptides: the power of simple models. *Eur Biophys J* 2010;39:609-21.
- [186] Ramadurai S, Holt A, Schäfer LV, Krasnikov VV, Rijkers DT, Marrink SJ, et al. Influence of hydrophobic mismatch and amino acid composition on the lateral diffusion of transmembrane peptides. *Biophys J* 2010;99:1447-54.
- [187] Shahmiri M, Enciso M, Mechler A. Controls and constraints of the membrane disrupting action of Aurein 1.2. *Sci Rep* 2015;5:16378.
- [188] Haney EF, Nazmi K, Lau F, Bolscher JG, Vogel HJ. Novel lactoferrampin antimicrobial peptides derived from human lactoferrin. *Biochimie* 2009;91:141-54.
- [189] Ciornei CD, Sigurdardóttir T, Schmidtchen A, Bodelsson M. Antimicrobial and chemoattractant activity, lipopolysaccharide neutralization, cytotoxicity, and inhibition by serum of analogs of human cathelicidin LL-37. *Antimicrob Agents Chemother* 2005;49:2845-50.
- [190] Malmsten M. Antimicrobial peptides. *Upsala J Med Sci* 2014;119:199-204.
- [191] Ringstad L, Schmidtchen A, Malmsten M. Effect of peptide length on the interaction between consensus peptides and DOPC/DOPA bilayers. *Langmuir* 2006;22:5042-50.
- [192] Deslouches B, Phadke SM, Lazarevic V, Cascio M, Islam K, Montelaro RC, et al. De novo generation of cationic antimicrobial peptides: influence of length and tryptophan substitution on antimicrobial activity. *Antimicrob Agents Chemother* 2005;49:316-22.
- [193] Park Y, Park SC, Park HK, Shin SY, Kim Y, Hahm KS. Structure-activity relationship of HP (2–20) analog peptide: Enhanced antimicrobial activity by N-terminal random coil region deletion. *J Pept Sci* 2007;88:199-207.
- [194] Bernal J. William Thomas Astbury, 1898-1961. The Royal Society; 1963.
- [195] Gellman SH. Foldamers: a manifesto. *Acc Chem Res* 1998;31:173-80.
- [196] Ganz T. Defensins: antimicrobial peptides of innate immunity. *Nat Rev Immunol* 2003;3:710-20.

- [197] Kawano K, Yoneya T, Miyata T, Yoshikawa K, Tokunaga F, Terada Y, et al. Antimicrobial peptide, tachyplesin I, isolated from hemocytes of the horseshoe crab (*Tachyplesus tridentatus*). NMR determination of the beta-sheet structure. *J Biol Chem* 1990;265:15365-7.
- [198] Hwang PM, Zhou N, Shan X, Arrowsmith CH, Vogel HJ. Three-dimensional solution structure of lactoferricin B, an antimicrobial peptide derived from bovine lactoferrin. *Biochemistry* 1998;37:4288-98.
- [199] Chan DI, Prenner EJ, Vogel HJ. Tryptophan-and arginine-rich antimicrobial peptides: structures and mechanisms of action. *BBA-Biomembranes* 2006;1758:1184-202.
- [200] Falla TJ, Karunaratne DN, Hancock RE. Mode of action of the antimicrobial peptide indolicidin. *J Biol Chem* 1996;271:19298-303.
- [201] Selsted ME, Novotny MJ, Morris WL, Tang Y-Q, Smith W, Cullor JS. Indolicidin, a novel bactericidal tridecapeptide amide from neutrophils. *J Biol Chem* 1992;267:4292-5.
- [202] Rozek A, Friedrich CL, Hancock RE. Structure of the bovine antimicrobial peptide indolicidin bound to dodecylphosphocholine and sodium dodecyl sulfate micelles. *Biochemistry* 2000;39:15765-74.
- [203] Rokitskaya TI, Kolodkin NI, Kotova EA, Antonenko YN. Indolicidin action on membrane permeability: carrier mechanism versus pore formation. *BBA-Biomembranes* 2011;1808:91-7.
- [204] Yeaman MR, Yount NY. Mechanisms of antimicrobial peptide action and resistance. *Pharmacological reviews* 2003;55:27-55.
- [205] Ebenhan T, Gheysens O, Kruger HG, Zeevaert JR, Sathekge MM. Antimicrobial peptides: their role as infection-selective tracers for molecular imaging. *Biomed Res Int* 2014;2014.
- [206] Matsuzaki K. Control of cell selectivity of antimicrobial peptides. *BBA-Biomembranes* 2009;1788:1687-92.
- [207] Turner J, Cho Y, Dinh N-N, Waring AJ, Lehrer RI. Activities of LL-37, a cathelin-associated antimicrobial peptide of human neutrophils. *Antimicrob Agents Chemother* 1998;42:2206-14.
- [208] Raymond P, Narayanan A, Pradet A. Evidence for the presence of 3', 5'-cyclic AMP in plant tissues. *Biochem Biophys Res Commun* 1973;53:1115-21.
- [209] Koppelman C-M, Den Blaauwen T, Duursma MC, Heeren RM, Nanninga N. *Escherichia coli* minicell membranes are enriched in cardiolipin. *J Bacteriol* 2001;183:6144-7.
- [210] Matsuzaki K. Why and how are peptide-lipid interactions utilized for self-defense? Magainins and tachyplesins as archetypes. *BBA-Biomembranes* 1999;1462:1-10.
- [211] Van Meer G, Voelker DR, Feigenson GW. Membrane lipids: where they are and how they behave. *Nat Rev Mol Cell Biol* 2008;9:112.
- [212] Marín-Medina N, Ramírez DA, Trier S, Leidy C. Mechanical properties that influence antimicrobial peptide activity in lipid membranes. *Appl Microbiol Biot* 2016;100:10251-63.
- [213] Zhang L, Rozek A, Hancock RE. Interaction of cationic antimicrobial peptides with model membranes. *J Biol Chem* 2001;276:35714-22.
- [214] Bessalle R, Haas H, Gorla A, Shalit I, Fridkin M. Augmentation of the antibacterial activity of magainin by positive-charge chain extension. *Antimicrob Agents Chemother* 1992;36:313-7.
- [215] Dathe M, Wieprecht T, Nikolenko H, Handel L, Maloy WL, MacDonald DL, et al. Hydrophobicity, hydrophobic moment and angle subtended by charged residues modulate antibacterial and haemolytic activity of amphipathic helical peptides. *FEBS Lett* 1997;403:208-12.
- [216] Dathe M, Nikolenko H, Meyer J, Beyersmann M, Bienert M. Optimization of the antimicrobial activity of magainin peptides by modification of charge. *FEBS Lett* 2001;501:146-50.
- [217] Taheri-Araghi S, Ha B-Y. Physical basis for membrane-charge selectivity of cationic antimicrobial peptides. *Phys Rev Lett* 2007;98:168101.
- [218] Oren Z, Shai Y. A class of highly potent antibacterial peptides derived from pardaxin, a pore-forming peptide isolated from Moses sole fish *Pardachirus marmoratus*. *Eur J Biochem* 1996;237:303-10.
- [219] Bahar AA, Ren D. Antimicrobial peptides. *Pharmaceuticals* 2013;6:1543-75.
- [220] Lee DG, Kim HN, Park Y, Kim HK, Choi BH, Choi C-H, et al. Design of novel analogue peptides with potent antibiotic activity based on the antimicrobial peptide, HP (2–20), derived from N-terminus of *Helicobacter pylori* ribosomal protein L1. *BBA-Proteins Proteom* 2002;1598:185-94.

- [221] Tam JP, Wu C, Yang JL. Membranolytic selectivity of cystine-stabilized cyclic protegrins. *Eur J Biochem* 2000;267:3289-300.
- [222] Unger T, Oren Z, Shai Y. The effect of cyclization of magainin 2 and melittin analogues on structure, function, and model membrane interactions: implication to their mode of action. *Biochemistry* 2001;40:6388-97.
- [223] Saberwal G, Nagaraj R. Cell-lytic and antibacterial peptides that act by perturbing the barrier function of membranes: facets of their conformational features, structure-function correlations and membrane-perturbing abilities. *BBA-Rev Biomembranes* 1994;1197:109-31.
- [224] Chen Y, Guarnieri MT, Vasil AI, Vasil ML, Mant CT, Hodges RS. Role of peptide hydrophobicity in the mechanism of action of α -helical antimicrobial peptides. *Antimicrob Agents Chemother* 2007;51:1398-406.
- [225] Blondelle SE, Simpkins LR, Pérez-Payá E, Houghten RA. Influence of tryptophan residues on melittin's hemolytic activity. *BBA-Biomembranes* 1993;1202:331-6.
- [226] Blondelle SE, Houghten RA. Hemolytic and antimicrobial activities of the twenty-four individual omission analogs of melittin. *Biochemistry* 1991;30:4671-8.
- [227] Wieprecht T, Dathe M, Beyermann M, Krause E, Maloy WL, MacDonald DL, et al. Peptide hydrophobicity controls the activity and selectivity of magainin 2 amide in interaction with membranes. *Biochemistry* 1997;36:6124-32.
- [228] Avrahami D, Shai YJB. Conjugation of a magainin analogue with lipophilic acids controls hydrophobicity, solution assembly, and cell selectivity. *Biochemistry* 2002;41:2254-63.
- [229] Yin LM, Edwards MA, Li J, Yip CM, Deber CM. Roles of hydrophobicity and charge distribution of cationic antimicrobial peptides in peptide-membrane interactions. *J Biol Chem* 2012;287:7738-45.
- [230] TEwards IA, Elliott AG, Kavanagh AM, Zuegg J, Blaskovich MA, Cooper MA. Contribution of amphipathicity and hydrophobicity to the antimicrobial activity and cytotoxicity of β -hairpin peptides. *ACS Infect Dis* 2016;2:442-50.
- [231] Cun-Bao L, Bin S, Hong-Mei B, Jing T, Long-Zong Y, Yan-Bing M. Hydrophilic/hydrophobic characters of antimicrobial peptides derived from animals and their effects on multidrug resistant clinical isolates. *Zool Res* 2015;36:41.
- [232] Pathak N, Salas-Auvert R, Ruche G, Janna Mh, McCarthy D, Harrison RGJPS, Function,, et al. Comparison of the effects of hydrophobicity, amphiphilicity, and α -helicity on the activities of antimicrobial peptides. *Proteins* 1995;22:182-6.
- [233] Fernández-Vidal M, Jayasinghe S, Ladokhin AS, White SH. Folding amphipathic helices into membranes: amphiphilicity trumps hydrophobicity. *J Mol Biol* 2007;370:459-70.
- [234] Eisenberg D. Three-dimensional structure of membrane and surface proteins. *Annu Rev Biochem* 1984;53:595-623.
- [235] Chen Y, Mant CT, Farmer SW, Hancock RE, Vasil ML, Hodges RS. Rational design of α -helical antimicrobial peptides with enhanced activities and specificity/therapeutic index. *J Biol Chem* 2005;280:12316-29.
- [236] Bílikova K, Huang S-C, Lin I-P, Šimuth J, Peng C-C. Structure and antimicrobial activity relationship of royalisin, an antimicrobial peptide from royal jelly of *Apis mellifera*. *Peptides* 2015;68:190-6.
- [237] Talandashti R, Mahdiuni H, Jafari M, Mehrnejad F. Molecular Basis for Membrane Selectivity of Antimicrobial Peptide Pleurocidin in the Presence of Different Eukaryotic and Prokaryotic Model Membranes. *J Chem Inf Model* 2019.
- [238] Zhang Y-P, Lewis RN, Henry GD, Sykes BD, Hodges RS, McElhaney RN. Peptide models of helical hydrophobic transmembrane segments of membrane proteins. 1. Studies of the conformation, intralayer orientation, and amide hydrogen exchangeability of Ac-K2-(LA) 12-K2-amide. *Biochemistry* 1995;34:2348-61.
- [239] Hale JD, Hancock RE. Alternative mechanisms of action of cationic antimicrobial peptides on bacteria. *Expert Rev Anti-infect Ther* 2007;5:951-9.
- [240] Wimley WC. Describing the mechanism of antimicrobial peptide action with the interfacial activity model. *ACS Chem Biol* 2010;5:905-17.

- [241] Lee M-T, Chen F-Y, Huang HW. Energetics of pore formation induced by membrane active peptides. *Biochemistry* 2004;43:3590-9.
- [242] Baumann G, Mueller P. A molecular model of membrane excitability. *J Supramol Struct* 1974;2:538-57.
- [243] Boheim G. Statistical analysis of alamethicin channels in black lipid membranes. *J Membr Biol* 1974;19:277-303.
- [244] Oren Z, Shai Y. Mode of action of linear amphipathic α -helical antimicrobial peptides. *J Pept Sci* 1998;47:451-63.
- [245] Cafiso D. Alamethicin: a peptide model for voltage gating and protein-membrane interactions. *Annu Rev Biophys* 1994;23:141-65.
- [246] Boheim G, Hanke W, Jung G. Alamethicin pore formation: voltage-dependent flip-flop of α -helix dipoles. *Biophys Struct Mech* 1983;9:181-91.
- [247] Boheim G, Benz R. Charge-pulse relaxation studies with lipid bilayer membranes modified by alamethicin. *BBA-Biomembranes* 1978;507:262-70.
- [248] Mak D, Webb WW. Two classes of alamethicin transmembrane channels: molecular models from single-channel properties. *Biophys J* 1995;69:2323-36.
- [249] Zemel A, Fattal DR, Ben-Shaul A. Energetics and self-assembly of amphipathic peptide pores in lipid membranes. *Biophys J* 2003;84:2242-55.
- [250] Hall J. Toward a molecular understanding of excitability. Alamethicin in black lipid films. *Biophys J* 1975;15:934-9.
- [251] Sansom MS. The biophysics of peptide models of ion channels. *Prog Biophys Mol Biol* 1991;55:139-235.
- [252] Matsubara A, Asami K, Akagi A, Nishino N. Ion-channels of cyclic template-assembled alamethicins that emulate the pore structure predicted by the barrel-stave model. *Chem Comm* 1996:2069-70.
- [253] He K, Ludtke SJ, Huang HW, Worcester DL. Antimicrobial peptide pores in membranes detected by neutron in-plane scattering. *Biochemistry* 1995;34:15614-8.
- [254] Goode J. Antimicrobial Peptides, Ciba Symposium 186. Wiley, Chichester, UK; 1994.
- [255] Sengupta D, Leontiadou H, Mark AE, Marrink SJ. Toroidal pores formed by antimicrobial peptides show significant disorder. *Biochim Biophys Acta* 2008;1778:2308-17.
- [256] Hallock KJ, Lee D-K, Ramamoorthy A. MSI-78, an analogue of the magainin antimicrobial peptides, disrupts lipid bilayer structure via positive curvature strain. *Biophys J* 2003;84:3052-60.
- [257] Cruciani RA, Barker JL, Durell SR, Raghunathan G, Guy HR, Zasloff M, et al. Magainin 2, a natural antibiotic from frog skin, forms ion channels in lipid bilayer membranes. *Eur J Pharmacol* 1992;226:287-96.
- [258] Pouny Y, Rapaport D, Mor A, Nicolas P, Shai Y. Interaction of antimicrobial dermaseptin and its fluorescently labeled analogs with phospholipid membranes. *Biochemistry* 1992;31:12416-23.
- [259] Mani R, Buffy JJ, Waring AJ, Lehrer RI, Hong M. Solid-state NMR investigation of the selective disruption of lipid membranes by protegrin-1. *Biochemistry* 2004;43:13839-48.
- [260] Shai Y, Oren Z. From "carpet" mechanism to de-novo designed diastereomeric cell-selective antimicrobial peptides. *Peptides* 2001;22:1629-41.
- [261] Gazit E, Boman A, Boman HG, Shai Y. Interaction of the mammalian antibacterial peptide cecropin P1 with phospholipid vesicles. *Biochemistry* 1995;34:11479-88.
- [262] Mechler A, Praporski S, Atmuri K, Boland M, Separovic F, Martin LL. Specific and selective peptide-membrane interactions revealed using quartz crystal microbalance. *Biophys J* 2007;93:3907-16.
- [263] Ambroggio EE, Separovic F, Bowie JH, Fidelio GD, Bagatolli LA. Direct visualization of membrane leakage induced by the antibiotic peptides: maculatin, citropin, and aurein. *Biophys J* 2005;89:1874-81.
- [264] Ganz T, Lehrer RI. Defensins. *Pharmacol Therapeut* 1995;66:191-205.
- [265] Lehrer R, Barton A, Daher KA, Harwig S, Ganz T, Selsted ME. Interaction of human defensins with *Escherichia coli*. Mechanism of bactericidal activity. *J Clin Invest* 1989;84:553-61.

- [266] Dathe M, Wieprecht T. Structural features of helical antimicrobial peptides: their potential to modulate activity on model membranes and biological cells. *BBA-Biomembranes* 1999;1462:71-87.
- [267] Epand RM, Vogel HJ. Diversity of antimicrobial peptides and their mechanisms of action. *BBA-Biomembranes* 1999;1462:11-28.
- [268] Bals R. Epithelial antimicrobial peptides in host defense against infection. *Respir Res* 2000;1:5.
- [269] Zasloff MJ. Antimicrobial peptides of multicellular organisms. *Nature* 2002;415:389.
- [270] Brogden KA. Antimicrobial peptides: pore formers or metabolic inhibitors in bacteria? *Nature Reviews Microbiology* 2005;3:238.
- [271] Lu N, Yang K, Yuan B, Ma Y. Molecular response and cooperative behavior during the interactions of melittin with a membrane: dissipative quartz crystal microbalance experiments and simulations. *J Phys Chem B* 2012;116:9432-8.
- [272] Dufrêne YF. Atomic force microscopy, a powerful tool in microbiology. *J Bacteriol* 2002;184:5205-13.
- [273] Avci FG, Sariyar Akbulut B, Ozkirimli E. Membrane active peptides and their biophysical characterization. *Biomolecules* 2018;8:77.
- [274] Mechler A, Praporski S, Atmuri K, Boland M, Separovic F, Martin LLJBj. Specific and selective peptide-membrane interactions revealed using quartz crystal microbalance. 2007;93:3907-16.
- [275] Tamm LK, Tatulian SA. Infrared spectroscopy of proteins and peptides in lipid bilayers. *Q Rev Biophys* 1997;30:365-429.
- [276] Galdiero S, Falanga A, Cantisani M, Vitiello M, Morelli G, Galdiero M. Peptide-Lipid Interactions: Experiments and Applications. *Int J Mol Sci* 2013;14:18758-89.
- [277] Oravcova J, Bo B, Lindner W. Drug-protein binding studies new trends in analytical and experimental methodology. *J chromatogr B, Biomed sci appl* 1996;677:1-28.
- [278] Connors KA. Binding constants: the measurement of molecular complex stability: Wiley-Intersci; 1987.
- [279] Otagiri M, Masuda K, Imai T, Imamura Y, Yamasaki M. Binding of pirprofen to human serum albumin studied by dialysis and spectroscopy techniques. *Biochem Pharmacol* 1989;38:1-7.
- [280] Santos N, Castanho M. Fluorescence spectroscopy methodologies on the study of proteins and peptides. *Trends Appl Spectrosc* 2002;4:113-25.
- [281] Separovic F, Naito A. *Advances in Biological Solid-State NMR: Proteins and Membrane-Active Peptides*: R. Soc. Chem.; 2014.
- [282] Shenkarev ZO, Balandin SV, Trunov KI, Paramonov AS, Sukhanov SV, Barsukov LI, et al. Molecular mechanism of action of β -hairpin antimicrobial peptide arenicin: oligomeric structure in dodecylphosphocholine micelles and pore formation in planar lipid bilayers. *Biochemistry* 2011;50:6255-65.
- [283] Usachev KS, Efimov SV, Kolosova O, Filippov A, Klockhov VV. High-resolution NMR structure of the antimicrobial peptide protegrin-2 in the presence of DPC micelles. *J Biomol NMR* 2015;61:227-34.
- [284] Chignell CF. Recent advances in methodology: Spectroscopic techniques. *Ann N Y Acad Sci* 1973;226:44-59.
- [285] Chignell CF. Optical studies of drug-protein complexes: II. Interaction of phenylbutazone and its analogues with human serum albumin. *Mol Pharmacol* 1969;5:244-52.
- [286] Chignell CF. Optical Studies of Drug-Protein Complexes: III. Interaction of Flufenamic Acid and Other N-Arylanthranilates with Serum Albumin. *Mol Pharmacol* 1969;5:455-62.
- [287] Barbosa S, Taboada P, Mosquera V. Analysis of the interactions between human serum albumin/amphiphilic penicillin in different aqueous media: an isothermal titration calorimetry and dynamic light scattering study. *Chem Phys* 2005;310:51-8.
- [288] Perozzo R, Folkers G, Scapozza L. Thermodynamics of protein-ligand interactions: history, presence, and future aspects. *J Recept Sig Transd* 2004;24:1-52.

- [289] Al-Kaddah S, Reder-Christ K, Kloczek G, Wiedemann I, Brunschweiler M, Bendas G. Analysis of membrane interactions of antibiotic peptides using ITC and biosensor measurements. *Biophys Chem* 2010;152:145-52.
- [290] Henriksen JR, Andresen TL. Thermodynamic profiling of peptide membrane interactions by isothermal titration calorimetry: a search for pores and micelles. *Biophys J* 2011;101:100-9.
- [291] McCubbin GA, Praporski S, Piantavigna S, Knappe D, Hoffmann R, Bowie JH, et al. QCM-D fingerprinting of membrane-active peptides. *Eur Biophys J* 2011;40:437-46.
- [292] Tang Y, Wang Z, Xiao J, Yang S, Wang YJ, Tong P. Studies of phospholipid vesicle deposition/transformation on a polymer surface by dissipative quartz crystal microbalance and atomic force microscopy. *J Phys Chem B* 2009;113:14925-33.
- [293] Seantier B, Breffa C, Felix O, Decher G. Dissipation-enhanced quartz crystal microbalance studies on the experimental parameters controlling the formation of supported lipid bilayers. *J Phys Chem B* 2005;109:21755-65.
- [294] Shahmiri M, Enciso M, Mechler A. Controls and constraints of the membrane disrupting action of Aurein 1.2. *Scientific Reports* 2015;5:16378.
- [295] Lv Y, Wang J, Gao H, Wang Z, Dong N, Ma Q, et al. Antimicrobial properties and membrane-active mechanism of a potential α -helical antimicrobial derived from cathelicidin PMAP-36. *PloS One* 2014;9:e86364.
- [296] Kalfa V, Jia H, Kunkle R, McCray P, Tack B, Brogden K. Congeners of SMAP29 kill ovine pathogens and induce ultrastructural damage in bacterial cells. *Antimicrob Agents Chemother* 2001;45:3256-61.
- [297] Shaw JE, Epand RF, Sinnathamby K, Li Z, Bittman R, Epand RM, et al. Tracking peptide-membrane interactions: Insights from in situ coupled confocal-atomic force microscopy imaging of NAP-22 peptide insertion and assembly. *J Struct Biol* 2006;155:458-69.
- [298] Pawley J. *Handbook of biological confocal microscopy*: SSBM; 2006.

Chapter Two

Methodology

2. 1. Quartz Crystal Microbalance (QCM)

QCM is based on the simple principle that addition of mass to the surface of a mechanical oscillator changes its resonance frequency. The QCM oscillator is a piezoelectric quartz crystal plate equipped with two electrodes [1]. Because quartz is a piezoelectric material, applying AC voltage causes this piezoelectric plate to oscillate at a specific frequency (f_0) determined by the mechanical and geometric properties of the crystal [2], as defined by

$$f_0 = \frac{\sqrt{\frac{Mq}{\rho q}}}{2t_q}$$

Eq. 2. 1

where M_q , ρ_q and t_q are the elastic shear modulus of quartz, quartz density and the quartz crystal thickness, respectively. This formula allows for quantifying mass change from frequency change, as shown by Sauerbrey [3] for the addition of thin solid layers:

$$\Delta m = -C \Delta f$$

Eq. 2. 2

Where C is a constant for a quartz crystal plate:

$$C = \frac{t_q \rho_q}{f_0}$$

Eq. 2. 3

Here t_q and ρ_q are thickness and density of quartz plate, respectively.

The Sauerbrey equation is valid within specific boundary conditions [1, 3-5]. The mass adsorbed should be rigid, distribute uniformly and it should be much smaller than the mass of the quartz plate.

QCM can also provide information about energy dissipation into the adlayer [6]. The dissipation (D) in a mechanical oscillator is related to the quality factor (Q) of the resonance and the oscillatory decay time constant (τ) when excitation is removed as follows:

$$D = \frac{1}{Q} = \frac{1}{\pi f \tau} = \frac{E_{dissipated}}{2\pi E_{stored}}$$

Eq. 2. 4

Where $E_{dissipated}$ and E_{stored} are the dissipated energy during one period of oscillation and stored energy in the system, respectively.

There is a simple QCM technology for measuring frequency and dissipation simultaneously [7]. In the absence of a continuous drive signal, the amplitude of the

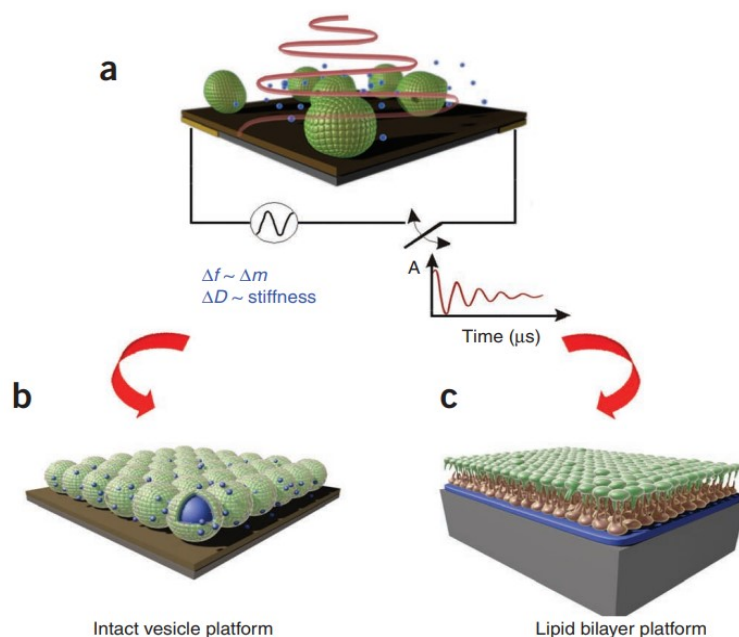


Figure 2.1. QCM-D principles. (a) Schematic representation of the QCM-D principle. The spheres resemble unruptured vesicles and blue balls resemble attached solvent. (b) A monolayer of unruptured vesicles formed on substrates e.g., gold and titanium oxide. (c) A supported lipid bilayer [12]

oscillation will decay exponentially. Energy dissipation (D) is the exponent, that can be described as per Eq 2.4 as energy loss per stored energy during one oscillation cycle [8]. In the absence of an electronic drive signal, the oscillating piezoelectric crystal generates an AC voltage, the magnitude of which is proportional to the amplitude of the mechanical oscillation, providing a direct readout. During the decay dissipation and frequency can be recorded simultaneously for multiple eigenmodes of the crystal ($n= 1, 3, 5, \dots, 13$) corresponding to 5, 15, 25, ..., 65 MHz, respectively [9]. The frequency and dissipation values of different eigenmodes can be used to determine the adsorbed mass and viscoelastic properties of the adsorbed layers, properties such as viscosity, elasticity, density and thickness [10]. The complex (dissipating) shear modulus of the adsorbed film on the sensor can be defined by:

$$G = G' + iG'' = \mu_f + 2\pi i f \eta_f$$

Equation 2. 5

In the equation, μ_f and η_f are the elastic (storage) and viscosity (loss) shear, respectively, and f is the frequency of oscillation [11]. Adsorbed layers with larger viscous loss will have larger dissipation change than more rigid films, due to the larger ratio between stored and loss energy [12]. Therefore, QCM-D can provide in situ information about mass and structure changes during the measurement, is proved to be a powerful technique

not only to investigate the deposition of materials on the sensor surface, but also to monitor the interaction between the surface and other material added such as peptides or proteins [13].

2. 1. 1. Biomimetic membrane formation on QCM sensor surface

A widely accepted model for mimicking natural cell membrane is using supported lipid bilayers (SLBs) [14, 15]. While the first study on the formation of SLB by spontaneous vesicle fusion on hydrophilic substrate was published in 1985 [16], precise control of the deposited membrane structural characteristics used to be a challenge [6, 17] which was resolved and confirmed precisely by using different techniques [18, 19]. QCM is one of the techniques widely used to monitor the formation of SLB on different substrates and study their interaction with peptides [1, 20-28].

It was shown that using silicon dioxide coated chips promotes membrane formation; the deposition yields a non-dissipative membrane due to the strong surface binding [6, 17, 29]. It is also possible to create suitable conditions by functionalizing the gold electrode surface directly by a self-assembled monolayer (SAM) of suitable chemistry, such as mercaptopropionic acid or mercaptoundecanoic acid; such SAM surfaces support the formation of partially suspended, that is, dissipative membranes [18, 21, 30]. Partially suspended single bilayer DMPC membrane on mercaptopropionic acid (MPA) modified gold chips exhibits frequency and dissipation values of $\sim -13\text{Hz}$ and $\sim 3 \times 10^6$ arb.u. values, respectively [31].

2. 1. 2. Viscoelastic fingerprinting analysis

Plotting dissipation energy change (ΔD) against frequency change (Δf) provides a quick and useful picture of the viscoelastic processes in a QCM deposition or interaction assay. It shows characteristic interaction vectors in f-D space defined by the mass and viscosity of the deposited material during adlayer formation, or the structural change that disrupt the native viscosity and elasticity of this adlayer when exposed to an interacting partner, such as membranes and membrane disrupting AMPs. These interaction vectors, or trendlines, provide a fingerprint of multi-step processes by highlighting each mechanistic subprocesses [32, 33]. Δf values are often plotted in reverse, i.e. positive to negative on the x-axis, to demonstrate mass uptake (that correspond to negative frequency change) while ΔD values are plotted negative to positive on the y-axis [33].

In viscoelastic fingerprinting analysis, the overall process is divided into individual sub-processes or steps. The characteristic trendline of each step is interpreted by correlating the viscoelastic change to the possible underlying processes. While there is a slight crosstalk between the signals [34], in an idealized system the frequency change shows mass change on the surface and dissipation change shows structural rearrangement in the system [18, 33]. However pure elasticity change also appears as frequency change, while the addition of viscoelastic mass increases dissipation parallel to frequency. Consistently different processes may give identical trendlines, thus QCM analysis must be informed by results from other techniques. Nevertheless, there are some general rules in interpreting fingerprints. The trendline toward $[-f, +D]$ is normally indicative of mass uptake whereas $[+f, -D]$ shows mass loss. If the trend proceeds toward other quadrants, it indicates structural changes in the system. The different shear wave penetration depth of the different sensor resonance modes also offers a qualitative depth profile: in terms of AMP-membrane interaction, different responses over eigenmodes indicate surface acting peptides and equal responses across eigenmodes suggest trans-membrane action [27].

2.2 Dye leakage experiments

Self-quenching arises between two identical molecules or ions when the first molecule that is initially in an excited state exchanges energy with its' ground state counterpart, resulting both molecules simultaneously changing to excited states that are intermediate in energy between the two initial states. Therefore, the energy drop for the first molecule

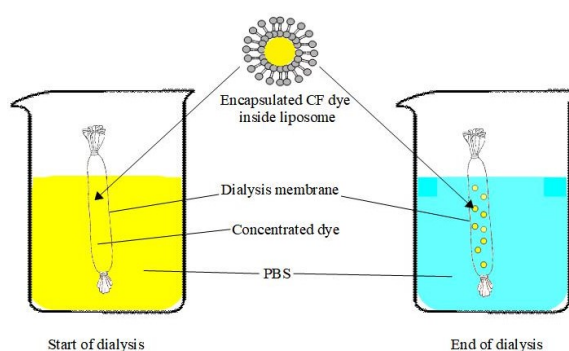


Figure 2.2. The simple schematic representation of dialysis process

is equal to the energy increase for the second molecule, causing conserving energy but no photon emission.

In practical dye leakage experiments, the light from an excitation lamp source is absorbed by the dye, followed by some of the energy emitted as fluorescence; the emitted photons

are collected by a photomultiplier detector [35]. In this thesis, The concentration of carboxyfluorescein (CF) dye encapsulated in liposomes was with the absorption at 470 nm and emission at 515 nm [36, 37].

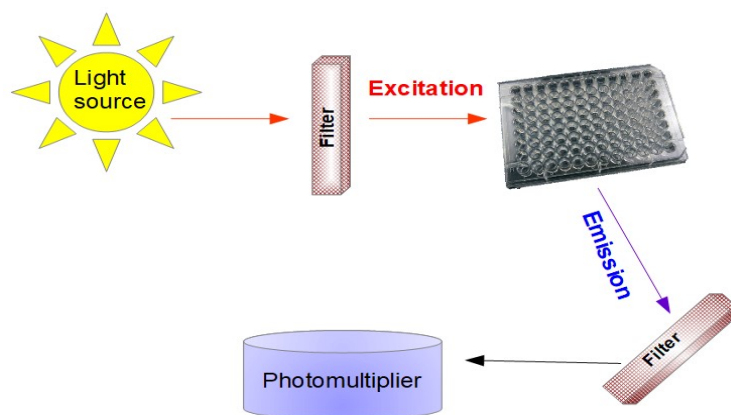


Figure 2.3. Schematic figure of dye leakage process

In order to assess disruption action of AMPs, 0.02 M 5(6)-carboxyfluorescein dye as incorporated in liposomes by preparing the liposomes in dye solution. The excess amount of dye was removed by using snakeskinTM dialysis tube and dialysis process until a clear solution remained (figure 2.2). The amount of dye release after addition of different concentration of peptide was recorded by using Spectramax M5 spectrophotometer (Molecular Devices, Silicon Valley, CA, USA).

The data is analyzed by subtracting a blank containing only dye loaded liposomes to remove photobleaching. Release intensity was normalized to the time zero intensity. Positive control was not used due to the errors inherent in variations between the intensities of the liposome suspensions in each cell. The data in this case is a yes/no indicator of membrane disrupting activity or the absence thereof.

2. 3. Dynamic light scattering (DLS)

Dynamic light scattering, also known as photon correlation spectroscopy, is a technique used to measure the size and size distribution of particles in suspension, such as polymers, proteins and liposomes in a liquid medium. It covers the size range from 1 nm up to a few μm [38, 39].

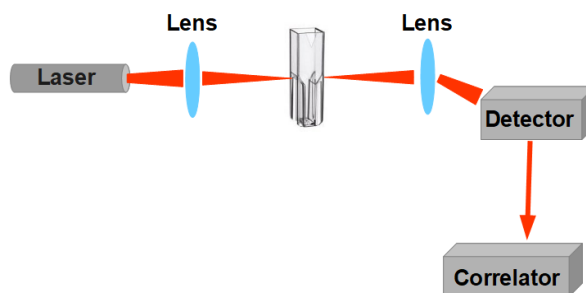


Figure 2.4. Block diagram of DLS

The DLS setup consists of a monochromatic light source, usually a laser light used to illuminate the sample. The light will then be scattered by particles of sample, and the fluctuations of the scattered light will be collected at a known scattering angle by a fast photon detector. The suspended particles in the sample move in random directions with certain correlation properties, known as Brownian motion, which leads to fluctuation of the scattering intensity characteristic of a particular sample size. Movement of particles changes the noise pattern with a time function based on the particle size [40]. The dynamic movement of the particles is derived from autocorrelation of the intensity trace recorded

The relation between the diffusion coefficient of the particles speed and the particle size is given by the Stokes-Einstein equation:

$$D = \frac{kT}{6\pi\eta R}$$

Eq. 2. 5

where D is the diffusion coefficient (m^2/s), k the Boltzmann constant ($\text{m}^2\text{kg}/\text{Ks}^2$), T the temperature (K), η the viscosity of the medium (Pa.s), and R is the hydrodynamic radius (m). Consistently the particle movement depends not only on size, shape and structure, but also on temperature and viscosity of medium [39].

The main advantage of using DLS is its simplicity, none destructive, no calibration required and short time of measurement, on the other hand, in case of polydisperse colloids, there is a risk of small objects being screened by bigger ones and cannot be detected [41]. Furthermore, particles greater than $\sim 5000\text{nm}$ cannot be measured by DLS [39].

2.4. Atomic Force Microscopy (AFM)

To visualize nanometre scale structures Atomic Force Microscopy (AFM) is frequently used [42-44]. The principle is shown schematically in Figure 2.5. AFM senses surfaces with a sharp tip attached to a soft cantilever-type spring with approximately 100-450 μm length with typical resonance frequencies of 7–120 kHz [45]. When the tip is pushed against the surface, the forces between the molecules of the tip and sample surface cause the cantilever to bend based on Hooke's law. Cantilever bending is measured by monitoring the deflection of a laser beam reflected from the back of cantilever, by a position sensitive photodiode detector. Feedback maintains constant bending and thus

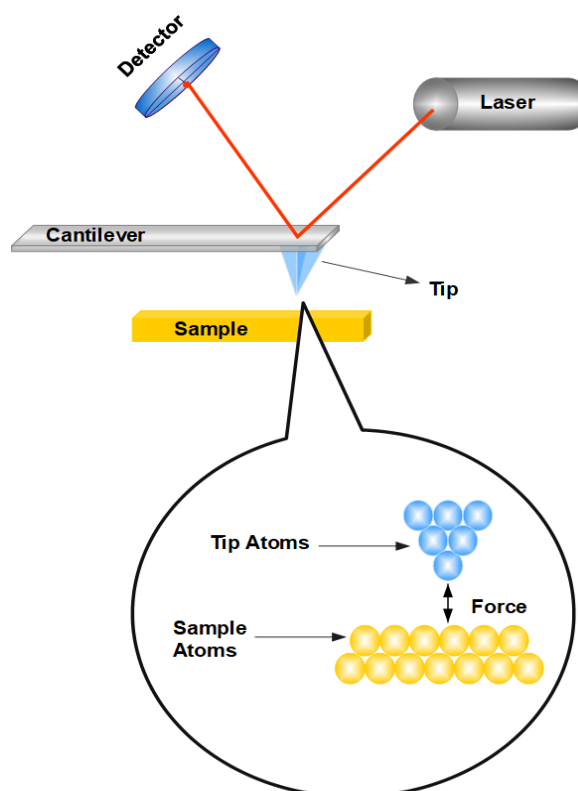


Figure 2.5. The schematic figure of AFM

constant interaction force; the control signal after feedback is used to produce a topographic map of the sample surface [46]. The interaction forces include van der Waals, capillary, elastic, electrostatic and magnetic forces. There are three general modes for AFM operation [47, 48]:

- Constant force (contact mode)
- Noncontact mode
- Constant amplitude (Tapping) mode

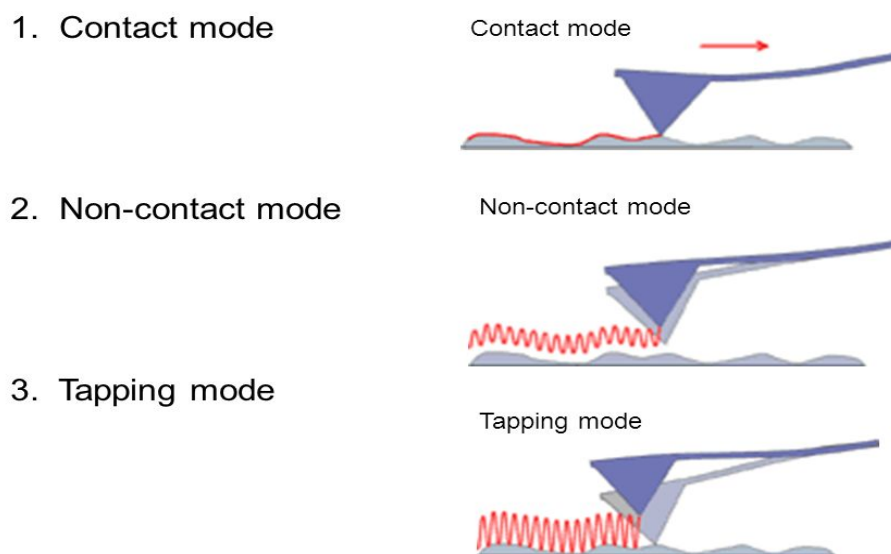


Figure 2.6. Schematic figure of different modes of AFM

In the first mode, as the name shows, the probe is in a constant contact with the sample surface throughout the scan. This can be achieved by controlling the cantilever bending and thus the constant push force to the surface to maintain a constant height from the surface. Soft or poorly bound biological samples are challenging to image by this mode.

It should be noted that both non-contact mode and tapping mode can be performed in constant amplitude scanning modes. However, non-contact scanning provides lower resolution due to its high sensitivity to noise [49].

In tapping mode, the cantilever oscillates at or near its resonance frequency. Usually the amplitude of this oscillation varies from several nm to 200 nm. Compared with contact mode, tapping mode lowers the probable damage done to the sample and the tip, because of the lower shear forces between tip and sample. Therefore, tapping mode is used to study biological samples, such as supported lipid bilayers.

AFM found to be a crucial instrument in physical and life sciences as it can probe the nano scale samples under physiological liquid environment [50-52]. Tapping mode is the most preferable mode for liquid scanning [53]. AFM liquid imaging requires a liquid cell, or a droplet formed by capillary forces between sample surface and the cantilever holder to immerse the sample and probe while the probe scanning the surface. Use of AFM in liquid has some valuable advantages such as elimination of capillary forces [54], reduction of van der Waals forces [55] and more importantly the capability of creating in situ high-resolution images of samples in physiological conditions [56, 57].

2. 5. Neutron reflectometry (NR)

Neutrons have strong interaction with nuclei and magnetic moments of the substrate [58]. Neutron reflectometry is a non-destructive technique to study the structure of thin layer materials, with wide range of applications on soft matter problems including surface confined liquids, biosensors and artificial biological membranes [59-62].

Neutron reflectometry involves directing a pulsed neutron beam to a flat surface and measure the intensity of reflected beam as a function of reflection angle or wavelength [63]. The specular reflectometry of neutron, in which the angle of reflected and incident beams are equal, provides chemical composition profile perpendicular to the surface. The

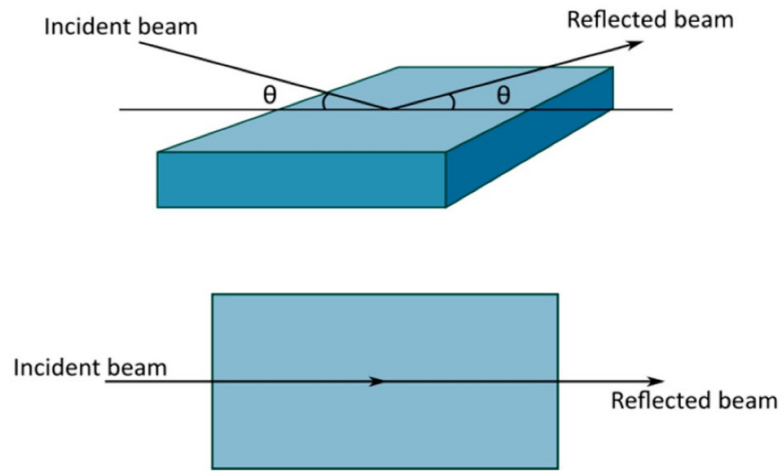


Figure 2.7. Reflection on an infinite planar surface [45]

specular reflectivity profile will provide detailed information about the surface structure, such as thickness, roughness and density of the thin films or layers on the substrate [64].

The specular reflectivity from a thin film can be calculated by:

$$R(q) = \frac{16\pi^2}{q^4} \Delta\rho^2$$

Equation 2. 6

Where $\Delta\rho$ is the changes of scattering length density throughout the interface and q is the wave-vector transferring perpendicular to the surface [65].

The energy of the neutron can be calculated by:

$$E = \frac{\hbar^2 K^2}{2m}$$

Equation 2. 7

Where \hbar is the reduced Planck constant and m the mass of neutron and K is the wave vector of an incident neutron in vacuum [66].

This technique has many similarities to X-ray reflectometry, however with some significant advantages. As the neutron is uncharged, it can penetrate deep into the sample that enables the study of buried layers and it can be used at complex sample environment (very low or high temperature). Furthermore, it can differentiate between neighbouring elements (such as iron and magnesium) based on the contrast in scattering potentials, which is particularly large for hydrogen and deuterium, which enables isotope detection [67]. In the case of biological systems, neutron has the advantage over X-rays of the sensitivity to light elements that are important in these materials [68].

In this thesis, neutron reflectometry was used to find the orientation of two well-known antimicrobial peptides in the membrane throughout peptide-membrane interaction. By using deuterated molecules, and choosing a suitable solvent contrast different segments of the lipid bilayer can be explored. In this thesis, neutron reflectometry has been used to find the orientation of antimicrobial peptides in the membrane.

References

- [1] Dixon MC. Quartz crystal microbalance with dissipation monitoring: enabling real-time characterization of biological materials and their interactions. *J Biomol Tech* 2008;19:151.
- [2] Curie J, Curie P. An oscillating quartz crystal mass detector. *Rendu* 1880;91:294-7.
- [3] Sauerbrey G. Verwendung von Schwingquarzen zur Wägung dünner Schichten und zur Mikrowägung. *Z Phys* 1959;155:206-22.
- [4] Cho N-J, Kanazawa KK, Glenn JS, Frank CW. Employing two different quartz crystal microbalance models to study changes in viscoelastic behavior upon transformation of lipid vesicles to a bilayer on a gold surface. *Anal Chem* 2007;79:7027-35.
- [5] Lu C, Czanderna AW. Applications of piezoelectric quartz crystal microbalances: Elsevier; 2012.
- [6] Keller C, Kasemo B. Surface specific kinetics of lipid vesicle adsorption measured with a quartz crystal microbalance. *Biophys J* 1998;75:1397-402.
- [7] Rodahl M, Kasemo B. A simple setup to simultaneously measure the resonant frequency and the absolute dissipation factor of a quartz crystal microbalance. *Rev Sci Instrum* 1996;67:3238-41.
- [8] Spencer W, Smith W. Defects in natural quartz. *J Appl Phys* 1966;37:2557-63.
- [9] Liu SX, Kim J-T. Application of Kelvin—Voigt model in quantifying whey protein adsorption on polyethersulfone using QCM-D. *JALA-J LAB AUTOM* 2009;14:213-20.
- [10] McCubbin GA, Praporski S, Piantavigna S, Knappe D, Hoffmann R, Bowie JH, et al. QCM-D fingerprinting of membrane-active peptides. *Eur Biophys J* 2011;40:437-46.
- [11] Tammelin T, Merta J, Johansson L-S, Stenius P. Viscoelastic properties of cationic starch adsorbed on quartz studied by QCM-D. *Langmuir* 2004;20:10900-9.
- [12] Cho N-J, Frank CW, Kasemo B, Höök F. Quartz crystal microbalance with dissipation monitoring of supported lipid bilayers on various substrates. *Nature Protocols* 2010;5:1096.
- [13] Tang Y, Wang Z, Xiao J, Yang S, Wang YJ, Tong P. Studies of phospholipid vesicle deposition/transformation on a polymer surface by dissipative quartz crystal microbalance and atomic force microscopy. *J Phys Chem B* 2009;113:14925-33.
- [14] Sackmann E. Supported membranes: scientific and practical applications. *Science* 1996;271:43-8.
- [15] Watts TH, Brian AA, Kappler JW, Marrack P, McConnell HM. Antigen presentation by supported planar membranes containing affinity-purified I-Ad. *PNAS* 1984;81:7564-8.
- [16] Tamm LK, McConnell HM. Supported phospholipid bilayers. *Biophys J* 1985;47:105-13.
- [17] Richter R, Mukhopadhyay A, Brisson A. Pathways of lipid vesicle deposition on solid surfaces: a combined QCM-D and AFM study. *Biophys J* 2003;85:3035-47.
- [18] Mechler A, Praporski S, Piantavigna S, Heaton SM, Hall KN, Aguilar M-I, et al. Structure and homogeneity of pseudo-physiological phospholipid bilayers and their deposition characteristics on carboxylic acid terminated self-assembled monolayers. *Biomaterials* 2009;30:682-9.
- [19] Hasan IY, Mechler A. Formation of planar unilamellar phospholipid membranes on oxidized gold substrate. *Biointerphases* 2016;11:031017.
- [20] Richter RP, Bérat R, Brisson AR. Formation of solid-supported lipid bilayers: an integrated view. *Langmuir* 2006;22:3497-505.
- [21] Evans KO. Supported phospholipid membrane interactions with 1-butyl-3-methylimidazolium chloride. *J Phys Chem B* 2008;112:8558-62.
- [22] Briand E, Zäch M, Svedhem S, Kasemo B, Petronis S. Combined QCM-D and EIS study of supported lipid bilayer formation and interaction with pore-forming peptides. *Analyst* 2010;135:343-50.
- [23] Lu N-Y, Yang K, Li J-L, Yuan B, Ma Y-Q. Vesicle deposition and subsequent membrane–melittin interactions on different substrates: A QCM-D experiment. *BBA-Biomembranes* 2013;1828:1918-25.
- [24] Wang KF, Nagarajan R, Camesano TA. Antimicrobial peptide alamethicin insertion into lipid bilayer: a QCM-D exploration. *Colloids Surf B Biointerfaces* 2014;116:472-81.

- [25] Losada-Pérez P, Khorshid M, Hermans C, Robijns T, Peeters M, Jiménez-Monroy K, et al. Melittin disruption of raft and non-raft-forming biomimetic membranes: A study by quartz crystal microbalance with dissipation monitoring. *Colloids Surf B Biointerfaces* 2014;123:938-44.
- [26] Fernandez DI, Le Brun AP, Whitwell TC, Sani M-A, James M, Separovic F. The antimicrobial peptide aurein 1.2 disrupts model membranes via the carpet mechanism. *Phys Chem Chem Phys* 2012;14:15739-51.
- [27] Mechler A, Praporski S, Atmuri K, Boland M, Separovic F, Martin LL. Specific and selective peptide-membrane interactions revealed using quartz crystal microbalance. *Biophys J* 2007;93:3907-16.
- [28] Sherman PJ, Jackway RJ, Gehman JD, Praporski S, McCubbin GA, Mechler A, et al. Solution structure and membrane interactions of the antimicrobial peptide fallaxidin 4.1 a: an NMR and QCM study. *Biochemistry* 2009;48:11892-901.
- [29] Reimhult E, Höök F, Kasemo B. Intact vesicle adsorption and supported biomembrane formation from vesicles in solution: influence of surface chemistry, vesicle size, temperature, and osmotic pressure. *Langmuir* 2003;19:1681-91.
- [30] Piantavigna S, McCubbin GA, Boehnke S, Graham B, Spiccia L, Martin LL. A mechanistic investigation of cell-penetrating Tat peptides with supported lipid membranes. *BBA-Biomembranes* 2011;1808:1811-7.
- [31] Hasan IY, Mechler A. Viscoelastic changes measured in partially suspended single bilayer membranes. *Soft Matter* 2015;11:5571-9.
- [32] Rodahl M, Höök F, Fredriksson C, Keller CA, Krozer A, Brzezinski P, et al. Simultaneous frequency and dissipation factor QCM measurements of biomolecular adsorption and cell adhesion. *Faraday Discuss* 1997;107:229-46.
- [33] McCubbin GA, Praporski S, Piantavigna S, Knappe D, Hoffmann R, Bowie JH, et al. QCM-D fingerprinting of membrane-active peptides. *Eur Biophys J* 2011;40:437-46.
- [34] Voinova M, Jonson M, Kasemo B. 'Missing mass' effect in biosensor's QCM applications. *Biosens Bioelectron* 2002;17:835-41.
- [35] Lakowicz JR. Instrumentation for fluorescence spectroscopy. *Principles of Fluorescence Spectroscopy*: Springer; 1999. p. 25-61.
- [36] Suenaga M, Lee S, Park NG, Aoyagi H, Kato T, Umeda A, et al. Basic amphipathic helical peptides induce destabilization and fusion of acidic and neutral liposomes. *BBA-Biomembranes* 1989;981:143-50.
- [37] Lee T-H, Heng C, Swann MJ, Gehman JD, Separovic F, Aguilar M-I. Real-time quantitative analysis of lipid disordering by aurein 1.2 during membrane adsorption, destabilisation and lysis. *BBA-Biomembranes* 2010;1798:1977-86.
- [38] Tomaszewska E, Soliwoda K, Kadziola K, Tkacz-Szczesna B, Celichowski G, Cichomski M, et al. Detection limits of DLS and UV-Vis spectroscopy in characterization of polydisperse nanoparticles colloids. *J Nanomater* 2013;2013:60.
- [39] Goldburg W. Dynamic light scattering. *Am J Phys* 1999;67:1152-60.
- [40] Pecora R. Dynamic light scattering: applications of photon correlation spectroscopy: SSBM; 2013.
- [41] Brar SK, Verma M. Measurement of nanoparticles by light-scattering techniques. *TrAC, Trends Anal Chem* 2011;30:4-17.
- [42] Hugel T, Seitz M. The study of molecular interactions by AFM force spectroscopy. *Macromol Rapid Commun* 2001;22:989-1016.
- [43] Shi Y, Cai M, Zhou L, Wang H. The structure and function of cell membranes studied by atomic force microscopy. *Semin Cell Dev Biol*: Elsevier; 2017.
- [44] Quate C, Gerber C, Binnig C. Atomic force microscope. *Phys Rev Lett* 1986;56:930-3.
- [45] Meyer E. Atomic force microscopy. *Prog Surf Sci* 1992;41:3-49.
- [46] Binnig G, Gerber C, Stoll E, Albrecht T, Quate C. Atomic resolution with atomic force microscope. *EPL* 1987;3:1281.
- [47] Giessibl FJ. Advances in atomic force microscopy. *Rev Mod Phys* 2003;75:949.
- [48] Geisse NA. AFM and combined optical techniques. *Mater Today* 2009;12:40-5.

- [49] Prater C, Maivald P, Kjoller K, Heaton M. Tapping mode imaging applications and technology. Digital Instruments Nanonotes, Santa Barbara, California, USA 1995.
- [50] Han W, Lindsay S, Jing T. A magnetically driven oscillating probe microscope for operation in liquids. *Appl Phys Lett* 1996;69:4111-3.
- [51] van Noort SJT, Willemsen OH, van der Werf KO, de Grooth BG, Greve J. Mapping electrostatic forces using higher harmonics tapping mode atomic force microscopy in liquid. *Langmuir* 1999;15:7101-7.
- [52] Ivanovska I, De Pablo P, Ibarra B, Sgalari G, MacKintosh F, Carrascosa J, et al. Bacteriophage capsids: tough nanoshells with complex elastic properties. *PNAS* 2004;101:7600-5.
- [53] Hansma P, Cleveland J, Radmacher M, Walters D, Hillner P, Bezanilla M, et al. Tapping mode atomic force microscopy in liquids. *Appl Phys Lett* 1994;64:1738-40.
- [54] Drake B, Prater C, Weisenhorn A, Gould S, Albrecht T, Quate C, et al. Imaging crystals, polymers, and processes in water with the atomic force microscope. *Science* 1989;243:1586-9.
- [55] Garcia N, Binh VT. van der Waals forces in atomic force microscopy operating in liquids: A spherical-tip model. *Phys Rev B* 1992;46:7946.
- [56] Butt H-J, Wolff E, Gould S, Northern BD, Peterson C, Hansma P. Imaging cells with the atomic force microscope. *JSB* 1990;105:54-61.
- [57] Putman CA, Van der Werf KO, De Grooth BG, Van Hulst NF, Greve J. Tapping mode atomic force microscopy in liquid. *Appl Phys Lett* 1994;64:2454-6.
- [58] Sears VF. Electromagnetic neutron-atom interactions. *Phys Rep* 1986;141:281-317.
- [59] Felcher G, Hilleke R, Crawford R, Haumann J, Kleb R, Ostrowski G. Polarized neutron reflectometer: A new instrument to measure magnetic depth profiles. *Rev Sci Instrum* 1987;58:609-19.
- [60] Majkrzak C, Cable J, Kwo J, Hong M, McWhan D, Yafet Y, et al. Observation of a magnetic antiphase domain structure with long-range order in a synthetic Gd-Y superlattice. *Phys Rev Lett* 1986;56:2700.
- [61] Lee L, Langevin D, Farnoux B. Neutron reflectivity of an oil-water interface. *Phys Rev Lett* 1991;67:2678.
- [62] Penfold J, Lee E, Thomas R. The structure of aqueous tetramethylammonium dodecylsulphate solutions at the air-water interface studied by the specular reflection of neutrons. *Mol Phys* 1989;68:33-47.
- [63] Wood MH, Clarke SM. Neutron reflectometry for studying corrosion and corrosion inhibition. *Metals* 2017;7:304.
- [64] Schmitt J, Gruenewald T, Decher G, Pershan PS, Kjaer K, Loesche M. Internal structure of layer-by-layer adsorbed polyelectrolyte films: a neutron and X-ray reflectivity study. *Macromolecules* 1993;26:7058-63.
- [65] Penfold J. Principles of reflectometry with reactors and pulsed sources. *Neutron Reflectometry—A Probe for Materials Surfaces*; International Atomic Energy Agency: Vienna, Austria 2004:29-44.
- [66] Cousin F, Menelle A. Neutron reflectivity. *EPJ Web of Conferences*: EDP Sciences; 2015. p. 01005.
- [67] Brown AS, Holt SA, Reynolds PA, Penfold J, White JW. Growth of Highly Ordered Thin Silicate Films at the Air– Water Interface. *Langmuir* 1998;14:5532-8.
- [68] Krueger S. Neutron reflection from interfaces with biological and biomimetic materials. *Curr Opin Colloid Interface Sci* 2001;6:111-7.

Chapter Three

Mechanism of action of melittin

Preamble

As it was discussed in chapter one, AMPs represent a broad category of natural innate weapon in virtually all organisms. For decades, bee venom therapy has been used to treat different ailments[1]. Bee venom is an efficient and complex mixture of substances including several biologically active peptides and enzymes. Melittin is the main constituent of European honey bee (*Apis mellifera*) venom [2]. This unique peptide found to have various biological activities, such as antibacterial [3], antiviral [4] and antifungal [5] effect as well as a potential for use in anticancer therapy[6].

Melittin is one of the most well-known “cationic α -helical” membrane disrupting peptides yet it has also given rise to the most controversy as far as its specificity, selectivity and especially mechanism of action is concerned[2, 7]. Melittin is perhaps the most extensively studied AMP. Its structure was determined experimentally by X-ray diffraction[8] and NMR spectroscopy [9] as well as by molecular dynamics (MD) simulations[7, 10]. It is thus known to have a bent rod-like conformation due to a proline “kink”[11, 12]. This characteristic geometry leads to an amphiphilic molecular configuration by symmetrically allocation of the polar and nonpolar residues[13]. Melittin, as a venom, has the ability to interact with neutral and negatively charged membranes, however it often shows greater affinity for the latter that is explained with the cationic charge of the peptide [14].

A widely accepted two-state model describes the mechanism of melittin action with initial binding on the membrane surface followed by transmembrane insertion that yields directly the formation of pores[15, 16]. The pore formation itself was initially believed to follow the barrel-stave model[17, 18] but soon experimental and simulation studies revised that to toroidal pore formation [15, 19-22]. However there are further controversies that suggest different mechanistic pathways on different membrane types, and even non-pore-forming mechanism[23-25]. Indeed despite all the studies, the interaction mechanism of melittin is still unclear and there are lots of uncertainties probably due to complexity of interaction and the small size of peptide[24, 26].

The focus of this chapter will be the mechanism of action of melittin, by using state-of-the-art methodology that became widely available only recently. I will aim at finding clues to the molecular stages of melittin action. In the first paper, the mechanism of action of melittin was studied on different type of membranes, aiming to identify the effect of charge and cholesterol in the peptide behaviour.

In the second part of chapter three I focus on the effect of different membrane morphologies of DMPC and DMPC:DMPG 4:1 membranes on peptide behaviour by analysing QCM viscoelastic fingerprints for single bilayer, multiple bilayer and liposome containing deposit. This chapter will be a validation of the methodology for transmembrane membrane disrupting peptides, describing

melittin action while also laying the groundwork for the following chapters, including even more advanced methodologies.

References

- [1] Lee J-D, Park H-J, Chae Y, Lim S. An overview of bee venom acupuncture in the treatment of arthritis. *Evidence-based complementary and alternative medicine* 1970;2.
- [2] Son DJ, Lee JW, Lee YH, Song HS, Lee CK, Hong JT. Therapeutic application of anti-arthritis, pain-releasing, and anti-cancer effects of bee venom and its constituent compounds. *Pharmacology & therapeutics* 2007;115:246-70.
- [3] Shi W, Li C, Li M, Zong X, Han D, Chen Y. Antimicrobial peptide melittin against *Xanthomonas oryzae* pv. *oryzae*, the bacterial leaf blight pathogen in rice. *Applied microbiology and biotechnology* 2016;100:5059-67.
- [4] Skalickova S, Heger Z, Krejcova L, Pekarik V, Bastl K, Janda J, et al. Perspective of use of antiviral peptides against influenza virus. *Viruses* 2015;7:5428-42.
- [5] Do N, Weindl G, Grohmann L, Salwiczek M, Koksche B, Korting HC, et al. Cationic membrane-active peptides—anticancer and antifungal activity as well as penetration into human skin. *Experimental dermatology* 2014;23:326-31.
- [6] Gajski G, Garaj-Vrhovac V. Melittin: a lytic peptide with anticancer properties. *Environmental toxicology and pharmacology* 2013;36:697-705.
- [7] Terwilliger TC, Weissman L, Eisenberg D. The structure of melittin in the form I crystals and its implication for melittin's lytic and surface activities. *Biophysical journal* 1982;37:353.
- [8] Terwilliger TC, Eisenberg D. The structure of melittin. I. Structure determination and partial refinement. *Journal of Biological Chemistry* 1982;257:6010-5.
- [9] BAZZO R, TAPPIN MJ, PASTORE A, HARVEY TS, CARVER JA, CAMPBELL ID. The structure of melittin. *European Journal of Biochemistry* 1988;173:139-46.
- [10] Andersson M, Ulmschneider JP, Ulmschneider MB, White SH. Conformational states of melittin at a bilayer interface. *Biophysical journal* 2013;104:L12-L4.
- [11] Oren Z, Shai Y. Selective lysis of bacteria but not mammalian cells by diastereomers of melittin: structure–function study. *Biochemistry* 1997;36:1826-35.
- [12] Naito A, Nagao T, Norisada K, Mizuno T, Tuzi S, Saitô H. Conformation and dynamics of melittin bound to magnetically oriented lipid bilayers by solid-state ³¹P and ¹³C NMR spectroscopy. *Biophysical Journal* 2000;78:2405-17.
- [13] Hong J, Lu X, Deng Z, Xiao S, Yuan B, Yang K. How Melittin inserts into cell membrane: Conformational changes, inter-peptide cooperation, and disturbance on the membrane. *Molecules* 2019;24:1775.
- [14] Sani M-A, Separovic F. How membrane-active peptides get into lipid membranes. *Accounts of chemical research* 2016;49:1130-8.
- [15] Yang L, Harroun TA, Weiss TM, Ding L, Huang HW. Barrel-stave model or toroidal model? A case study on melittin pores. *Biophysical journal* 2001;81:1475-85.
- [16] Huang HW. Action of antimicrobial peptides: two-state model. *Biochemistry* 2000;39:8347-52.
- [17] Vogel H, Jähnig F. The structure of melittin in membranes. *Biophysical journal* 1986;50:573-82.

- [18] Sansom MS. The biophysics of peptide models of ion channels. *Progress in biophysics and molecular biology* 1991;55:139-235.
- [19] Huang HW. Molecular mechanism of antimicrobial peptides: the origin of cooperativity. *Biochimica et Biophysica Acta (BBA)-Biomembranes* 2006;1758:1292-302.
- [20] Sengupta D, Leontiadou H, Mark AE, Marrink S-J. Toroidal pores formed by antimicrobial peptides show significant disorder. *Biochimica et Biophysica Acta (BBA)-Biomembranes* 2008;1778:2308-17.
- [21] Leveritt III JM, Pino-Angeles A, Lazaridis T. The structure of a melittin-stabilized pore. *Biophysical journal* 2015;108:2424-6.
- [22] Fox SJ, Lakshminarayanan R, Beuerman RW, Li J, Verma CS. Conformational Transitions of Melittin between Aqueous and Lipid Phases: Comparison of Simulations with Experiments. *The Journal of Physical Chemistry B* 2018;122:8698-705.
- [23] Knowles BH, Farndale RW. Activation of insect cell adenylate cyclase by *Bacillus thuringiensis* δ -endotoxins and melittin. Toxicity is independent of cyclic AMP. *Biochemical journal* 1988;253:235-41.
- [24] Dempsey CE. The actions of melittin on membranes. *Biochimica et Biophysica Acta (BBA)-Reviews on Biomembranes* 1990;1031:143-61.
- [25] Liao C, Esai Selvan M, Zhao J, Slimovitch JL, Schneebeil ST, Shelley M, et al. Melittin aggregation in aqueous solutions: insight from molecular dynamics simulations. *The Journal of Physical Chemistry B* 2015;119:10390-8.
- [26] Mihajlovic M, Lazaridis T. Antimicrobial peptides in toroidal and cylindrical pores. *Biochimica et Biophysica Acta (BBA)-Biomembranes* 2010;1798:1485-93.

Part 1:

Nano-viscosimetry analysis of the
membrane disrupting action of the
bee venom peptide melittin

<https://www.nature.com/articles/s41598-019-47325-y>

SCIENTIFIC REPORTS

OPEN

Nano-viscosimetry analysis of the membrane disrupting action of the bee venom peptide melittin

Sara Pandidan & Adam Mechler 

Received: 8 May 2019

Accepted: 10 July 2019

Published online: 25 July 2019

Melittin is one of the most studied α -helical cationic membrane disrupting peptides. It is the main component of bee venom, however it is considered an antimicrobial peptide for its ability to kill bacteria. Melittin is believed to act by opening large toroidal pores in the plasma membrane of the targeted cells/bacteria, although this is questioned by some authors. Little is known, however, about the molecular mechanism leading to this activity. In this study the mechanism of action of melittin was studied by dye leakage and quartz crystal microbalance fingerprinting analysis in biomimetic model membranes. The results revealed the existence of multiple stages in the membrane disrupting action with characteristic differences between different membrane types. In bacterial-mimetic (charged) lipid mixtures the viscoelastic fingerprints suggest a surface-acting mechanism, whereas in mammalian-mimetic (neutral) membranes melittin appears to penetrate the bilayer already at low concentrations. In domain-forming mixed membranes melittin shows a preference for the domain containing predominantly zwitterionic lipids. The results confirm membrane poration but are inconsistent with the insertion-to-toroidal pore pathway. Therefore hypotheses of the two membrane disrupting pathways were developed, describing the membrane disruption as either surface tension modulation leading to toroidal pore formation, or linear aggregation leading to fissure formation in the membrane.

The emergence of bacterial resistance to conventional antibiotics is one of the most significant international health problems of our time that requires an urgent solution¹. A potential answer to this near-crisis situation is using antimicrobial peptides (AMPs)². AMPs represent one of the oldest, highly effective forms of antimicrobial defence in all complex organisms, including plants, insects, amphibians and even mammals, typically released in response to stress³ and hazardous situations, such as facing the risk of a predator's attack⁴. Many AMPs can kill both Gram-positive and Gram-negative bacteria, while some of them have anticancer and antiviral activities as well⁵. Particularly interesting are cationic α -helical AMPs that kill bacteria by disrupting their plasma membrane, offering a specific class of potential therapeutic agents that are complementary to existing antibiotics, and which bacteria may not be able to develop resistance toward^{6,7}.

To identify sources of bioactive natural products traditional medicine is often a good guidance. Bee venom therapy is one of the methods in traditional medicine, used to treat different ailments^{8,9}. Bee venom is a complex mixture of peptides and enzymes, and the peptide melittin is the main component that constitutes 50% of the dry weight of European honey bee (*Apis mellifera*) venom¹⁰. Melittin is essentially a broad spectrum cell lysing agent¹¹ that is nevertheless generally known as an antimicrobial peptide in the literature¹² as it exerted strong antibacterial activity on 51 strains of both Gram-positive and Gram-negative bacteria, as well as rapidly growing mycobacteria¹³. However, melittin's potent antimicrobial activity is hitherto inseparable from its haemolytic action¹². Hence, melittin is a case study of membrane disrupting peptides; its potential for drug development can only be realized once its mechanism of action is fully understood, and its sequence is engineered in a way that it can selectively target bacteria.

Melittin is α -helical, cationic and amphiphilic peptide that consists of 26 amino acids (NH₂-GIGAVLKVLTTGLPALISWIKRKRQQ-CONH₂). Its C-terminal domain contains positively charged residues and hence is hydrophilic, while the N-terminal region is mostly hydrophobic^{10,14}. Despite the high proportion of hydrophobic side chains in its sequence, melittin is highly soluble in water, and moderately soluble in methanol¹⁵. The structure of melittin was determined by X-ray diffraction¹⁶ and NMR spectroscopy in methanol solution¹⁷. The folding of melittin consists of two α -helical domains (residues 1–10 and 13–26) intersecting at an angle of 120°, due to a

La Trobe Institute for Molecular Science, La Trobe University, Melbourne, Australia. Correspondence and requests for materials should be addressed to A.M. (email: a.mechler@latrobe.edu.au)

proline “kink” to form a bent structure; in the longer helix the hydrophilic and hydrophobic residues are aligned, facing in opposite directions^{15,18}. According to CD measurements melittin remains unfolded in aqueous solution, but becomes 68% α -helical when interacting with a DMPC bilayer; notably, the helicity is only 32% when cholesterol is mixed to the phospholipid¹⁹, suggesting that mammalian cells are protected against lysis and thus melittin exhibits some degree of specificity towards bacterial membranes. That is, however, inconsistent with the reported haemolytic activity¹² and pore forming activity in membranes of small cholesterol content²⁰. However, efforts to develop melittin-based antibiotics have not progressed beyond preclinical phase; like most of AMP derivatives, melittin based drug candidates could not obtain Food & Drug Administration approval²¹.

The key challenge facing drug development from membrane disrupting AMPs is the absence of a clearly defined drug target. The mechanism of action is based solely on a rearrangement of the lipid molecules around the peptides to breach the membrane integrity, such as forming a pore structure of a defined geometry^{22–24}. Specifics of this process are challenging to obtain due to the molecular dimensions of the interacting structures^{23,25}. Only the end result: the membrane disruption itself can be confirmed with high confidence using dye leakage assays^{26,27}, while the details of the pathway leading to membrane breach remain elusive^{28–30}. The dynamic nature of the peptide-lipid interaction limits microscopic methods to the capture of large-scale morphology changes, while the location, orientation or even aggregation of the peptides in real time cannot be resolved^{31–33}. The same dynamics limit the achievable detail from spectroscopic and surface characterization methods. In the absence of permanent interactions between lipid and peptide moieties, the only sub-molecular resolution data is gleaned by solid-state nuclear magnetic resonance (ss-NMR) measurements that identify disturbances in specific lipid moieties by the interaction with the peptide^{34–39}. The generally accepted membrane disruption models were developed with reliance on ss-NMR data^{40,41}. However even ss-NMR cannot distinguish multiple, co-existing membrane-bound states of the peptide, and, given that it essentially averages over all present molecules of a given species, it requires very high peptide to lipid ratios to clearly show the effect of the peptide⁴².

Consistently, there is no consensus in the literature about the mechanism of action of melittin, even though it is perhaps the best-known and most studied membrane disrupting peptide⁴³. Initially it was believed that melittin induced barrel-stave pores^{43,44}. Consecutively a range of studies argued that melittin forms toroidal pores^{27,43,45–51}. Molecular dynamics simulations also support the toroidal pore forming mechanism⁵². However a surface plasmon resonance study suggested that melittin can change its mechanism of action as a function of membrane properties, inserting into the membrane core in zwitterionic membranes (incl. 10% cholesterol), and acting in a detergent-like manner in anionic membranes⁵⁰. Dual-colour fluorescence-burst analysis studies using pure DOPC and DOPC:cholesterol 9:1 membranes showed concentration dependent action: at low concentrations, pore formation with the pore size dependent on melittin concentration, whereas at high concentrations and/or on charged membranes melittin triggered liposome fusion and aggregation without specific dye leakage⁵³. Melittin-induced pores have never been imaged at a quality that would clearly confirm the toroidal pore hypothesis; indeed an AFM imaging study suggested that melittin is not forming pores at all, rather fissures in the membrane⁵⁴. Thus, there is no clear consensus on the membrane disrupting pathway of melittin; even less is known about the molecular process leading to membrane disruption.

Recent improvement in multimodal surface characterizing methods such as quartz crystal microbalance “with dissipation” (QCM) opened new ways to glean further insights into AMP-membrane interactions. QCM measures mass with nanogram sensitivity simultaneously with recording any changes in the viscosity of the sample^{55–58}. This can be used to produce viscoelastic fingerprints of the membrane interaction, revealing distinct stages of the process^{51,59–64}. It should be noted that these stages differ in their viscoelastic character; to assign them to actual molecular processes either further information is needed about the peptide-membrane interaction, or at least a model based on the physical chemistry of peptide-membrane interactions.

In this work the mechanism of melittin interaction with different lipid mixtures was studied using QCM as the main method, while dye leakage measurements were used to benchmark the peptide activity. Based on viscoelastic fingerprint analysis to identify stages of the membrane interaction, two new mechanistic pathways were proposed for these model membranes.

Materials and Methods

Buffer preparation. Potassium dihydrogen phosphate (KH_2PO_4) was purchased from Sigma Aldrich (Castle Hill, NSW, Australia) and Fluka branded potassium hydrogen phosphate (K_2HPO_4) was purchased from Honeywell (Shanghai, China). Sodium chloride (NaCl) was purchased from Chem-Supply Pty Ltd, Gillman SA, Australia. The phosphate buffered saline (PBS) assay buffer contained 20 mM phosphate and 100 mM NaCl at pH 7.2. Deionized water of 18.2 M Ω cm resistivity (Ultrapure, Sartorius AG, Germany) was used for all solutions.

Vesicle preparation. 1,2-dimyristoyl-sn-glycero-3-phosphocholine (DMPC), 1,2-dioleoyl-sn-glycero-3-phosphocholine (DOPC), sodium salt of 1,2-dimyristoyl-sn-glycero-3-phosphoglycerol (DMPG), and cholesterol were purchased from Avanti Polar Lipids (Alabaster, AL, USA). Chloroform (ACS Reagent, 99.8%) and methanol (>99.9%, spectrophotometric grade) were purchased from Sigma-Aldrich (Castle Hill, NSW, Australia).

Lyophilized lipids were dissolved in chloroform; in case of DMPG 3% methanol was also added to increase solubility. Lipid solutions were mixed in desired ratios in a clean test tube. As described before, the solvent was evaporated with a gentle flow of nitrogen gas upon continuous moderate vortexing to obtain a uniform layer. Afterward, the tubes were stored in a desiccator. Before use the lipid aliquots were hydrated in 1 ml PBS in a 37°C incubator for 30 minutes, followed by one minute vortexing and brief sonication. This method yields a broad distribution of mostly unilamellar liposomes; the membrane deposition process is optimized for using this precursor⁵⁹. Lipid suspensions were used immediately.

As mammalian-mimetic membrane model, neat DMPC, DOPC, DMPC:cholesterol (9:1) and DMPC:chol (8:2) mixtures were used; as bacteria-mimetic model membranes DMPC:DMPG (4:1) and DMPC:DMPG (3:2)

mixtures were used. While this approach reduces the complexity of natural membrane, it allows for studying the effect of each membrane constituent, in line with our previous work and also a common practice in the literature^{64–68}.

Dye leakage assay. Vesicles were loaded with 5(6)-Carboxyfluorescein purchased from Sigma-Aldrich (Castle Hill, Australia). The lipid samples were suspended in PBS buffer containing 0.02 M CF dye solution and incubated for 30 minutes, following with one-minute vortex and one-minute sonication. Excess CF was removed from the medium by dialysis using SnakeSkin Dialysis Tubing 10000 MWCO, replacing the buffer solution 3 times until a clear solution was obtained. All experiments were performed using a SpectraMax M5 Multi-Mode Microplate Reader. Intensities were recorded every 60 s for 45 min after adding 1, 3, 5, 7 and 10 μ M melittin at 25 °C with excitation and emission wavelengths of 480 nm and 517 nm, respectively. The measurements were repeated at least three times for each membrane type and peptide concentration; the results showed high qualitative and quantitative agreement.

Quartz crystal microbalance. All experiments were conducted with a Q-SENSE E4 system (Q-SENSE, Sweden) using AT-cut gold-coated quartz chips with a fundamental resonance frequency of 5 MHz. QCM chips were cleaned and oxidised with a base piranha solution consisting of 1:1:3 of hydrogen peroxide (aqueous solution, 30%) purchased from ChemSupply Pty Ltd, Australia, Gillman, SA; ammonia solution (28–30%) purchased from Merck, Darmstadt Germany; and deionized water, at 70 °C for 20 minutes.

The cleaned chips were rinsed with ultra-pure water and dried under a gentle stream of N₂. The chips were modified in a solution of 2% 3-mercaptopropionic acid (MPA) (HPLC Grade, >99%, Fluka branded product from Sigma Aldrich, Castle Hill, NSW, Australia) in propan-2-ol overnight. Next, the chips were soaked in propan-2-ol to remove any excess thiol from the surface. After subsequent drying the chips were placed in deionized water for a few hours to hydrate the MPA self-assembled monolayer.

QCM is primarily used for measuring mass changes, such as peptide binding to a specific membrane. The second information channel, energy dissipation, is often neglected as most model membrane platforms restrain dissipative processes in supported membranes. By using a partially suspended membrane system, the dissipation signal becomes a useful measure of viscoelastic changes in the membrane properties and thus it can be also used to glean further insights into the peptide-membrane interaction^{69,70}.

Lipid deposition and fingerprinting assays. After installing the MPA modified chips in to the QCM chambers, baselines were recorded first in deionized water and in PBS for reference and also to confirm the stability of the sensor signals. Next, the lipid suspensions were injected into the chambers. Deposition was monitored in real time and, when a stable baseline was reached, mild osmotic stress (20 mM phosphate buffer solution without salt) was also used to clean the membrane surface of liposome residues. Assay buffer was then returned into the chamber and melittin (GL Biochem Ltd., Shanghai) was introduced in desired concentrations. All experiments were repeated at least three times at 19 °C and at a flow rate of 50 μ L/min. The frequency and dissipation changes were only plotted for four eigenmodes (3rd, 5th, 7th and 9th; 15–45 MHz) as these provide the most reliable data on lipid membranes⁵⁹.

In order to analyse the peptide mechanism of action, the QCM results were converted into f-D curves. These viscoelastic fingerprints show different stages of the membrane disruption process as distinct trendlines, and may be analysed to reveal the molecular process of peptide-membrane interaction as described before.

Dynamic light scattering (DLS) assay. DLS measurements were performed using a Malvern Zetasizer Nano instrument (Malvern Instruments, Ltd., Malvern Worcestershire, UK) and disposable micro cuvettes (ZEN0040). Measurements were done at 25 °C on 2 μ M DMPC before and after adding 10 μ M melittin. In the latter case the samples were centrifuged at 3000 rpm for 10 min and the supernatant was passed through a 200 nm pore size syringe filter to remove any intact liposomes that may obscure the small populations.

Results and Discussion

Dye leakage assays. Figure 1 shows the dye leakage results. In this work, the dye concentration was only slightly higher than the lower limit of self-quenching concentration to avoid interference from osmotic effects. Consistently, the intensity increases are moderate.

Exposing DMPC liposomes to melittin causes immediate, thresholdless and concentration-independent intensity increase to 4–8% (Fig. 1a). The result is nearly identical if DMPC is mixed with 20% cholesterol (Fig. 1c). However, in case of 10% cholesterol content the dye leakage is both higher and clearly concentration dependent, starting from ~12% at 1 μ M melittin and reaching 20% at 10 μ M concentration (Fig. 1b). The dye leakage trend on the unsaturated DOPC membrane (Fig. 1d) was near identical to the DMPC:cholesterol (9:1).

In case of the bacteria-mimetic membranes, the kinetics of the dye leakage appear different. For DMPC:DMPG (4:1) the intensity reaches a maximum of ~10% increase in approximately 20 minutes, in a concentration-independent manner. However when increasing the DMPG content to 40%, the dye leakage is again immediate, with an apparent decreasing trend from 1 μ M to 5 μ M melittin concentration, then a step increase in intensity from 13% to 30%. All the presented results are highly reproducible.

The variations confirm that, while melittin is an indiscriminate cell killer, it exhibits higher activity against the bacteria-mimetic DMPC:DMPG (3:2) membrane. The results also suggest that its action is affected by the structure of the membrane core, that is, whether the lipid molecules are saturated or unsaturated, and the presence and amount of cholesterol⁶⁴.

QCM assays. Mammalian-mimetic membranes. As shown in Fig. 2, in the case of neat zwitterionic DMPC membrane, the f-D fingerprints only change in proportion as a function of melittin concentration, but not in their

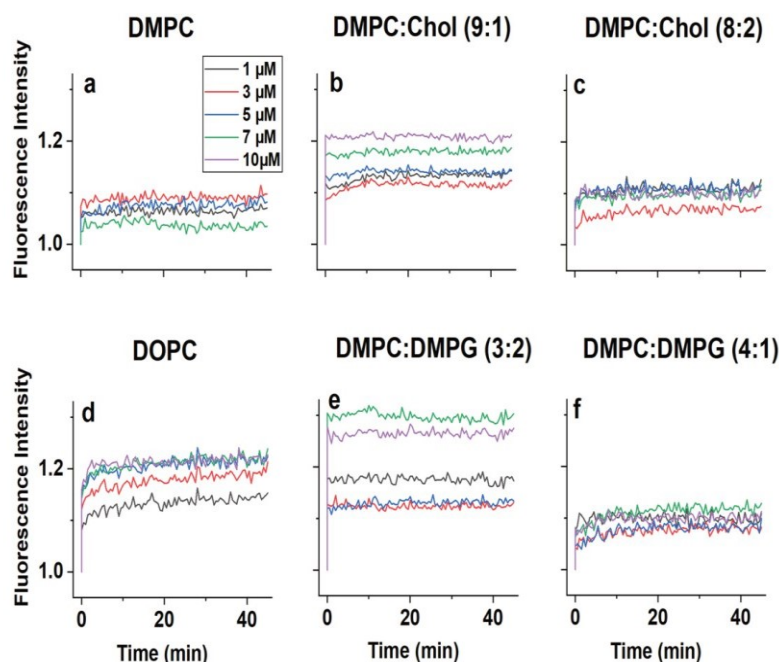


Figure 1. Results of dye leakage experiments. Normalized intensity of dye release shown as a function of time for a range of membrane mixtures and peptide concentrations as indicated. (a) DMPC; (b) DMPC:cholesterol (9:1); (c) DMPC:cholesterol (8:2); (d) DOPC; (e) DMPC:DMPG (3:2); (f) DMPC:DMPG (4:1). The fluorescence intensity of dye loaded liposomes before the addition of the peptide was set as unity.

shape. The first noticeable feature is that the first trendline is $[-f, -D]$, unlike the typical $[-f, +D]$ that is common in previously studied peptides^{61,64,70–72}. The $[-f, -D]$ trendline suggests that, parallel with mass gain due to the peptides binding to the membrane, an immediate structural change takes place, one that reduces the freedom of the membrane to dissipate energy. This is consistent with immediate peptide penetration into the membrane, altering the lipid packing order and inhibiting out of plane motion, which is the main pathway of energy dissipation in suspended membranes. The fingerprints at different eigenmodes almost perfectly overlap, suggesting that the changes in the membrane structure are more elastic than viscous in character, and may indicate transmembrane insertion of the peptides³¹. This stage reaches approximately the same values at all concentrations: $\Delta f = -4$ – 5 Hz and $\Delta D = -0.2$ – 0.5 arb. u., suggesting that the occupancy of the membrane inserted monomeric state reaches maximum at these values. Importantly that is achieved already at micromolar bulk peptide concentrations. Thus, melittin appears to preferentially absorb into the membrane from the solution phase in spite of its well-known high aqueous solubility.

Mass uptake ($-f$) continues in the second stage; however energy dissipation increases after the minimum reached at the end of stage 1, suggesting weakening in-plane interactions that re-introduce freedom of out-of-plane motion and hence dissipative processes. This is consistent with the formation of structures that break the continuity of the membrane, offering several pathways for energy dissipation. Membrane breach takes place parallel with further peptide insertion into the membrane, which contributes to further mass increase ($-f$). Finally, a slight $[+f, -D]$ mass loss trendline suggests that some fragments of the membrane break free from the surface, likely as a result of expansion of the membrane and “flaking” at the edges (stage 3).

In the presence of 10% cholesterol at low melittin concentrations the frequency trend of the f - D curve is similar to neat DMPC, however the dissipation change is significantly less (Fig. 2b). At $7 \mu\text{M}$ melittin concentration the fingerprint changes, with a loop continuing towards $[+f, -D]$; this becomes a sharp turn at $10 \mu\text{M}$ concentration.

Increasing the amount of cholesterol to 20% in the membrane lead to a substantial change in the shape of the f - D curves. The fingerprints reveal three distinct stages. The brief first stage shows a $[-f, 0]$ trend. A second stage appears as a sudden dissipation drop at ~ -2 Hz. At low peptide concentrations this drop takes place without any frequency change, however it acquires an increasingly $+f$ direction as the peptide concentration is increased. This trend is similar to the sudden $-D$ turn observed at $10 \mu\text{M}$ melittin concentration for DMPC:cholesterol (9:1).

The cause of this sudden drop in dissipation is unclear. In light of the dye leakage results, such a major structural change in the membrane has to be related to membrane disruption; yet if it is pore formation it is very different from the neat DMPC membrane. This is followed by a stage of significant negative frequency change with very small changes in dissipation. In previous works on surface acting peptides it was identified as the collapse of the partially suspended membrane after disruption with continuing adsorption of more peptide^{64,70}. Considering

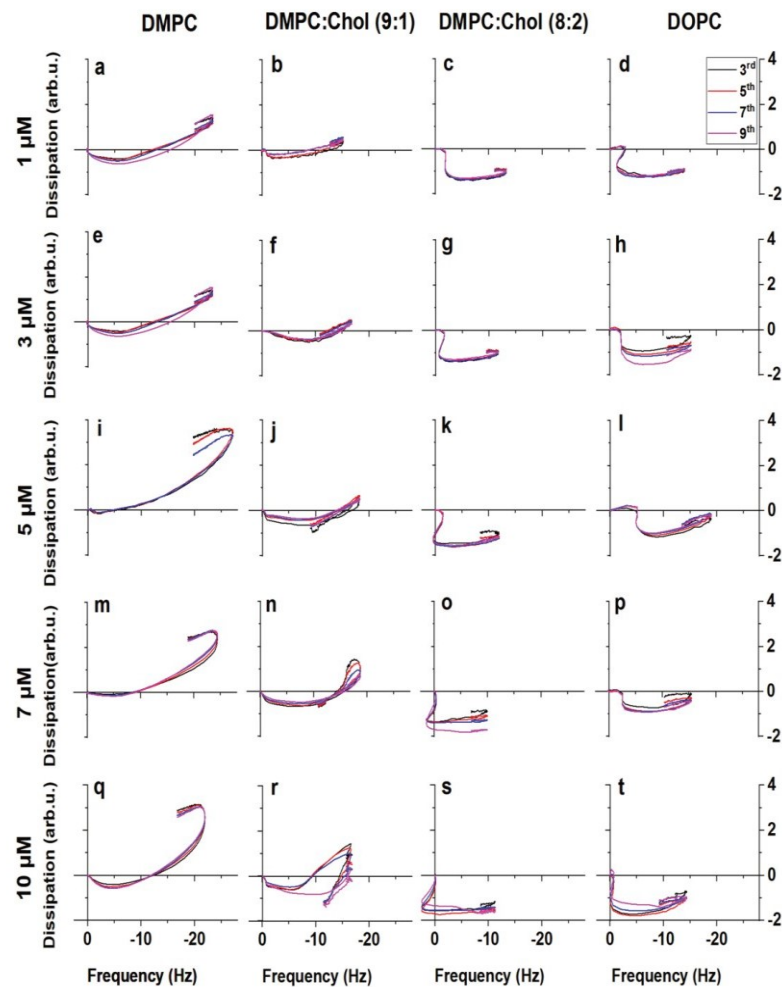


Figure 2. Viscoelastic fingerprints of interactions of melittin at varied concentrations with neutral membranes as follows. (a–d) 1 μ M melittin, (a) DMPC, (b) DMPC:cholesterol (9:1), (c) DMPC:cholesterol (8:2), (d) DOPC. (e–h) 3 μ M melittin, (e) DMPC, (f) DMPC:cholesterol (9:1), (g) DMPC:cholesterol (8:2), (h) DOPC. (i–l) 5 μ M melittin, (i) DMPC, (j) DMPC:cholesterol (9:1), (k) DMPC:cholesterol (8:2), (l) DOPC. (m–p) 7 μ M melittin, (m) DMPC, (n) DMPC:cholesterol (9:1), (o) DMPC:cholesterol (8:2), (p) DOPC. (q–t) 10 μ M melittin, (q) DMPC, (r) DMPC:cholesterol (9:1), (s) DMPC:cholesterol (8:2), (t) DOPC.

the dye leakage results it is feasible to assume a similar process. There is again a small amount of material removal at the end of the process likely due to desorption of peptides upon buffer wash.

The difference between the two cholesterol-containing membranes may be understood based on their structural characteristics. It is known that adding cholesterol to DMPC yields the formation of two domains: DMPC-rich and cholesterol-rich. The DMPC-rich domain shrinks progressively with increasing cholesterol content, disappearing at $\sim 20\%$ cholesterol⁷³. It was reported before that the existence of domains of different cholesterol content can influence peptide-membrane interaction, as cholesterol may inhibit penetration and fragmentation of the membrane by some AMPs^{74,75}. The QCM data suggest that at 10% cholesterol concentration melittin first interacts with the DMPC-rich domain, hence the similar trend; the lower dissipation is the result of the rigidifying effect of the cholesterol-rich domains. At high melittin concentration the peptides start to interact with the cholesterol-rich domain, resulting in the sudden $-D$ trend, but do not proceed to the $[-f, 0]$ trendline likely due to the different viscoelastic character of the domain separated nature of the membrane. Thus, the results for 10% cholesterol reflect the composite effect of the two distinct membrane domains.

To separate cholesterol effects from the lipid packing in the membrane core, experiments were also performed with unsaturated DOPC membrane and the results are shown in Fig. 2d. The fingerprints show a high degree of similarity to the DMPC:cholesterol (8:2) membrane, that is, to the case when cholesterol distributes evenly in

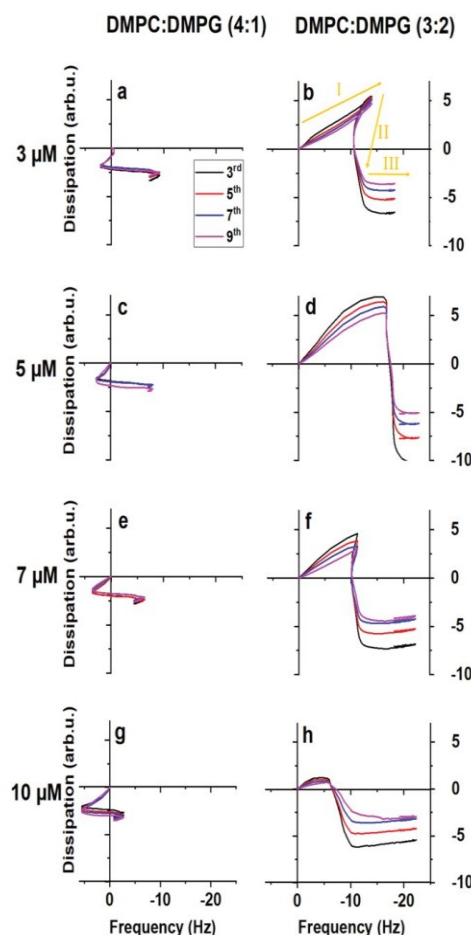


Figure 3. Viscoelastic fingerprints of melittin interactions with anionic membranes at different concentrations as follows. 3 μ M melittin: (a) DMPC/DMPG (4:1), (b) DMPC/DMPG (3:2). 5 μ M melittin: (c) DMPC/DMPG (4:1), (d) DMPC/DMPG (3:2). 7 μ M melittin: (e) DMPC/DMPG (4:1), (f) DMPC/DMPG (3:2). 10 μ M melittin: (g) DMPC/DMPG (4:1), (h) DMPC/DMPG (3:2). The arrows in panel (b) indicate stages of the interaction with Roman numerals.

the membrane without forming any domains. This suggests that the peptide insertion is directly affected by the packing and/or viscosity of the membrane core, not by a specific interaction with cholesterol.

Bacteria - mimetic membranes. Figure 3 shows f-D curves of melittin interaction with the bacteria-mimetic DMPC:DMPG (4:1) mixture. There are three distinct stages. In all cases, the fingerprints start with a [+f, -D] trend, that abruptly switches into a [-f, 0] trendline with a final stage where this trend is inverted (upon rinsing with assay buffer). The maximum positive frequency change in the first trend is proportional to peptide concentration, whereas the negative frequency change of the second trendline appears to be largely independent of the concentration.

Increasing the anionic (PG) lipid content of the mixture from 20% to 40% yields a much altered fingerprint, as shown in Fig. 2b. The first stage is now a viscoelastic mass increase [-f, +D], consistent with peptides binding to the membrane surface as in case of surface acting peptides; this is followed by a drastic structural change [0, -D], and finally further non-viscous frequency increase [-f, 0] and a very short reverse trend upon washing. The first stage is concentration dependent, however there is a change after 5 μ M peptide concentration that has the maximum frequency and dissipation change values: these are reduced again at 7 μ M and even more at 10 μ M. Importantly, in this lipid mixture the fingerprints show a spreading of the harmonics of the sensor resonance (that overlap in most other cases), which is normally observed in case of surface acting peptides.

The substantial difference in the fingerprints between 20% and 40% anionic lipid content suggests that there is a specific interaction between the PG headgroups and the peptide. DMPC:DMPG (3:2) is the only mixture where the initial trend is similar to the one observed for surface acting peptides; it is also the mixture yielding the strongest dye leakage. Hence it is feasible to assume that here peptides initially stay on the membrane surface, interact with the headgroups and appear as added viscous mass (stage 1). In stage 2 a major structural change

commences: as the presence of the peptide increases asymmetric tension, local blistering and/or immediate pore opening leads to a sudden stiffening of the membrane (+f) parallel with a significant reduction of dissipative out-of-plane motion (e.g. undulation) of the membrane (-D). The structural change however allows increased water penetration; this and/or the negative effect of the growing pores on overall membrane elasticity leads to a slight (-f) trend again, especially towards the end of the stage and at higher concentrations. Hence the stage is characterized by curved trendlines. The growing of the pores eventually leads to the membrane collapsing back to the surface (stage 3) as observed before for surface acting peptides⁶⁴.

The difference between the two anionic membranes is analogous to the case of varied cholesterol content as described above. Indeed at a first glance the DMPC:DMPG (4:1) fingerprint is very similar to that of melittin interaction with DMPC:cholesterol (9:1) mixture at 10 μ M concentration. It was shown before that DMPC:DMPG (4:1) mixture is also prone to domain separation³⁹; it is feasible to assume that the f-D fingerprint reflects a composite effect, similarly to the one described for DMPC:cholesterol (9:1). Therefore in the six studied membranes, we can observe only four clearly different fingerprints: in neat DMPC, neat DOPC, DMPC:cholesterol (8:2) and DMPC:DMPG (3:2). Consistently, the controls of the peptide-membrane interaction are the structure of the membrane core and the presence of phosphatidylglycerol lipids.

DLS measurements. In order to confirm membrane breakup/dissolution into mixed micelles at high peptide concentrations, DLS measurements have been carried out. DMPC liposomes formed by the method described above typically exhibit two populations: one at ~ 100 nm and a larger, broader size distribution centred at 300–400 nm. When this liposome suspension is exposed to 10 μ M melittin, two dominant populations are detected: monomeric peptides at ~ 1 nm of diameter and a distinct population of uniform sized micelles of approx. 20 nm. A third, small population of intact liposomes of ~ 300 nm diameter was also detected (Fig. S1). These results confirm the formation of mixed micelles/nanodisks as the product of membrane disruption. It should be noted that formation of such mixed micelles was reported before for mutants of magainin2 and melittin^{41,75}.

Mechanism

QCM fingerprints highlighted specific changes in the viscoelastic character of the peptide-membrane interaction, identifying distinct stages of the membrane disrupting process. The identification of these stages is, however, not straightforward, given the complexities of relating the viscoelastic characteristics to ensemble effects of molecular interactions. Therefore further considerations are required. Descriptions of the mechanism of melittin action focus on the final stage, i.e. the membrane poration; thus far not much attention was paid to the pathway that leads to this outcome. In the physicochemical sense the peptide traverses through a number of states characterized by different free energies resulting from the specific physical interactions between the peptide and its environment. Identifying these states helps to assign the viscoelastic trends seen in the QCM experiments.

Geometric analysis. To establish the physicochemical states of peptide membrane interaction, the membrane-inserted geometry of the peptide is a key clue, of which only indirect data is available in the literature; from the effect on the packing and interactions between the lipid tail groups it is inferred that melittin achieves membrane poration by inserting in a transmembrane manner^{15,76–80}. This is based on i) the fact that melittin forms pores without dissolving the membrane, and ii) its length of 26 amino acids, which is considered to be sufficient to form a membrane spanning α -helix. It is important to assess the validity of this argument. It is reported that melittin is unstructured in solution but becomes helical in the membrane environment⁸¹. In the accepted membrane disruption models the helical form is the prerequisite of membrane penetration and consecutive disruption, since helicity creates the longitudinal amphiphilic character of the N-terminal domain of the peptide. Melittin structure also exhibits a characteristic “kink” due to a proline residue. It is argued that the proline residue plays a key role in both the antimicrobial activity and the (undesired) cytotoxicity of the peptide⁸². Adjacent to the proline the C-terminal domain has a single apolar loop with a tryptophan residue, followed by a “tail” of charged residues.

In a membrane inserted monomeric state the mostly apolar regions of the peptide (residues 1–19) would reach energy minimum in the membrane core. It can be approximated that this helical segment is ~ 2.8 nm long⁸³. If this helix enters the hydrophobic membrane core, the tryptophan residue is located close to the ester moieties; by analogy to the role of aromatic rings in other peptides^{84–89} it is feasible to assume that the tryptophan side chain is associated with the esters. This anchoring effect and the following highly charged C-terminal segment that is likely associated to the phosphate moieties set a firm upper limit to membrane penetration at 2.8 nm. However it is unlikely that this helix is inserted normal to the membrane plane, given the polar residues occupying one side that likely retain some hydration and/or association to the polar headgroup area. If the helix is tilted to e.g. 45°, the insertion depth is reduced to ~ 2 nm. Hence the question is whether such a penetration depth is able to destabilize two membrane leaflets.

Neutron diffraction methods established that the hydrophobic thickness of the membrane core is 2.6–3.05 nm^{90–92}. At the lower limit, a vertically inserted peptide could bridge the two leaflets, however at the upper limit a tilted peptide may only interact with a single leaflet. A temperature-resolved Raman spectroscopy study using DMPC established that, even at a 14:1 lipid:peptide ratio, melittin interacts only with 5–7 lipid molecules, while simple geometrical considerations would suggest 14 nearest neighbours if the peptide penetrates both leaflets vertically⁹³. Based on this it is highly possible that there are circumstances where melittin molecules interact only with a single membrane leaflet. Potentially the tilt of the peptide depends on the strength of the interactions of the polar moieties of the N-terminal helix with the membrane headgroups, explaining the differences between the mammalian and bacterial-mimetic membranes. However, even if melittin does not insert in a transmembrane manner, it is well established that it disrupts most natural and biomimetic membranes. This suggests that melittin

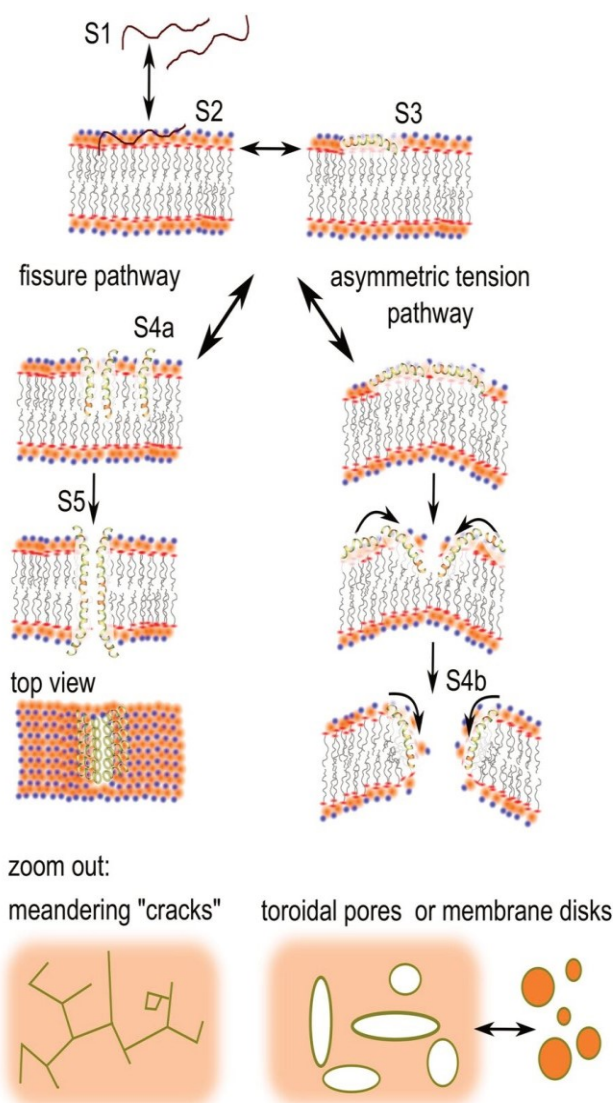


Figure 4. Hypothetic pathways of melittin pore forming mechanism. In the schematic representation of the lipid headgroups, red are ester, orange are phosphate and blue are choline moieties. The peptides are shown fully helical according to melittin crystal structure; it is likely that under physiological conditions the C-terminal segment is unstructured and in that form it directly associates to the lipid headgroups.

can trigger distortion of the membrane structure even if it is not in a transmembrane orientation. In the followings two hypotheses are presented to describe such a mechanism.

Fissure hypothesis. In terms of the mechanism, first the peptide has to adsorb to the membrane surface; this is a reversible dynamic process, yielding an equilibrium between the solvated (Fig. 4S1) and adsorbed (Fig. 4S2) states. The adsorbed peptide then folds into a helix (Fig. 4S3), in equilibrium with the unstructured S2 state. The folded peptide penetrates the membrane (Fig. 4S4a). Potentially, folding and penetration happen simultaneously, hence it is unclear whether S3 is a distinct state.

It should be assessed whether monomeric or aggregated forms are more likely to penetrate the membrane. The argument for the latter is that aggregation of amphiphiles is energetically favoured and it may promote membrane insertion by obscuring hydrophilic regions and exposing hydrophobic areas that would reduce the energy of the insertion into the hydrophobic membrane core. Such bundling-and-insertion process was described for the barrel-stave pore forming alamethicin^{94–96}. However, this is not consistent with a toroidal pore model where lipid molecules separate the peptides in the torus. Furthermore, if the peptides are still exposed to the aqueous environment on the membrane surface at the time of aggregation, it is more likely that the aggregation would be

driven by hydrophobic interaction, exposing the hydrophilic residues, and thus inhibiting insertion instead of promoting it. Hence, the membrane insertion is assumed to be in monomeric form in this pathway.

The peptides may also aggregate after insertion. Considering that the polar residues are distributed over ~23%⁹⁷ of the helix circumference, a dimeric, or even a circular aggregate would not be stable (i.e. melittin is unlikely to form a barrel-stave pore); however a linear aggregate is possible (Fig. 4S5). The formation of such linear aggregates may allow increased water penetration along these “cracks”.

Considering the shallow penetration of the peptide into the membrane, in the absence of a lipid torus it cannot open a pore, unless there is a pathway for the peptides to transfer to the inner leaflet. Direct transfer is energetically prohibited due to the high charge of the hydrophilic terminus. However it is possible that crack formation as per above would reduce the energy barrier and allow peptide flip-flopping to the inner leaflet, likely through density fluctuations (transient pores) along the crack. That way the cracks can potentially open into fissures, stabilized by arrays of peptides embedded in the opposite leaflets. There is microscopy evidence of the formation of such fissures⁵⁴. Importantly, this fissure model does not necessitate the formation of a toroidal structure, i.e. no need for lipid interdigitation between the peptides. The peptide transfer to the inner leaflet does not represent a different energetic state.

Asymmetric tension hypothesis. The formation of toroidal pores requires a different pathway. The peptide has to alter the membrane curvature, hence it has to remain associated with the headgroup zone (Fig. 4 right). This is possible in the presence of phosphatidylglycerol lipids that allow deeper water penetration into the headgroup zone due to the smaller size than the choline group of the neutral lipids, and the ability of water to hydrogen bond to the alcohol moieties of the glycerol. Water can thus access the side chains of the polar residues of the N-terminal helix of melittin and restrict their ability to “sink” into the hydrophobic membrane core. These side chains may also bind directly to the phosphate or ester oxygens of the lipids, as mentioned above. Thus melittin would act on the surface, remain embedded at the boundary between the apolar core and the headgroup zone, and, due to its size, apply lateral pressure to the outer leaflet. Continuous adhesion of peptides would introduce an increasing difference in the surface tension between the two membrane leaflets. When the difference reaches a threshold, the membrane would break, with a high likelihood that the peptides are carried into the breach, forming a toroidal pore; this is a distinct energetic state (Fig. 4S4b).

Interpretation of melittin action as a function of membrane composition. It is clear from the experimental data that melittin interaction, and hence the disruption pathway is a function of membrane composition. A key outcome of the experiments is that in domain separated membranes DMPC:cholesterol 9:1 and DMPC:DMPG 4:1 melittin interacts preferentially with one of the domains. Due to the similarity of the fingerprints to the neat DMPC case, melittin appears to preference the DMPC rich domain. Hence, in a competitive environment, the membrane-inserted state is the lower free energy state for melittin. According to the models outlined above, melittin can follow the fissure pathway in these cases, as in neat DMPC, including up to 4 membrane bound states (unstructured; structured on the surface; membrane penetrated; aggregated). The analysis of the f-D curves suggests that the first stage is a composite of the individually opposing dissipation trends of the population of the two surface bound and the membrane penetrated states, whereas the second stage is the result of crack formation. The membrane remains mostly intact.

It is also clear that DMPC:DMPG (3:2) case shows melittin as a surface acting peptide that breaches the membrane once a certain surface concentration is reached; it follows the asymmetric tension pathway through the surface bound unstructured, surface bound structured and torus bound states (the latter one would differ in free energy due to the altered local membrane curvature). The first two, as in case of the fissure pathway, cannot be distinguished from the viscoelastic fingerprints, yielding the first stage of the mechanism; the second stage is consistent with pore opening. The third stage is thus the collapse of the membrane back to the sensor surface as seen, and explained, with other surface acting peptides^{64,70}.

DLS results confirmed the dissolution of the membrane into uniform sized mixed micelles. While literature normally classifies the peptides into pore formers and carpet-like membrane disruptors, it is easy to see that the mechanism can switch between the two as a function of peptide concentration. The edge of the “toroidal pore” can have convex or concave curvatures; structurally and energetically it is not much different from a peptide-stabilized membrane nanodisc (Fig. 4 bottom right). Therefore, it is highly likely that high concentrations of the peptide can invert the pore structure into a series of islands. The same is true for the fissures described above. Hence at high peptide concentration melittin may dissolve the membrane; cracks in a melittin-exposed DMPC:DMPG (4:1) membrane have been imaged before⁵⁴.

Melittin action was much attenuated and slightly altered in unsaturated or high cholesterol content (8:2) membranes compared to neat DMPC. It is likely that this is a simple effect of a physical obstruction. In both cases the membrane core is less accessible to the peptide hence the membrane inserted monomeric state has a higher free energy than in neat saturated lipids, shifting the equilibrium towards the surface bound state. Co-existence of the two states explains the brief [-f, 0] trendline. The second stage of the QCM fingerprints is thus the result of retaining a substantial population of peptides in the headgroup zone and concomitant modulation of membrane tension (blistering), but dampened by the presence of a population of membrane inserted peptides, explaining the observed limitation of the dissipative processes. The final stage indicates the collapsed membrane as discussed before.

Conclusion

The action of melittin on different lipids and mixtures was characterized by using dye leakage and QCM fingerprinting measurements. The results demonstrate that melittin is able to breach all type of membranes: neutral and charged, made of saturated or unsaturated lipids, and irrespective of whether the membranes contained cholesterol. The QCM results revealed melittin-membrane interaction is a multi-step process, and that melittin can

follow different disrupting pathways in different membranes, switching between a surface acting and an inserting mode. The main controls of the mode of action were identified as the presence or absence of phosphatidylglycerol and the structure of the membrane core. It was noted that in domain separated membranes melittin shows a preference for the DMPC-rich domain. The data allowed the construction of two hypothetical disruption models: the fissure-forming model describing a membrane penetrating pathway and the asymmetric tension model leading to toroidal pores through surface action.

References

- Cohen, M. L. & Tauxe, R. V. Drug-resistant Salmonella in the United States: an epidemiologic perspective. *Science* **234**, 964–969 (1986).
- Hancock, R. E. & Sahl, H.-G. Antimicrobial and host-defense peptides as new anti-infective therapeutic strategies. *Nat. Biotechnol.* **24**, 1551–1557 (2006).
- Conlon, J. M. & Sonnevend, A. Antimicrobial peptides in frog skin secretions. *Antimicrob. Peptide Methods Protoc.*, 3–14 (2010).
- Zaslouff, M. Antimicrobial peptides of multicellular organisms. *Nature* **415**, 389–395 (2002).
- Hancock, R. E. & Diamond, G. The role of cationic antimicrobial peptides in innate host defences. *Trends Microbiol.* **8**, 402–410 (2000).
- Dürr, U. H., Sudheendra, U. & Ramamoorthy, A. LL-37, the only human member of the cathelicidin family of antimicrobial peptides. *Biochim. Biophys. Acta* **1758**, 1408–1425 (2006).
- Henzler Wildman, K. A., Lee, D.-K. & Ramamoorthy, A. Mechanism of lipid bilayer disruption by the human antimicrobial peptide, LL-37. *Biochemistry* **42**, 6545–6558 (2003).
- Oršolić, N. Bee venom in cancer therapy. *Cancer Metastasis Rev.* **31**, 173–194 (2012).
- Ali, M. A. A.-S. M. Studies on bee venom and its medical uses. *Int. J. Advancements Res. Technol.* **1**, 69–83 (2012).
- Son, D. J. *et al.* Therapeutic application of anti-arthritis, pain-releasing, and anti-cancer effects of bee venom and its constituent compounds. *Pharmacol. Ther.* **115**, 246–270 (2007).
- Blondelle, S. E. & Houghton, R. A. Hemolytic and antimicrobial activities of the twenty-four individual omission analogs of melittin. *Biochemistry* **30**, 4671–4678 (1991).
- Tossi, A., Sandri, L. & Giangaspero, A. Amphipathic, α -helical antimicrobial peptides. *Pept. Sci.* **55**, 4–30 (2000).
- Issam, A.-A., Zimmermann, S., Reichling, J. & Wink, M. Pharmacological synergism of bee venom and melittin with antibiotics and plant secondary metabolites against multi-drug resistant microbial pathogens. *Phytomedicine* **22**, 245–255 (2015).
- Terwilliger, T. C., Weissman, L. & Eisenberg, D. The structure of melittin in the form I crystals and its implication for melittin's lytic and surface activities. *Biophys. J.* **37**, 353 (1982).
- Naito, A. *et al.* Conformation and dynamics of melittin bound to magnetically oriented lipid bilayers by solid-state ³¹P and ¹³C NMR spectroscopy. *Biophys. J.* **78**, 2405–2417 (2000).
- Terwilliger, T. C. & Eisenberg, D. The structure of melittin. I. Structure determination and partial refinement. *J. Biol. Chem.* **257**, 6010–6015 (1982).
- BAZZO, R. *et al.* The structure of melittin. *Eur. J. Biochem.* **173**, 139–146 (1988).
- Oren, Z. & Shai, Y. Selective lysis of bacteria but not mammalian cells by diastereomers of melittin: structure–function study. *Biochemistry* **36**, 1826–1835 (1997).
- Sharma, V. K., Mamontov, E., Anunciado, D. B., O'Neill, H. & Urban, V. S. Effect of antimicrobial peptide on the dynamics of phosphocholine membrane: role of cholesterol and physical state of bilayer. *Soft Matter* **11**, 6755–6767 (2015).
- Papo, N. & Shai, Y. Exploring peptide membrane interaction using surface plasmon resonance: differentiation between pore formation versus membrane disruption by lytic peptides. *Biochemistry* **42**, 458–466 (2003).
- Steckbeck, J. D., Deslouches, B. & Montelaro, R. C. *Antimicrobial peptides: new drugs for bad bugs?* (Taylor & Francis, 2014).
- Brogden, K. A. Antimicrobial peptides: pore formers or metabolic inhibitors in bacteria? *Nat. Rev. Microbiol.* **3**, (238) (2005).
- Galdiero, S. *et al.* Peptide-lipid interactions: experiments and applications. *Int. J. Mol. Sci.* **14**, 18758–18789 (2013).
- Fjell, C. D., Hiss, J. A., Hancock, R. E. & Schneider, G. Designing antimicrobial peptides: form follows function. *Nat. Rev. Drug Discov.* **11**, 37–51, <https://doi.org/10.1038/nrd3591> (2011).
- Sun, D., Forsman, J. & E Woodward, C. Current understanding of the mechanisms by which membrane-active peptides permeate and disrupt model lipid membranes. *Curr. Top. Med. Chem.* **16**, 170–186 (2016).
- Matsuzaki, K., Yoneyama, S. & Miyajima, K. Pore formation and translocation of melittin. *Biophys. J.* **73**, 831–838 (1997).
- Allende, D., Simon, S. & McIntosh, T. J. Melittin-induced bilayer leakage depends on lipid material properties: evidence for toroidal pores. *Biophys. J.* **88**, 1828–1837 (2005).
- Heitz, F., Morris, M. C. & Divita, G. Twenty years of cell-penetrating peptides: from molecular mechanisms to therapeutics. *Br. J. Pharmacol.* **157**, 195–206 (2009).
- Tamba, Y., Ariyama, H., Levadny, V. & Yamazaki, M. Kinetic pathway of antimicrobial peptide magainin 2-induced pore formation in lipid membranes. *J. Phys. Chem. B* **114**, 12018–12026 (2010).
- Melo, M. N., Ferre, R. & Castanho, M. A. Antimicrobial peptides: linking partition, activity and high membrane-bound concentrations. *Nat. Rev. Microbiol.* **7**, 245 (2009).
- Mechler, A. *et al.* Specific and selective peptide-membrane interactions revealed using quartz crystal microbalance. *Biophys. J.* **93**, 3907–3916 (2007).
- Milov, A. D. *et al.* PELDOR conformational analysis of bis-labeled alamethicin aggregated in phospholipid vesicles. *J. Phys. Chem. B* **112**, 13469–13472 (2008).
- Ding, B. & Chen, Z. Molecular interactions between cell penetrating peptide Pep-1 and model cell membranes. *J. Phys. Chem. B* **116**, 2545–2552, <https://doi.org/10.1021/jp209604m> (2012).
- Lee, D.-K. *et al.* Lipid composition-dependent membrane fragmentation and pore-forming mechanisms of membrane disruption by pexiganan (MSI-78). *Biochemistry* **52**, 3254–3263 (2013).
- Porcelli, F. *et al.* Structure and orientation of pardaxin determined by NMR experiments in model membranes. *J. Biol. Chem.* **279**, 45815–45823 (2004).
- Smith, R., Separovic, F., Bennett, F. & Cornell, B. Melittin-induced changes in lipid multilayers. A solid-state NMR study. *Biophys. J.* **63**, 469–474 (1992).
- Jamasbi, E., Mularski, A. & Separovic, F. Model membrane and cell studies of antimicrobial activity of melittin analogues. *Curr. Top. Med. Chem.* **16**, 40–45 (2016).
- Balla, M., Bowie, J. & Separovic, F. Solid-state NMR study of antimicrobial peptides from Australian frogs in phospholipid membranes. *Eur. Biophys. J.* **33**, 109–116 (2004).
- Separovic, F. & Naito, A. *Advances in Biological Solid-State NMR: Proteins and Membrane-Active Peptides*. (Royal Society of Chemistry, 2014).
- Ramamoorthy, A., Thennarasu, S., Lee, D.-K., Tan, A. & Maloy, L. Solid-state NMR investigation of the membrane-disrupting mechanism of antimicrobial peptides MSI-78 and MSI-594 derived from magainin 2 and melittin. *Biophys. J.* **91**, 206–216 (2006).

41. Hallock, K. J., Lee, D.-K. & Ramamoorthy, A. MSI-78, an analogue of the magainin antimicrobial peptides, disrupts lipid bilayer structure via positive curvature strain. *Biophys. J.* **84**, 3052–3060 (2003).
42. Pott, T., Dufourcq, J. & Dufourc, E. Fluid or gel phase lipid bilayers to study peptide-membrane interactions? *Eur. Biophys. J.* **25**, 55–59 (1996).
43. Guha, S., Ghimire, J., Wu, E. & Wimley, W. C. Mechanistic Landscape of Membrane-Permeabilizing Peptides. *Chem. Rev.* **119**, 6040–6085 (2019).
44. Rex, S. Pore formation induced by the peptide melittin in different lipid vesicle membranes. *Biophys. Chem.* **58**, 75–85 (1996).
45. Yang, L., Harroun, T. A., Weiss, T. M., Ding, L. & Huang, H. W. Barrel-stave model or toroidal model? A case study on melittin pores. *Biophys. J.* **81**, 1475–1485 (2001).
46. Park, S.-C. *et al.* Investigation of toroidal pore and oligomerization by melittin using transmission electron microscopy. *Biochem. Biophys. Res. Commun.* **343**, 222–228 (2006).
47. Sengupta, D., Leontiadou, H., Mark, A. E. & Marrink, S.-J. Toroidal pores formed by antimicrobial peptides show significant disorder. *Biochim. Biophys. Acta* **1778**, 2308–2317 (2008).
48. Mihajlovic, M. & Lazaridis, T. Antimicrobial peptides in toroidal and cylindrical pores. *Biochim. Biophys. Acta* **1798**, 1485–1493 (2010).
49. Lee, M.-T., Sun, T.-L., Hung, W.-C. & Huang, H. W. Process of Inducing Pores in Membranes by Melittin. *Biophys. J.* **106**, 293a (2014).
50. Vogel, H. & Jähnig, F. The structure of melittin in membranes. *Biophys. J.* **50**, 573–582 (1986).
51. Irudayam, S. J. & Berkowitz, M. L. Influence of the arrangement and secondary structure of melittin peptides on the formation and stability of toroidal pores. *Biochim. Biophys. Acta* **1808**, 2258–2266 (2011).
52. Lin, J.-H. & Baumgaertner, A. Stability of a melittin pore in a lipid bilayer: a molecular dynamics study. *Biophys. J.* **78**, 1714–1724 (2000).
53. Van Den Bogaart, G., Mika, J. T., Krasnikov, V. & Poolman, B. The lipid dependence of melittin action investigated by dual-color fluorescence burst analysis. *Biophys. J.* **93**, 154–163 (2007).
54. Lee, T.-H. *et al.* In *Peptides for Youth* 313–315 (Springer, 2009).
55. Rodahl, M., Höök, F., Krozer, A., Brzezinski, P. & Kasemo, B. Quartz crystal microbalance setup for frequency and Q-factor measurements in gaseous and liquid environments. *Rev. Sci. Instrum.* **66**, 3924–3930 (1995).
56. Rodahl, M. *et al.* Simultaneous frequency and dissipation factor QCM measurements of biomolecular adsorption and cell adhesion. *Faraday Discuss.* **107**, 229–246 (1997).
57. Cho, N.-J., Frank, C. W., Kasemo, B. & Höök, F. Quartz crystal microbalance with dissipation monitoring of supported lipid bilayers on various substrates. *Nat. Protoc.* **5**, 1096 (2010).
58. Voinova, M., Jonson, M. & Kasemo, B. 'Missing mass' effect in biosensor's QCM applications. *Biosens. Bioelectron.* **17**, 835–841 (2002).
59. Mechler, A. *et al.* Structure and homogeneity of pseudo-physiological phospholipid bilayers and their deposition characteristics on carboxylic acid terminated self-assembled monolayers. *Biomaterials* **30**, 682–689, <https://doi.org/10.1016/j.biomaterials.2008.10.016> (2009).
60. Piantavigna, S. *et al.* Cell penetrating apidaecin peptide interactions with biomimetic phospholipid membranes. *Int. J. Pept. Res. Ther.* **15**, 139–146 (2009).
61. Praporski, S., Mechler, A., Separovic, F. & Martin, L. L. Subtle differences in initial membrane interactions underpin the selectivity of small antimicrobial peptides. *ChemPlusChem* **80**, 91–96 (2015).
62. Knappe, D. *et al.* Oncocin (VDKPPYLPRPPRRRIYNR-NH₂): a novel antibacterial peptide optimized against gram-negative human pathogens. *J. Med. Chem.* **53**, 5240–5247 (2010).
63. McCubbin, G. A. *et al.* QCM-D fingerprinting of membrane-active peptides. *Eur. Biophys. J.* **40**, 437–446 (2011).
64. Shahmiri, M., Enciso, M. & Mechler, A. Controls and constraints of the membrane disrupting action of Aurein 1.2. *Sci. Rep.* **5**, 16378 (2015).
65. Lee, T.-H., Heng, C., Separovic, F. & Aguilar, M.-I. Comparison of reversible membrane destabilisation induced by antimicrobial peptides derived from Australian frogs. *Biochim. Biophys. Acta* **1838**, 2205–2215 (2014).
66. Fernandez, D. I., Lee, T.-H., Sani, M.-A., Aguilar, M.-I. & Separovic, F. Proline facilitates membrane insertion of the antimicrobial peptide maculatin 1.1 via surface indentation and subsequent lipid disordering. *Biophys. J.* **104**, 1495–1507 (2013).
67. Lee, T.-H. *et al.* Real-time quantitative analysis of lipid disordering by aurein 1.2 during membrane adsorption, destabilisation and lysis. *Biochim. Biophys. Acta* **1798**, 1977–1986 (2010).
68. Separovic, F., Gehman, J. D., Lee, T.-H., Bowie, J. H. & Aguilar, M.-I. Effect of Antimicrobial Peptides from Australian Tree Frogs on Anionic Phospholipid Membranes. *Biophys. J.* **96**, 156a (2009).
69. Hasan, I. Y. & Mechler, A. Viscoelastic changes measured in partially suspended single bilayer membranes. *Soft Matter* **11**, 5571–5579, <https://doi.org/10.1039/c5sm00278h> (2015).
70. Shahmiri, M. *et al.* Membrane Core-Specific Antimicrobial Action of Cathelicidin LL-37 Peptide Switches Between Pore and Nanofibre Formation. *Sci. Rep.* **6**, 38184, <https://doi.org/10.1038/srep38184> (2016).
71. Wang, K. F., Nagarajan, R. & Camesano, T. A. Differentiating antimicrobial peptides interacting with lipid bilayer: molecular signatures derived from quartz crystal microbalance with dissipation monitoring. *Biophys. Chem.* **196**, 53–67 (2015).
72. Joshi, T., Voo, Z. X., Graham, B., Spiccia, L. & Martin, L. L. Real-time examination of aminoglycoside activity towards bacterial mimetic membranes using Quartz Crystal Microbalance with Dissipation monitoring (QCM-D). *Biochim. Biophys. Acta* **1848**, 385–391 (2015).
73. Hasan, I. Y. & Mechler, A. Cholesterol Rich Domains Identified in Unilamellar Supported Biomimetic Membranes via Nano-Viscosity Measurements. *Anal. Chem.* **88**, 5037–5041 (2016).
74. Arsov, Z. *et al.* Cholesterol prevents interaction of the cell-penetrating peptide transportan with model lipid membranes. *J. Pept. Sci.* **14**, 1303–1308 (2008).
75. Lee, D.-K., Bhunia, A., Kotler, S. A. & Ramamoorthy, A. Detergent-type membrane fragmentation by MSI-78, MSI-367, MSI-594, and MSI-843 antimicrobial peptides and inhibition by cholesterol: a solid-state nuclear magnetic resonance study. *Biochemistry* **54**, 1897–1907 (2015).
76. Frey, S. & Tamm, L. K. Orientation of melittin in phospholipid bilayers. A polarized attenuated total reflection infrared study. *Biophys. J.* **60**, 922–930 (1991).
77. Chen, X., Wang, J., Boughton, A. P., Kristalyn, C. B. & Chen, Z. Multiple orientation of melittin inside a single lipid bilayer determined by combined vibrational spectroscopic studies. *J. Am. Chem. Soc.* **129**, 1420–1427 (2007).
78. Vogel, H., Jähnig, F., Hoffmann, V. & Stümpel, J. The orientation of melittin in lipid membranes. A polarized infrared spectroscopy study. *Biochim. Biophys. Acta* **733**, 201–209 (1983).
79. Brown, L. R., Braun, W., Kumar, A. & Wüthrich, K. High resolution nuclear magnetic resonance studies of the conformation and orientation of melittin bound to a lipid-water interface. *Biophys. J.* **37**, 319–328 (1982).
80. Smith, R. *et al.* Structure and orientation of the pore-forming peptide melittin, in lipid bilayers. *J. Mol. Biol.* **241**, 456–466 (1994).
81. Vogel, H. Incorporation of melittin into phosphatidylcholine bilayers. *FEBS Lett.* **134**, 37–42 (1981).
82. Jamasbi, E. *et al.* Melittin peptides exhibit different activity on different cells and model membranes. *Amino Acids* **46**, 2759–2766 (2014).

83. Eisenberg, D., Weiss, R. M. & Terwilliger, T. C. The helical hydrophobic moment: a measure of the amphiphilicity of a helix. *Nature* **299**, 371 (1982).
84. Hong, H., Park, S., Flores Jiménez, R. H., Rinehart, D. & Tamm, L. K. Role of aromatic side chains in the folding and thermodynamic stability of integral membrane proteins. *J. Am. Chem. Soc.* **129**, 8320–8327 (2007).
85. Haug, B. E. & Svendsen, J. S. The role of tryptophan in the antibacterial activity of a 15-residue bovine lactoferricin peptide. *J. Pept. Sci.* **7**, 190–196 (2001).
86. Haney, E. F., Lau, F. & Vogel, H. J. Solution structures and model membrane interactions of lactoferrampin, an antimicrobial peptide derived from bovine lactoferrin. *Biochim. Biophys. Acta* **1768**, 2355–2364 (2007).
87. Chan, D. L., Prenner, E. J. & Vogel, H. J. Tryptophan- and arginine-rich antimicrobial peptides: structures and mechanisms of action. *Biochim. Biophys. Acta* **1758**, 1184–1202 (2006).
88. Haug, B. E., Skar, M. L. & Svendsen, J. S. Bulky aromatic amino acids increase the antibacterial activity of 15-residue bovine lactoferricin derivatives. *J. Pept. Sci.* **7**, 425–432 (2001).
89. Wang, G., Li, Y. & Li, X. Correlation of three-dimensional structures with the antibacterial activity of a group of peptides designed based on a nontoxic bacterial membrane anchor. *J. Biol. Chem.* **280**, 5803–5811 (2005).
90. Douliez, J.-P., Léonard, A. & Dufourc, E. J. Conformational order of DMPC sn-1 versus sn-2 chains and membrane thickness: an approach to molecular protrusion by solid state ²H-NMR and neutron diffraction. *J. Phys. Chem.* **100**, 18450–18457 (1996).
91. Kučerka, N., Kiselev, M. A. & Balgavý, P. Determination of bilayer thickness and lipid surface area in unilamellar dimyristoylphosphatidylcholine vesicles from small-angle neutron scattering curves: a comparison of evaluation methods. *Eur. Biophys. J.* **33**, 328–334 (2004).
92. Cornell, B. & Separovic, F. Membrane thickness and acyl chain length. *Biochim. Biophys. Acta* **733**, 189–193 (1983).
93. Lavialle, F., Levin, I. W. & Mollay, C. Interaction of melittin with dimyristoyl phosphatidylcholine liposomes. Evidence for boundary lipid by Raman spectroscopy. *Biochim. Biophys. Acta* **600**, 62–71 (1980).
94. He, K., Ludtke, S. J., Worcester, D. L. & Huang, H. W. Neutron scattering in the plane of membranes: structure of alamethicin pores. *Biophys. J.* **70**, 2659–2666 (1996).
95. Sansom, M. Alamethicin and related peptaibols—model ion channels. *Eur. Biophys. J.* **22**, 105–124 (1993).
96. Hanke, W. & Boheim, G. The lowest conductance state of the alamethicin pore. *Biochim. Biophys. Acta* **596**, 456–462 (1980).
97. White, S. H. & Wimley, W. C. Hydrophobic interactions of peptides with membrane interfaces. *Biochim. Biophys. Acta* **1376**, 339–352 (1998).

Author Contributions

S.P. performed all experiments, analysed data and drafted the manuscript. A.M. devised the project, supervised the experimental work and data analysis and finalized the manuscript.

Additional Information

Supplementary information accompanies this paper at <https://doi.org/10.1038/s41598-019-47325-y>.

Competing Interests: The authors declare no competing interests.

Publisher's note: Springer Nature remains neutral with regard to jurisdictional claims in published maps and institutional affiliations.



Open Access This article is licensed under a Creative Commons Attribution 4.0 International License, which permits use, sharing, adaptation, distribution and reproduction in any medium or format, as long as you give appropriate credit to the original author(s) and the source, provide a link to the Creative Commons license, and indicate if changes were made. The images or other third party material in this article are included in the article's Creative Commons license, unless indicated otherwise in a credit line to the material. If material is not included in the article's Creative Commons license and your intended use is not permitted by statutory regulation or exceeds the permitted use, you will need to obtain permission directly from the copyright holder. To view a copy of this license, visit <http://creativecommons.org/licenses/by/4.0/>.

© The Author(s) 2019

Part 2:

Membrane morphology effects in
quartz crystal microbalance
characterization of antimicrobial
peptide activity

Biophysical Chemistry: in press

Membrane morphology effects in quartz crystal microbalance characterization of antimicrobial peptide activity

Sara Pandidan and Adam Mechler

La Trobe Institute for Molecular Science, La Trobe University, Melbourne, Australia

Abstract

The mechanism of action of membrane disrupting antimicrobial peptides (AMPs) and the basis of their specificity and selectivity to pathogens are often studied by using biomimetic model membranes. It is often assumed that all model membrane morphologies, e.g. liposomes, supported bilayers, tethered bilayers etc. are equivalent. In this work the validity of this assumption was assessed. Melittin was used as the reference AMP as it can disrupt both bacterial and mammalian-mimetic membranes. Quartz crystal microbalance (QCM) viscoelastic fingerprints show characteristic differences between the three model morphologies: single bilayer membranes, multilamellar membrane stacks and unilamellar liposomes. In the second and third case, initial trends show material removal instead of material addition as in the single bilayer case, consistent with dissolution of some bilayers, and bursting liposomes, respectively. The latter is accompanied by a characteristic drop in the dissipation signal as the liposomes collapse. The results also highlight an important limitation of the QCM method, the need for a well established reference system for qualitative analysis of the viscoelastic fingerprints, and thus the importance of using the right model system, i.e. single bilayer membrane, for studies of the mechanism of action of AMPs.

Introduction

The increasing prevalence of multidrug-resistant strains of bacteria has grown into one of the most important public health issues during the past decades[1]. Antimicrobial peptides (AMPs) offer an alternative to traditional antibiotics, as they can provide effective, non-specific defence against infections with low probability of induced resistance [2-4]. AMPs are produced by all organisms, from prokaryotes to mammals and even humans [5, 6].

However, AMPs are often haemolytic, hence there is a consensus that they are only suitable as topical and/or last minute emergency drugs[7]. Nevertheless, there is a steady effort of re-engineering AMPs into better drug candidates; this necessitates an in-depth understanding of their mechanism of action and the molecular basis of their specificity and selectivity[8, 9]. Studies to this effect regularly resort to *in vitro* methods and the use of biomimetic membrane systems.

In vitro studies necessarily have to rely on model membranes specifically suited to the characterization methods. Some common model membrane systems are supported bilayers, tethered bilayers [10], hydrated bulk lipid phases [11] and liposome suspensions [12]. The equality of all membrane morphologies is often assumed, even though there are indications that the morphology of the model membrane can influence the mechanism: it was reported that membrane binding affinity of some AMPs is affected by surface morphology[13, 14], and that multilamellar membranes can affect QCM characterization of AMPs[15-17].

A well-known membrane-active peptide secreted by honeybee (*Apis mellifera*) is melittin [18-20], essentially a venom with strong haemolytic action[21], but mostly known as an antimicrobial peptide in the literature as it shows strong activity against most bacterial strains [22, 23]. Melittin is perhaps the best known and most widely studied AMP, yet uncertainty persists about the way it disrupts membranes [24-28]. Most, but not all sources agree that it is a pore former [29-35]. Initially it was argued that melittin forms barrel-stave pores based on measurements using unilamellar vesicles of 12-53 nm diameter formed from unsaturated lipids [36]. However characteristics of toroidal pores were identified by several studies, e.g. in multiple bilayers studied by neutron diffraction [30] and by Raman spectroscopy on ditetradecyl glycerol phosphocholine (DPTC) membrane [29]. A study based on surface plasmon resonance measurements in bilayers and hybrid lipid monolayers argued that the peptide has different mechanism as a function of membrane composition, forming barrel-stave pores in zwitterionic membranes and acting detergent-like in anionic membranes [37]. An atomic force microscopy (AFM) study introduced a new model for melittin, a mixed carpet-toroidal pathway, and the peptide shows higher tendency to insert into curved regions of bilayer[14]. A solid-state NMR study identified nearly normal insertion and consecutive pore formation that leads to the formation of disc-type micelles and thus membrane

fragmentation[38]. A few studies came to opposing conclusions: finding similarity in the binding results on bilayer and monolayer membranes, the authors argued that the peptide does not interact with the hydrophobic core region of the membrane at all, and prefers localizing on the surface acting *via* carpet mechanism [39, 40]. A study by solid-state NMR on MSI_594, a hybrid of melittin, revealed nearly parallel orientation of peptide to the bilayer surface, suggesting carpet mechanism for membrane disruption [41]. An AFM imaging study showed evidence that in supported DMPC:DMPG (4:1) membrane melittin does not follow any of the suggested pathways, rather it opens fissures [42]. This was corroborated by QCM and dye leakage experiments[43]. Thus, there is a confusing array of results about the activity of melittin in the literature, depending on the experimental conditions, as it was also highlighted before by other authors [44].

Comparison of the experimental methodologies in these studies reveals that almost each work used a different model membrane, not only in terms of composition but also in morphology. This appears to be the only aspect of methodology that has not been addressed systematically thus far; it is, therefore, important to understand how the membrane model system influences the observation of membrane interactions of AMPs. Our prior QCM study of the mechanism of action of melittin on different model membranes[43] offers a suitable basis for a study of the role of membrane morphologies.

1. Materials and Methods

1.1. Buffer preparation

The assay buffer was phosphate buffered saline (PBS) containing 20mM phosphate and 100mM NaCl at pH 7.2. 18.2 MΩcm deionized water was used to prepare the solutions, deionized by an Utrapure system (Sartorius AG, Germany). Potassium dihydrogen phosphate (Fluka branded) was purchased from Sigma Aldrich (Castle Hill, NSW, Australia); potassium hydrogen phosphate was purchased from Honeywell (Shanghai, China), and sodium chloride (NaCl) was purchased from Chem-Supply Pty Ltd (Gillman SA, Australia).

1.2. Liposome preparation

Dimyristoyl lipids have been used extensively for characterizing AMP action by us and others and thus our work will focus on this group of lipids [15-17, 26, 28, 42, 44-46]. 1,2-dimyristoyl-sn-glycero-3-phosphocholine (DMPC) and sodium salt of 1,2-dimyristoyl-sn-

glycero-3-phosphoglycerol (DMPG) were purchased from Avanti Polar Lipids (Alabaster, AL, USA). The lipids were dissolved in chloroform (ACS Reagent, 99.8%) and in case of DMPG 3% methanol (>99.9%, spectrophotometric grade) was also added, both solvents were purchased from Sigma-Aldrich (Castle Hill, NSW, Australia). Lipid films were prepared by mixing the desired lipid compositions in cleaned test tube and evaporating the solvent under a gentle stream of nitrogen gas with continuous vortexing. 0.1 μ mol amounts of lipid were measured out in each tube. The lipid films were placed in a desiccator overnight. Liposome suspensions were formed as described before: the lipid films were hydrated in 1 ml PBS to yield a 0.1mM lipid concentration, incubated for 30 min at 37°C, followed by 1 min gentle vortexing and 1 min sonication. This protocol yields a suspension containing mostly unilamellar liposomes [45].

1.3. Quartz Crystal Microbalance

All measurements were performed using a Q-Sense E4 instrument (Q-Sense, Sweden), with gold-coated AT-cut quartz sensors, with a fundamental resonance frequency of 5 MHz. The QCM sensors were cleaned with a mixture of one part hydrogen peroxide (aqueous solution, 30%) purchased from ChemSupply Pty Ltd, Australia, Gillman, SA; one part ammonia solution (28-30%) purchased from Merck, Darmstadt Germany, and three parts of deionized water, heated to 70°C for 20 minutes. This is known as the base piranha solution and is extremely dangerous when activated, should be handled with appropriate precautions. The cleaned sensors were washed with deionized water, dried and modified with a solution of 2% 3-mercaptopropionic acid (MPA) (HPLC Grade, >99%, Fluka branded product from Sigma Aldrich, Castle Hill, NSW, Australia) in 2-propanol (HPLC Plus 99.9% from Sigma Aldrich) overnight. Before using the modified sensors, in order to remove any excess thiol from the surface, sensors were rinsed in propan-2-ol solution. After drying, the sensors were soaked in deionized water for a few hours before starting the experiment.

1.4. Lipid deposition and fingerprinting assays

After installing the MPA modified chips in to the QCM chambers, baselines were recorded in deionized water and then in PBS as reference and for verifying the stability of the sensor

signals. Afterwards the lipid solutions were added at 19°C at a flow rate of 50 $\mu\text{L}/\text{min}$. The key methodology follows our pervious article [43]. The Δf and ΔD values corresponding to single bilayer membranes ($\Delta f = \sim 13$ Hz and $\Delta D = \sim 3 \times 10^{-6}$) were established before [47, 48]. To ensure the deposit does not contain any intact liposomes, once these parameters were reached the measurement chamber was flushed with phosphate buffer solution without added NaCl in order to rupture any unopened liposomes by means of osmotic stress. To form liposome-containing deposits, the osmotic stress was completely omitted.

Multiple bilayers were prepared by sequential addition of, batches of liposome suspension alternated with osmotic stress, until stacks of three bilayers were obtained. The structure is confirmed from proportional increase in both Δf and ΔD to multiples of a single bilayer membrane [45]. Any liposome content would lead to higher dissipation values [48].

In all cases, PBS with 100 mM NaCl was used as the assay buffer. The representative sensograms of the frequency and dissipation changes against time for liposome containing deposition, single and multiple stacks bilayer can be seen in the supplementary material (S1). Table 1 shows the approximate average Δf and ΔD values for each membrane type used in this study. For multilayer structures the aim was to obtain three complete bilayers (i.e. 3 x the Δf and ΔD values of a single bilayer membrane). In case of liposome containing membranes, the actual continuous bilayer content is hard to define, given the large mass and dissipation contribution of liposomes; however by keeping the deposited mass low (with high dissipation) it was ascertained that the liposome content dominates the deposit. Importantly, the aim was not to form a vesicular layer that could have been achieved using a different support, rather to create a composite layer, modelling experimental conditions where liposomes remain in the membrane due to imperfect fusion.

Table 1. Typical Δf and ΔD values for the three studied membrane morphologies

	Single bilayer membrane	Multilamellar membrane (~3 bilayers)	Liposome containing membrane
Δf (Hz)	13-15	40-50	21-40
ΔD ($\times 10^{-6}$ arb. u.)	2-3	7-9	5-9

Before introducing the desired concentration of melittin (with 95.51% purity, purchased from GL Biochem Ltd., Shanghai), stable baseline was obtained in PBS in all cases. All experiments were repeated at least three times at 19°C and the frequency and dissipation changes were plotted only for four eigenmodes (3rd, 5th, 7th and 9th) that were shown to provide the most reliable results on lipid membrane [45]. The results were converted into Δf - ΔD curves known as viscoelastic fingerprints, in which any changes in the direction of the plot could be characteristic of different distinct trend lines [17]. It was shown previously by QCM that peptides that do not bind to membranes only cause a negligible shift in frequency and dissipation signals due to solution viscosity change; this effect is at least an order of magnitude lower than the changes observed for even the lowest concentrations of membrane binding peptides[48].

2. Results and discussions

2.1. Effect of membrane morphology on melittin-DMPC interactions

Figure 1 (panels a-d) shows the viscoelastic fingerprints of melittin interaction with multiple bilayer stacks (approx. three bilayers, as per above) of neat DMPC, compared to the fingerprints recorded in single bilayer membranes (Figure 1 panels e-h). The latter have been described and analysed before[43] and therefore here they are only shown for comparison. In case of multiple bilayers of DMPC the initial trend points toward [+f, -D] implying that the interaction starts with material removal, as opposed to the single bilayer case where the initial process is binding/penetration ([-f, -D] trend with very small dissipation change). This stage is followed by a [-f, +D] trendline that is similar to the second stage in the single bilayer case, although it does not yield the same mass uptake.

The initial material removal trendline suggests that bilayers on top of other bilayers interact differently with melittin than bilayers in direct contact with the support. The total frequency change of this first stage is ~6-7 Hz, i.e. much less than a complete bilayer. This could mean that bilayer islands are removed first; however, it is also feasible to assume that the material removal leads to peptide binding to the uncovered membrane surface, i.e. removal of material and further binding of peptides proceed in parallel. Therefore, the more likely explanation for the short removal trend is that the top bilayers break up continuously and once the top layers

are removed, the process becomes similar to the single bilayer case. Liposome deposition is prone to leave residual liposomes entrapped in the fused bilayer[45]. It is therefore important to assess the effect of such residual liposomes on the fingerprinting measurements. As seen in Figure 1, the f-D fingerprints of melittin action exhibit a dramatic difference between single bilayer and liposome containing deposits.

In the presence of the liposomes the initial trends are $\sim [0, -D]$: almost exclusively dissipation change, with a very small increase in frequency. This is consistent with bursting the highly dissipative liposomes. The lack of any mass loss is surprising at first. The water loss is expected to increase the frequency, whereas the collapse of the liposome to the surface leads to concomitant lipid mass increase. The balance of these two frequency trends depends on the

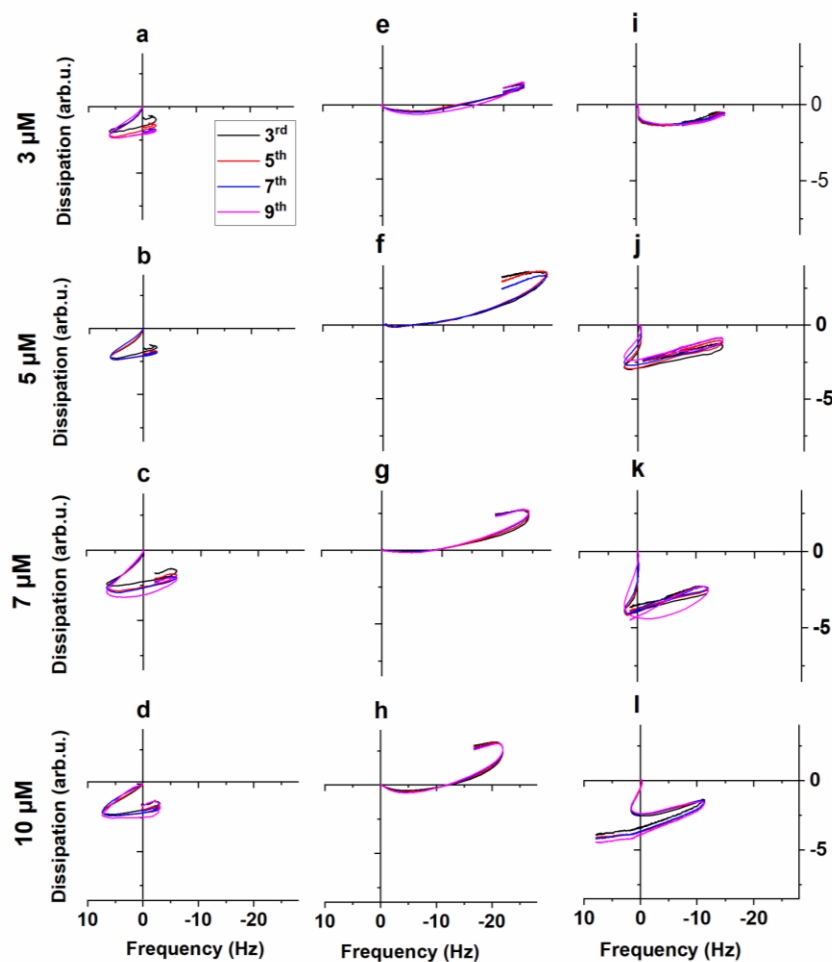


Fig 1 Comparison of viscoelastic fingerprints of the interaction of melittin with different DMPC membrane morphologies. (a-d) multiple bilayer stacks, (e-h) single bilayer membrane. (i-l) liposome containing deposit with 3 μ M, 5 μ M, 7 μ M, and 10 μ M melittin as indicated. Temperature 19°C, pH 7.2

size of the liposome. Small unilamellar liposomes (SUVs) are regularly used in vesicle deposition studies[49-51]. Here the membrane is bent at its persistence length[52], hence SUVs are rigid structures that mostly appear as added mass in QCM. In contrast, the membrane of a large unilamellar liposome is not geometrically constrained, allowing substantial membrane deformation[53]. Therefore, the shear wave produced by the QCM sensor oscillation could propagate nearly unhindered by the liposome-forming membrane, therefore the large liposomes mostly appear as viscous material. Hence, the entrapped water is in effect part of the environment and only a small fraction is measured as mass. The presence of such liposomes is obvious in dissipation, however, since the wobbling of the liposomes still dissipates energy. Therefore, the presence of the liposomes has a far more significant effect on the dissipation than the frequency channel.

Consistently, the first stage of the fingerprints is explained with peptide-induced bursting of

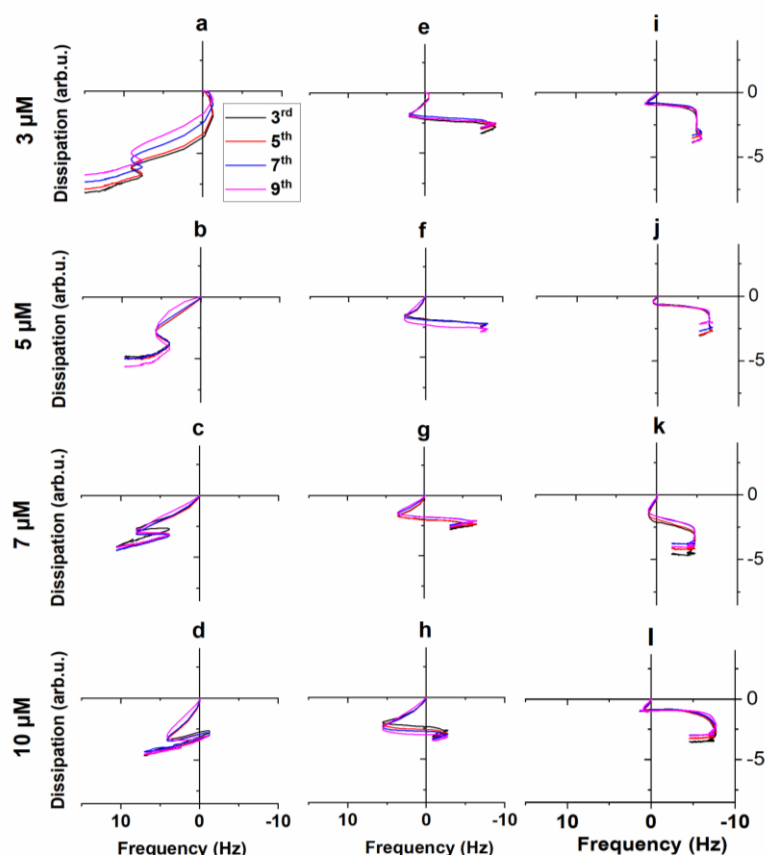


Fig 2 Comparison of viscoelastic fingerprints of interaction of melittin with different DMPC:DMPG (4:1) membrane morphologies as follows. (a-d) multiple bilayer stacks, (e-h) single bilayer, (i-l) liposome containing deposit with 3 μ M, 5 μ M, 7 μ M, and 10 μ M melittin as indicated. Temperature 19°C, pH 7.2

medium-large liposomes. The second stage is very similar to the single bilayer case, i.e. a binding trend; however, the third stage is net material removal, suggesting that the peptide can reach the inner leaflet of the “deflating” liposomes and that leads to easy dissolution of the membrane. This is the clearest in the 10 μM case. In case of the charged membrane, the difference is much less obvious, likely due to the ability of the peptide to target domain boundaries [43] and thus break up the liposomes before they collapse to the surface. It was reported before that melittin causes the formation of discs of phospholipid membranes in the gel-phase, which would be like inverted toroidal pores[26, 43]

2.2. Effect of membrane morphology on melittin – DMPC:DMPG 4:1 interactions

The peptide interaction with multiple bilayers of DMPC: DMPG (4:1) (Figure 2 a-d) starts with a [+f, -D] mass loss trend line in both cases, however in the multiple bilayer case the trend is longer; it terminates in a sudden “zigzag” [-f,-D] pattern before continuing in [+f, -D] direction, apparently lacking the [-f,0] collapse stage as in a single bilayer. The beginning of the [-f,-D] trendline is at $\sim 8\text{-}10\text{Hz}$, when a substantial amount of the top bilayer is already removed; therefore it is arguable that the zigzag is the indication of partial collapse of the membrane, which is however continuing in removal of more material, i.e. removal of an underlying membrane once the top bilayer is dissolved. Considering that at the beginning of

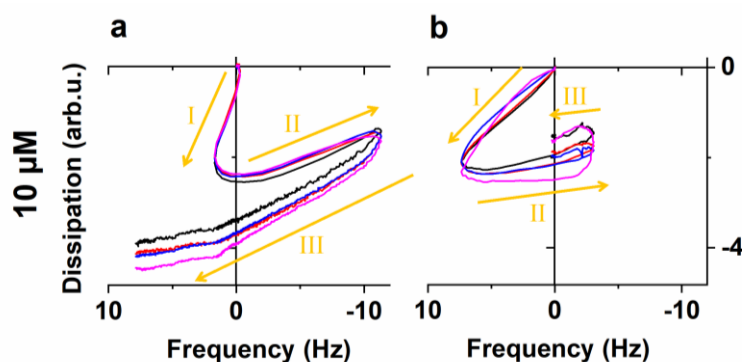


Fig 3 Viscoelastic fingerprints of the interaction of 10 μM melittin with DMPC membrane as a) liposome-containing deposit, b) multiple bilayer stacks. Temperature 19°C, pH 7.2

the experiment there were at least three bilayers on the surface, it appears that the membrane disruption does not proceed to the bilayer in direct contact to the support surface.

Melittin interaction with the liposome-containing deposits (Figure 2 i-l) show the same characteristic differences compared to single bilayer membranes as the neat DMPC. The main difference is the initial purely dissipative change in the first stage, consistent with the bursting of residual liposomes. The following stages are similar to the single bilayer case.

Discussion

Figure 3 shows a direct comparison of the interactions of DMPC multilayer and liposome containing deposits with 10 μM Melittin. The process is depicted schematically in Figure 4. In both the multiple bilayer and entrapped liposome case the mass uptake resulting from peptide binding is masked by the immediate structural changes, yielding [+f,-D] trends (Figure 3): the removal of top bilayer/patches, and the bursting of liposomes, respectively (Figure 4). In the direct comparison it is clear that the trend is mostly

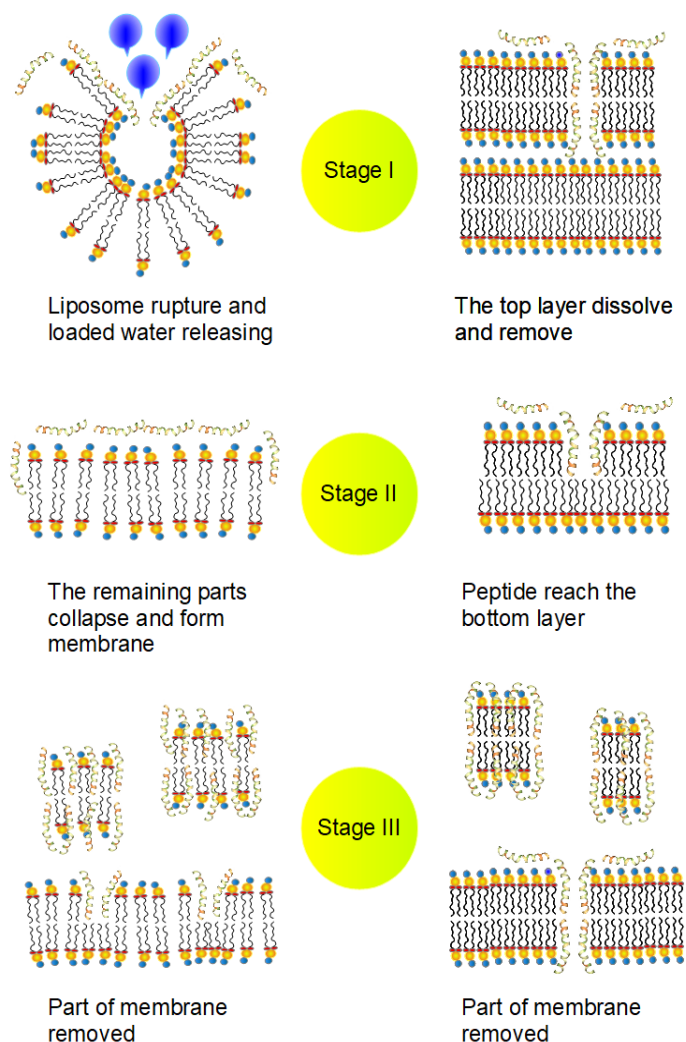


Fig 4 Schematic representation of the stages appearing in viscoelastic fingerprints of liposome containing and multilayer DMPC deposits. The schematics are not intended to represent a particular thermodynamic membrane state.

dissipative change for the liposome containing layer whereas mostly material removal for the multilayer case. The following stages in the respective systems appear similar in the fingerprints but the underlying mechanism is different, as shown in Figure 4; liposome collapse vs. further peptide binding. Finally, there is evidence of membrane dissolution in both cases.

The ability of melittin to dissolve membranes has been demonstrated before[14]; this study suggests that the dissolution takes place preferentially on the higher bilayers of multilayer stacks, that is, the support itself also affects the observed mechanism of action. The observations outlined here also explain variations in reported viscoelastic fingerprints for similar peptide-membrane interactions in cases when the membrane morphology was not controlled or monitored[16, 17, 46]. Consistently the results highlight the need to make comprehensive assessment of the conditions when interpreting qualitative QCM data. QCM has the resolving power to measure the addition of sub-nanogram masses to surfaces and the slight viscosity change accompanied by a shift in solvent viscosity caused by micromolar amounts of solutes. Its limitation as a method is in the complexity of the interpretation of the primary viscoelastic data in terms of molecular processes, as fundamentally different changes in the structure of an adlayer can lead to similar, or even identical f-D trends. The solution to this challenge is to control the experimental conditions, in the present study the membrane morphology, to the highest accuracy, keeping the number of variables as low as possible.

3. Conclusions

It is demonstrated that differences in membrane morphology can yield substantial differences in the viscoelastic fingerprint of the interactions of melittin with DMPC and DMPC:DMPG 4:1 membranes. These apparent differences reflect the underlying viscoelastic processes, but functionally they are artefacts in the analysis of peptide-membrane interactions. It is also shown that melittin can remove material when edges are exposed, such as membrane patches on top of another bilayer or in the case of liposome break-up. These results provide guidance for future QCM fingerprinting experiments.

References

- [1] Fair RJ, Tor Y. Antibiotics and Bacterial Resistance in the 21st Century. *Perspect Medicin Chem* 2014;6:PMC. S14459.
- [2] Hancock RE, Sahl H-G. Antimicrobial and host-defense peptides as new anti-infective therapeutic strategies. *Nat Biotechnol* 2006;24:1551-7.
- [3] Dürr UH, Sudheendra U, Ramamoorthy A. LL-37, the only human member of the cathelicidin family of antimicrobial peptides. *BBA-Biomembranes* 2006;1758:1408-25.
- [4] Henzler Wildman KA, Lee D-K, Ramamoorthy A. Mechanism of lipid bilayer disruption by the human antimicrobial peptide, LL-37. *Biochemistry* 2003;42:6545-58.
- [5] Conlon JM, Sonnevend A. Antimicrobial peptides in frog skin secretions. *Antimicrobial Peptides: Methods and Protocols* 2010:3-14.
- [6] Zasloff M. Antimicrobial peptides of multicellular organisms. *Nature* 2002;415:389.
- [7] Melicherčík P, Čerovský V, Nešuta O, Jahoda D, Landor I, Ballay R, et al. Testing the efficacy of antimicrobial peptides in the topical treatment of induced osteomyelitis in rats. 2018;63:97-104.
- [8] Matsuzaki K. Control of cell selectivity of antimicrobial peptides. *BBA-Biomembranes* 2009;1788:1687-92.
- [9] Tossi A, Sandri L, Giangaspero A. Amphipathic, α -helical antimicrobial peptides. *Peptide Sci* 2000;55:4-30.
- [10] He L, Robertson JW, Li J, Kärcher I, Schiller SM, Knoll W, et al. Tethered bilayer lipid membranes based on monolayers of thiolipids mixed with a complementary dilution molecule. 1. Incorporation of channel peptides. *Langmuir* 2005;21:11666-72.
- [11] Yang P, Ramamoorthy A, Chen Z. Membrane orientation of MSI-78 measured by sum frequency generation vibrational spectroscopy. *Langmuir* 2011;27:7760-7.
- [12] Litchfield WJ, Freytag JW, Adamich M. Highly sensitive immunoassays based on use of liposomes without complement. *Clin Chem* 1984;30:1441.
- [13] Lundquist A, Wessman P, Rennie AR, Edwards K. Melittin–Lipid interaction: A comparative study using liposomes, micelles and bilayerdisks. *BBA-Biomembranes* 2008;1778:2210-6.
- [14] Bodescu M, Rosenkötter F, Fritz J. Time lapse AFM on vesicle formation from mixed lipid bilayers induced by the membrane–active peptide melittin. *Soft Matter* 2017;13:6845-51.
- [15] Shahmiri M, Enciso M, Mechler A. Controls and constrains of the membrane disrupting action of Aurein 1.2. *Sci Rep* 2015;5:16378.
- [16] McCubbin GA, Praporski S, Piantavigna S, Knappe D, Hoffmann R, Bowie JH, et al. QCM-D fingerprinting of membrane-active peptides. *Eur Biophys J* 2011;40:437-46.
- [17] Praporski S, Mechler A, Separovic F, Martin LL. Subtle differences in initial membrane interactions underpin the selectivity of small antimicrobial peptides. *ChemPlusChem* 2015;80:91-6.
- [18] Killion J, Dunn J. Increased survival of lymphoma-bearing mice following therapy with melittin, a cytolytic molecule of bee-venom. *Proceeding of the American Association for Cancer Research: Amer assoc cancer research public BLDG, Suite 816, 150 S, Independence mall W., philadelphia, PA 19106; 1986. p. 310-.*
- [19] Oršolić N. Bee venom in cancer therapy. *Cancer and Metastasis Rev* 2012;31:173-94.
- [20] Son DJ, Lee JW, Lee YH, Song HS, Lee CK, Hong JT. Therapeutic application of anti-arthritis, pain-releasing, and anti-cancer effects of bee venom and its constituent compounds. *Pharmacol Therapeut* 2007;115:246-70.
- [21] Subbalakshmi C, Nagaraj R, Sitaram N. Biological activities of C-terminal 15-residue synthetic fragment of melittin: design of an analog with improved antibacterial activity. *FEBS Lett* 1999;448:62-6.

- [22] Raghuraman H, Chattopadhyay A. Melittin: a membrane-active peptide with diverse functions. *Biosci Rep* 2007;27:189-223.
- [23] Issam A-A, Zimmermann S, Reichling J, Wink M. Pharmacological synergism of bee venom and melittin with antibiotics and plant secondary metabolites against multi-drug resistant microbial pathogens. *Phytomedicine* 2015;22:245-55.
- [24] Hristova K, Dempsey CE, White SH. Structure, location, and lipid perturbations of melittin at the membrane interface. *Biophys J* 2001;80:801-11.
- [25] Lu NY, Yang K, Yuan B, Ma YQ. Molecular Response and Cooperative Behavior during the Interactions of Melittin with a Membrane: Dissipative Quartz Crystal Microbalance Experiments and Simulations. *J Phys Chem B* 2012;116:9432-8.
- [26] Dempsey CE. The actions of melittin on membranes. *Biochim Biophys Acta Rev* 1990;1031:143-61.
- [27] Steinem C, Galla HJ, Janshoff A. Interaction of melittin with solid supported membranes. *Phys Chem Chem Phys* 2000;2:4580-5.
- [28] Wimley WC. How does Melittin permeabilize membranes? *Biophys J* 2018;114:251-3.
- [29] Vogel H, Jähnig F. The structure of melittin in membranes. *Biophys J* 1986;50:573-82.
- [30] Yang L, Harroun TA, Weiss TM, Ding L, Huang HW. Barrel-stave model or toroidal model? A case study on melittin pores. *Biophys J* 2001;81:1475-85.
- [31] Allende D, Simon S, McIntosh TJ. Melittin-induced bilayer leakage depends on lipid material properties: evidence for toroidal pores. *Biophys J* 2005;88:1828-37.
- [32] Lee MT, Sun TL, Hung WC, Huang HW. Process of inducing pores in membranes by melittin. *Proc Natl Acad Sci U S A* 2013;110:14243-8.
- [33] Pan J, Khadka NK. Kinetic defects induced by melittin in model lipid membranes: A solution atomic force microscopy study. *J Phys Chem B* 2016;120:4625-34.
- [34] Van Den Bogaart G, Guzmán JV, Mika JT, Poolman B. On the mechanism of pore formation by melittin. *J Biol Chem* 2008;283:33854-7.
- [35] Juhaniewicz J, Sek S. Atomic Force Microscopy and Electrochemical Studies of Melittin Action on Lipid Bilayers Supported on Gold Electrodes. *Electrochim Acta* 2015;162:53-61.
- [36] Rex S. Pore formation induced by the peptide melittin in different lipid vesicle membranes. *Biophys Chem* 1996;58:75-85.
- [37] Papo N, Shai Y. Exploring peptide membrane interaction using surface plasmon resonance: differentiation between pore formation versus membrane disruption by lytic peptides. *Biochemistry* 2003;42:458-66.
- [38] Naito A, Nagao T, Norisada K, Mizuno T, Tuzi S, Saitô H. Conformation and dynamics of melittin bound to magnetically oriented lipid bilayers by solid-state ³¹P and ¹³C NMR spectroscopy. *Biophys J* 2000;78:2405-17.
- [39] Whitehouse C, Gidalevitz D, Cahuzac M, Koeppe RE, Nelson A. Interaction of gramicidin derivatives with phospholipid monolayers. *Langmuir* 2004;20:9291-8.
- [40] Papo N, Shai Y. Effect of drastic sequence alteration and D-amino acid incorporation on the membrane binding behavior of lytic peptides. *Biochemistry* 2004;43:6393-403.
- [41] Ramamoorthy A, Thennarasu S, Lee D-K, Tan A, Maloy L. Solid-state NMR investigation of the membrane-disrupting mechanism of antimicrobial peptides MSI-78 and MSI-594 derived from magainin 2 and melittin. *Biophys J* 2006;91:206-16.
- [42] Lee T-H, Hall K, Mechler A, Martin L, Popplewell J, Ronan G, et al. Molecular imaging and orientational changes of antimicrobial peptides in membranes. *Peptides for Youth: Springer*; 2009. p. 313-5.
- [43] Pandidan S, Mechler A. Nano-viscosimetry analysis of the membrane disrupting action of the bee venom peptide melittin. *Sci Rep* 2019;9:10841.

- [44] Jamasbi E, Mularski A, Separovic F. Model membrane and cell studies of antimicrobial activity of melittin analogues. *Curr Top Med Chem* 2016;16:40-5.
- [45] Mechler A, Praporski S, Piantavigna S, Heaton SM, Hall KN, Aguilar M-I, et al. Structure and homogeneity of pseudo-physiological phospholipid bilayers and their deposition characteristics on carboxylic acid terminated self-assembled monolayers. *Biomaterials* 2009;30:682-9.
- [46] Mechler A, Praporski S, Atmuri K, Boland M, Separovic F, Martin LL. Specific and selective peptide-membrane interactions revealed using quartz crystal microbalance. *Biophys J* 2007;93:3907-16.
- [47] Hasan IY, Mechler A. Viscoelastic changes measured in partially suspended single bilayer membranes. *Soft Matter* 2015;11:5571-9.
- [48] Hasan IY, Mechler A. Formation of planar unilamellar phospholipid membranes on oxidized gold substrate. *Biointerphases* 2016;11:031017.
- [49] Richter R, Mukhopadhyay A, Brisson A. Pathways of lipid vesicle deposition on solid surfaces: a combined QCM-D and AFM study. *Biophys J* 2003;85:3035-47.
- [50] Reimhult E, Höök F, Kasemo B. Intact vesicle adsorption and supported biomembrane formation from vesicles in solution: influence of surface chemistry, vesicle size, temperature, and osmotic pressure. *Langmuir* 2003;19:1681-91.
- [51] Richter RP, Him JLK, Brisson A. Supported lipid membranes. *Mat Today* 2003;6:32-7.
- [52] Lipowsky R, Seifert U. Adhesion of membranes: a theoretical perspective. *Langmuir* 1991;7:1867-73.
- [53] Smith A-S, Sengupta K, Goennenwein S, Seifert U, Sackmann E. Force-induced growth of adhesion domains is controlled by receptor mobility. *PNAS* 2008;105:6906-11.

Chapter Four

Mechanism of action of magainin 2

Preamble

As it was discussed in the previous chapters, AMPs can act via several pathways, however because of the simple structure and mechanism of action, as well as their various potential applications, pore forming membrane disruptor AMPs are perhaps the most studied and appealing class [1-10]. Following the thorough characterization of melittin, the focus of chapter four will be on finding the molecular interactions in the mechanism of action of magainin 2, another well-known pore forming membrane disruptor AMP. Magainin 2 is an α -helical, cationic peptide of 23 residues (H₂N-Gly-Ile-Gly-Lys-Phe-Leu-His-Ser-Ala-Lys-Lys-Phe-Gly-Lys-Ala-Phe-Val-Gly-Glu-Ile-Met-Asn-Ser-COOH), from the skin secretion of African clawed frog (*Xenopus laevis*) [11-14]. It is widely accepted that magainin 2 can permeabilize lipid bilayers by toroidal pore formation mechanism [15-18], that was deduced mainly from indirect measurements and findings, similar to many other AMPs [19-23]. However, like in case of melittin, there are discordant voices: it was suggested that in the case of phosphatidylserine or phosphatidylethanolamine lipids the disruption mechanism would be carpet-like [24]. Although nearly all sources agree with transient toroidal pore formation for magainin 2, as with melittin in the prior chapter, these pores have not been observed directly and their existence and structure was only supported by indirect evidence [17, 18].

In the previous chapter by revealing the molecular stages of melittin-membrane interaction I could propose the distinct mechanistic pathways for the peptide action on specific model membranes. Similarly, in this chapter my aim is to investigate the molecular interactions involved in the mechanism of magainin 2 against different type of membranes by using QCM fingerprinting analysis with the help of dye leakage and AFM imaging. In this I seek any hitherto hidden stages in the interaction and attempt to describe the overall mechanism of action of magainin 2. I also aim to find the similarities to or differences from the melittin model.

References

- [1] Shai Y, Oren Z. From “carpet” mechanism to de-novo designed diastereomeric cell-selective antimicrobial peptides. *Peptides* 2001;22:1629-41.
- [2] Wimley WC, Hristova K. Antimicrobial peptides: successes, challenges and unanswered questions. *J Membr Biol* 2011;239:27-34.
- [3] Pan H, Soman NR, Schlesinger PH, Lanza GM, Wickline SA. Cytolytic peptide nanoparticles (‘NanoBees’) for cancer therapy. *Wiley Interdiscip Rev Nanomed Nanobiotechnol* 2011;3:318-27.
- [4] Shai Y. Mode of action of membrane active antimicrobial peptides. *Peptide Sci* 2002;66:236-48.
- [5] Kauffman WB, Fuselier T, He J, Wimley WC. Mechanism matters: a taxonomy of cell penetrating peptides. *Trends Biochem Sci* 2015;40:749-64.
- [6] Liu S, Yang H, Wan L, Cai H-w, Li S-f, Li Y-p, et al. Enhancement of cytotoxicity of antimicrobial peptide magainin II in tumor cells by bombesin-targeted delivery. *Acta Pharmacol. Sin.* 2011;32:79.
- [7] Lehmann J, Retz M, Sidhu SS, Suttman H, Sell M, Paulsen F, et al. Antitumor activity of the antimicrobial peptide magainin II against bladder cancer cell lines. *Eur urol* 2006;50:141-7.
- [8] Raaymakers C, Verbrugghe E, Hernot S, Hellebuyck T, Betti C, Peleman C, et al. Antimicrobial peptides in frog poisons constitute a molecular toxin delivery system against predators. *Nat Commun* 2017;8:1495.
- [9] Gerlach SL, Rathinakumar R, Chakravarty G, Göransson U, Wimley WC, Darwin SP, et al. Anticancer and chemosensitizing abilities of cycloviolacin O2 from *Viola odorata* and psyle cyclotides from *Psychotria leptothyrsa*. *Peptide Sci* 2010;94:617-25.
- [10] Guha S, Ghimire J, Wu E, Wimley WC. Mechanistic Landscape of Membrane-Permeabilizing Peptides. *Chem Rev* 2019;119:6040-85.
- [11] Zasloff M. Magainins, a class of antimicrobial peptides from *Xenopus* skin: isolation, characterization of two active forms, and partial cDNA sequence of a precursor. *PNAS* 1987;84:5449-53.
- [12] Zasloff M, Martin B, Chen H-C. Antimicrobial activity of synthetic magainin peptides and several analogues. *PNAS* 1988;85:910-3.
- [13] Yang L, Harroun TA, Weiss TM, Ding L, Huang HW. Barrel-stave model or toroidal model? A case study on melittin pores. *Biophys J* 2001;81:1475-85.
- [14] Bechinger B, Zasloff M, Opella SJ. Structure and orientation of the antibiotic peptide magainin in membranes by solid-state nuclear magnetic resonance spectroscopy. *Protein Sci* 1993;2:2077-84.
- [15] Matsuzaki K, Harada M, Funakoshi S, Fujii N, Miyajima K. Physicochemical determinants for the interactions of magainins 1 and 2 with acidic lipid bilayers. *BBA-Biomembranes* 1991;1063:162-70.
- [16] Matsuzaki K, Murase O, Miyajima K. Kinetics of pore formation by an antimicrobial peptide, magainin 2, in phospholipid bilayers. *Biochemistry* 1995;34:12553-9.
- [17] Karal MAS, Alam JM, Takahashi T, Levadny V, Yamazaki M. Stretch-activated pore of the antimicrobial peptide, magainin 2. *Langmuir* 2015;31:3391-401.
- [18] Nguyen KT, Le Clair SV, Ye S, Chen Z. Molecular interactions between magainin 2 and model membranes in situ. *J Phys Chem B* 2009;113:12358-63.
- [19] Duclohier H, Molle G, Spach G. Antimicrobial peptide magainin I from *Xenopus* skin forms anion-permeable channels in planar lipid bilayers. *Biophys J* 1989;56:1017-21.
- [20] Hirsh DJ, Hammer J, Maloy WL, Blazys J, Schaefer J. Secondary structure and location of a magainin analogue in synthetic phospholipid bilayers. *Biochemistry* 1996;35:12733-41.
- [21] Ludtke SJ, He K, Heller WT, Harroun TA, Yang L, Huang HW. Membrane pores induced by magainin. *Biochemistry* 1996;35:13723-8.
- [22] Leontiadou H, Mark AE, Marrink SJ. Antimicrobial peptides in action. *J Am Chem Soc* 2006;128:12156-61.

- [23] Murzyn K, Pasenkiewicz-Gierula M. Construction of a toroidal model for the magainin pore. *J Mol Model* 2003;9:217-24.
- [24] Matsuzaki K, Sugishita K-i, Ishibe N, Ueha M, Nakata S, Miyajima K, et al. Relationship of membrane curvature to the formation of pores by magainin 2. *Biochemistry* 1998;37:11856-63.

Nano-viscosimetry analysis of antimicrobial peptide magainin 2 interactions with model membranes

Nano-viscosimetry analysis of antimicrobial peptide magainin 2 interactions with model membranes

Sara Pandidan and Adam Mechler

La Trobe Institute for Molecular Science, La Trobe University, Melbourne, Australia

Abstract

The rapid spread of antibiotic resistant strains of bacteria has created an urgent need for new alternative antibiotic agents. Antimicrobial peptides (AMPs) with bactericidal and fungicidal activity, may offer a solution. Magainin 2 is an AMP secreted by the African clawed frog (*Xenopus laevis*) that has been extensively studied for this purpose. Magainin 2 is described as a toroidal pore former membrane disrupting AMP. However, there are many uncertainties about the peptide-membrane interaction steps leading to the pore formation mechanism, of which only indirect evidence exists. In the present study, dye leakage experiments, quartz crystal microbalance (QCM) based viscoelastic fingerprinting analysis and atomic force microscopy (AFM) imaging were used to glean deeper insight into the peptide-membrane interactions. The effect of membrane charge, acyl chain unsaturation and different concentrations of cholesterol were investigated. The results show a complex membrane disruptive mechanism of magainin 2 action that is specific to the different model membranes. QCM nano viscosimetry measurement revealed the presence of distinct stages in the mechanism of magainin 2 action that, with the dye leakage data, confirm the existence of an initial transient pore stage resulting in peptide flip-flop between the outer and inner membrane leaflets. AFM imaging showed cylindrical mixed micelle structures as the end state of the peptide-membrane interaction at high peptide concentration. The results confirm some of the earliest hypotheses about magainin 2 action, while also highlighting the membrane modulating effect of the peptide.

Introduction

AMPs represent an effective innate weapon toward various type of bacteria, viruses and fungi in different living creatures from plants to insects, animals and human [11, 25, 26]. Since their discovery [26], they have represented a potential solution for global health threat of antibiotic resistant strains of bacteria [25, 27-29]. Magainins are a class of AMPs

found in the skin secretions of African clawed frog (*Xenopus laevis*) [11, 12]. Magainin 2 is a cationic peptide with 23 amino acid residues (H₂N-Gly-Ile-Gly-Lys-Phe-Leu-His-Ser-Ala-Lys-Lys-Phe-Gly-Lys-Ala-Phe-Val-Gly-Glu-Ile-Met-Asn-Ser-COOH) that forms α -helix structure in apolar environments, as in lipid membranes; under physiological conditions it acquires a cationic charge, believed to account for its specificity to anionic bacterial membranes that kills bacteria by opening pores in their membrane [13, 14, 20, 30].

Since its discovery, magainin 2 is described as a toroidal pore former peptide, based on indirect measurements by many studies with a range of different techniques [19-23]. In this pathway the peptide modulates the membrane surface into a torus, while remaining in contact with the headgroups throughout the entire process. Consistently the mechanism is described by almost all sources as a two-state transition [14, 17, 18, 21, 31-37]. The first step is the population of B_{ex} state, where magainin 2 in monomeric form [20, 31]) associates to the outer surface of the membrane and forms an α -helix that is oriented parallel to the head group region. Increased occupancy of B_{ex} leads to a transition to P state: excess of peptide expands the top leaflet laterally, decreases bilayer thickness, and leads to the formation of toroidal pores [21]. However, it was shown that on acidic phospholipids (phosphatidyl serine) magainin 2 may assemble on the surface of the membrane without proceeding to the P state, acting via carpet-like mechanism instead of pore formation [24].

The P state is mainly detected at high peptide concentration, with an apparent perpendicular insertion of peptide into the membrane caused by breakage of the membrane due to asymmetric tension [38]. As it involves membrane modulation, the formation of pores may be sensitive to membrane fluidity [39], which is a term to express range of disorder and molecular motion in a bilayer [40]. Even though there is a broad consensus about the formation of toroidal pores, such pores have not been observed by any microscopy methods, and thus the model is mainly based on interpretation of indirect evidence and speculation based on possible ways of magainin 2 binding to head group region. According to this reasoning at higher peptide concentration the membrane surface becomes saturated and increases the energy of adsorption; allowing access to other configurations that are comparatively lower energy states (inserted state), subsequently forming the transient toroidal pore [21]. The well-accepted model for magainin 2 predicts no peptide-peptide contact, i.e. no aggregation of peptides in the membrane, which was confirmed with NMR measurements [20], and it suggests an equilibrium distribution of

monomers at either side of the membrane leading to “closure” of the transient pores [21, 38, 41].

The evidence used to support the toroidal pore formation is multifold. For instance, losing the lipid orientation after membrane breach by magainin 2 as detected by polarized sum frequency generation (SFG) was interpreted as the tilt in side chains connecting two leaflets into a toroidal pore [18]. A study on single giant unilamellar vesicles (GUVs) using confocal laser scanning microscopy provided the most direct evidence of the mechanism: it was found that rapid binding of the peptide increases the area of lipid membrane (interpreted as an effect primarily on the outer leaflet), and that, by stretching the inner leaflet, would cause stochastic transfer of the peptide to the inner leaflet, forming transient toroidal pores in the process [17]. The translocation of peptides across the bilayer detected by Forster resonance energy transfer (FRET) using selective labelling of lipids of the outer leaflet was seen as proof of toroidal pore formation as well [38]. The most direct information is provided by neutron off-plane scattering analysis that reported, based on a model of circular symmetry, the internal and external radii for magainin 2 pore in DLPC membrane as 25Å and 42Å, respectively [42]. A pore of this size should be clearly visible in transmission electron microscopy, and hence the absence of any such data is remarkable.

Physicochemical models of magainin 2 activity are based on the assumption that a torus will form; the difference concerns the stability of this pore. In one view these pores are transient structures forming at the early stage of interaction to facilitate the translocation of peptides from the outer to the inner leaflet, until even distribution of peptide is achieved between leaflets [27, 35, 38]. If the peptide follows this mechanism, the P state would be a transition state and hence the equilibrium develops between B_{ex} and its equivalent in the inner leaflet (B_{in} state) [32]. However, X-ray diffraction results suggest that, at least at high peptide to lipid ratios, the pores are very stable [43]. Alternatively, if the presence of the peptide leads to modulation of the local membrane curvature, the P state is more stable than the planar surface bound state, hence once the initial pores form via membrane breakage, further peptides flip into the pores [44]. This is somewhat contradicted by dual polarisation interferometry studies suggesting that the membrane can recover after dissociation of Magainin 2 [45].

Overall, these models are descriptive and speculative, especially in the central tenet: the formation of circular holes in the membrane. Therefore in this work we ventured, by

using QCM viscoelastic measurements, dye leakage and AFM imaging, to identify the distinct stages of the peptide-membrane interaction that correlate to the respective physicochemical states of the mechanism, and to attempt direct visualization of the disruption product, i.e. the toroidal pore.

Materials and Methods

Buffer preparation

Potassium hydrogen phosphate (K_2HPO_4) was purchased from Honeywell (Shanghai, China) and potassium dihydrogen phosphate (KH_2PO_4) was Fluka branded and purchased from Sigma Aldrich (Castle Hill, NSW, Australia). Sodium chloride (NaCl) was purchased from ChemSupply (Australia). The water used for all solutions was deionized water of 18.2 M Ω cm resistivity (Ultrapure, Sartorius AG, Germany). The phosphate buffered saline (PBS) assay buffer contained 20mM phosphate and 100mM NaCl at pH 7.2.

Vesicle preparation

1,2-dimyristoyl-sn-glycero-3-phosphocholine (DMPC), sodium salt of 1,2-dimyristoyl-sn-glycero-3-phosphoglycerol (DMPG), 1,2-dioleoyl-sn-glycero-3-phosphocholine (DOPC), 1,2-Dioleoyl-sn-glycero-3-phosphoglycerol sodium salt and cholesterol were purchased from Avanti Polar Lipids (Alabaster, AL, USA). Chloroform (ACS Reagent, 99.8%) and methanol (>99.9%, spectrophotometric grade) were purchased from Sigma-Aldrich (Castle Hill, NSW, Australia).

Lyophilised lipids were dissolved in chloroform and for DMPG samples, 3% methanol was also added to increase solubility. Desired ratios of lipids were mixed in a clean test tube. As described before, with a gentle flow of nitrogen gas and continuous vortexing the solvent was evaporated, and then the prepared lipid test tubes were placed in desiccator overnight. Afterward, the dried lipid samples were suspended in 1 ml PBS buffer solution and incubated for 30 min at 37°C, following a 1 min vortex and sonication [46].

Dye leakage

Lipid vesicles (0.5 mM) were suspended in PBS buffer containing 20 mM 5(6)-carboxyfluoresceine (Sigma-Aldrich, Castle Hill, Australia) dye solution and incubated for 30 minutes, following with one-minute vortex and one-minute sonication. Excess CF was removed from the sample by dialysis using SnakeSkin Dialysis Tubing 10000 MWCO,

renewing the buffer solution until a clear solution obtained. All experiments were performed using a SpectraMax M5 Multi-Mode Microplate Reader. Intensities were recorded every 30 s for 55 min after adding 1, 3, 5, 7, 10 μM melittin at 25°C with excitation and emission wavelengths of 480 nm and 517 nm, respectively.

Quartz Crystal Microbalance (QCM)

The QCM experiments were conducted with a Q-SENSE E4 system (Q-SENSE, Sweden) using AT-cut gold-coated quartz chips with a fundamental resonance frequency of 5 MHz. Initially the QCM chips were cleaned in a piranha solution consisting of 1:1:3 of hydrogen peroxide (20%<c<60% aqueous solution), ammonia solution (aq 28-30%) and deionized water at 70°C for 20 minutes. H_2O_2 and ammonia solutions were purchased from ChemSupply Pty Ltd Australia and Merck Germany, respectively.

Biological membranes are too complex to study, therefore model membranes have been created to mimic the lipid bilayer structure [47]. In last few years different techniques have been progressed for forming model membrane systems: tethered vesicles [48], supported lipid bilayer [49], Giant unilamellar vesicles [50]. In this study, the bilayer formed on MPA modified QCM chips by using lipid liposomes, which explained, in material section.

The oxidised chips were rinsed with ultra-pure water and dried under a gentle stream of nitrogen gas. Then the chips were modified in a solution of 2% 3-mercaptopropionic acid (MPA) (HPLC Grade, > 99%, Fluka, Switzerland) in 2-propanol overnight. Next, the chips were soaked in 2-propanol (HPLC Plus, purchased from Sigma-Aldrich) to remove any excess thiol from the surface. After subsequent drying the chips were placed in deionized water for a few hours to hydrate the MPA self-assembled monolayer.

Atomic Force Microscopy (AFM)

Atomic force microscope imaging was performed with NT-MDT Ntegra (Zelenograd, Russia) and Digital Instruments Nanoscope IV Multimode (Santa Barbara, USA) instrumental platforms, in liquid cell. MicroMasch NSC15 and NT-MDT NSG 01/03 tapping probes were used, operated at resonance which was typically found in the range of 50-100kHz. Resonance peak was identified from the amplitude-distance curves following the method described by Kokavecz and Mechler [51]. Membranes were deposited onto freshly cleaved mica surface, washed with pure water to remove/burst intact liposomes and generate membrane islands, and imaged in assay buffer. Peptide solution was injected in situ, to achieve an approximate concentration of 15 μM .

Image processing was performed in Gwyddion freeware (by Czech Metrology Institute, www.gwyddion.net), using a sequence of plane fit, flattening and manual scar removal using Laplacian extrapolation, followed by matrix filters and three-dimensional rendering as needed.

Results and discussions

Dye leakage assay

Figure 1 shows the fluorescence intensity after adding 1, 3, 5, 7 and 10 μM magainin 2 on different lipid membrane structure. While the trends are very similar – there is an immediate dye release event after which the intensity is not changing over time - the amount of dye release is lower when the mixture contains charged lipids.

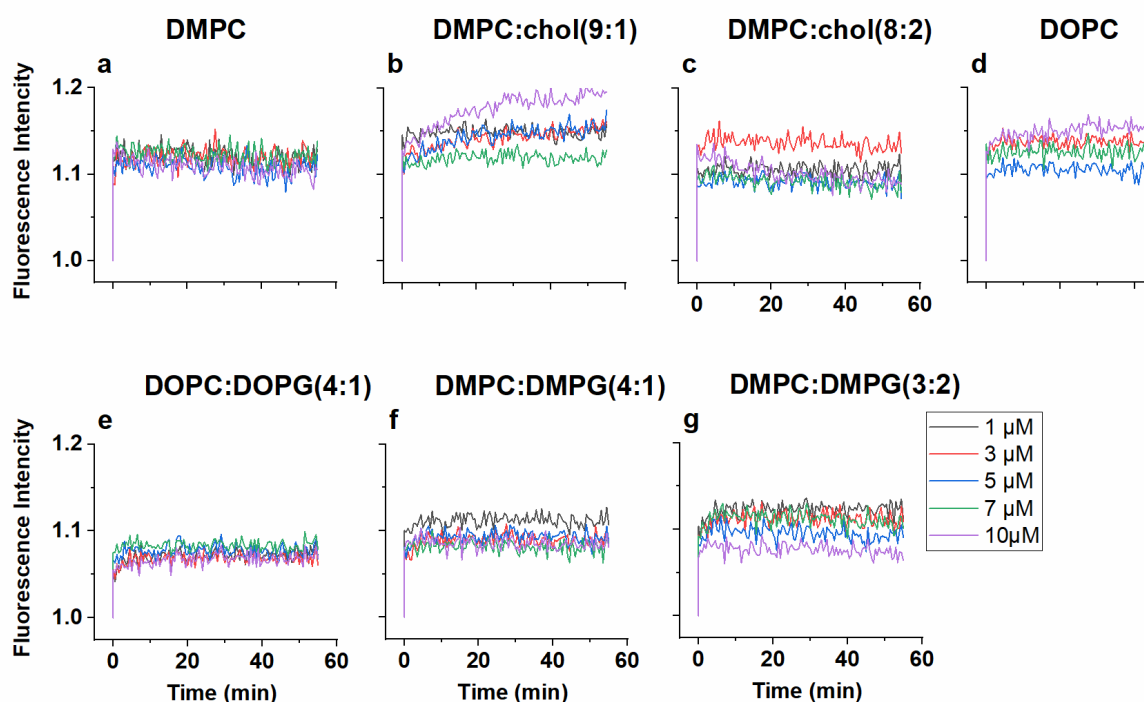


Figure 1. Fluorescence intensity after adding after adding different concentration of magainin2 on a) DMPC, b) DMPC:chol (9:1), c) DMPC:chol (8:2), d) DOPC, e) DOPC:DOPG (4:1), f) DMPC:DMPG (4:1), g) DMPC:DMPG (3:2) in 25°C

Adding 10% cholesterol to the saturated DMPC lipid, the amount of dye release only shows a small, unexpected increase, more pronounced at higher concentrations. The slow kinetics in the 10 μM case suggests that initial large scale pore formation is followed by a slow secondary process; considering the known propensity of the DMPC-cholesterol mixtures, this might imply that there is a variation between the cholesterol contents of the

liposomes, and the delayed release corresponds to liposomes of higher cholesterol content. It is notable, however, that increasing cholesterol content to 20% eliminates the effect. Hence the difference is likely related to the presence of domain boundaries in the 10% cholesterol containing membranes. The unsaturated DOPC behaves similarly to DMPC. Mixing PG to the mixture leads to substantially lower intensity in the dioleoyl lipids, but only a small change in the saturated dimyristoyl lipids.

Lipid deposition and QCM assays

Mammalian-Mimetic Membranes

Figure 2 shows the viscoelastic fingerprints for zwitterionic saturated lipid membranes of 0%, 10% and 20% cholesterol content. For the neat DMPC the fingerprint starts with small mass uptake ($-f$) and almost constant dissipation, consistent with binding to the membrane without a viscous element, by e.g. sinking into the headgroup region and restraining the dissipative movements of the membrane (e.g. undulations) and/or individual lipid molecules (e.g. out-of-plane “bobbing”). After this brief trend the mass uptake continues with a steep decrease in dissipation, which indicates a major structural change. The fingerprint shows a short ($+f$, 0) trend that suggests loss of membrane elasticity; this is preceded by some degree of membrane collapse indicated by a ($-f$, 0) trend at higher concentrations [52].

When mixing 10% cholesterol to the membrane, there is a noticeable difference: the first step is a ($-f$, $+D$) trend, consistent with viscoelastic mass uptake which can be the result of peptide binding on the membrane surface without much insertion; this suggests that the presence of cholesterol limits membrane penetration of the peptide. When comparing this to the DMPC trend it becomes apparent that in the latter the peptide is likely inserted deeper in the membrane than anticipated by the surface binding models. That would be consistent with the presence of a transient transmembrane state in case of neat DMPC as suggested by early models [21, 27, 35, 38] but that is constrained in some ways by the presence of cholesterol. This trend is followed by a ($-f$, $-D$) trend as in the neat DMPC case. Final step is a ($+f$, $-D$) trend upon washing the membrane with buffer, suggesting membrane recovery as reported before [45].

Upon increasing cholesterol concentration to 20% the fingerprints revert back to a pattern similar, but not identical to neat DMPC, with more material removal in last stage. This is consistent with the dye leakage results described above.

However, in the case of the unsaturated DOPC, the fingerprint shows a definite change.

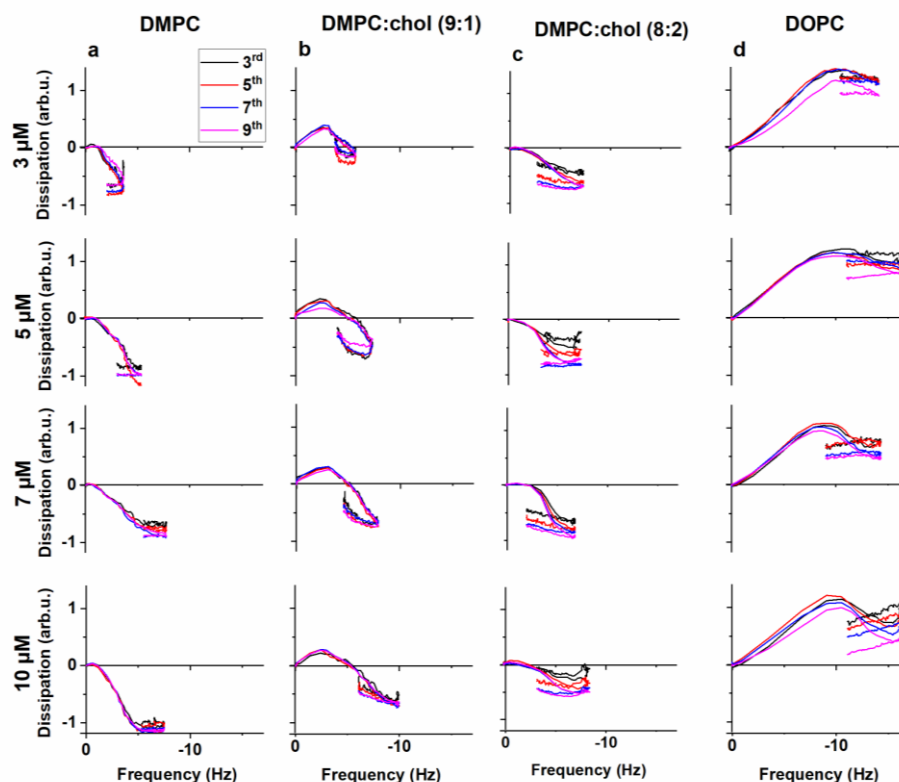


Figure 2. From top to bottom 3, 5, 7, 10 μ M magainin2 added on a) DMPC b) DMPC:chol (9:1) c) DMPC:chol (8:2) d) DOPC

The first trendline goes toward $(-f + D)$ with a steep slope that is consistent with peptide binding weakly on the membrane surface with substantial freedom of motion, adding to viscous energy loss. The mass uptake trend is followed by a relatively shallow $(-f, -D)$ trend, consistent with the 2nd stage for the DMPC membranes. The last step again goes toward $+f$ showing an obvious mass loss.

Hence, there is a high degree of similarity in the second trend between all of the neutral membranes, suggesting that the differences concern the means of initial peptide binding but the disruption pathway is the same for all, consistent with a two-stage process that might proceed to membrane disintegration.

Bacteria - mimetic membranes

One important difference between eukaryotic and prokaryotic cell membrane is their lipid composition [53]. In this study bacterial cell membrane is modelled by adding anionic lipids to the biomimetic membrane. Figure 3 shows the viscoelastic fingerprints for bacteria-mimetic membranes. In the case of DMPC: DMPG (4:1) the most significant difference from neat DMPC is the viscoelastic binding trend in the first stage. The trendline is not straight: it shows a gradual decrease of the dissipation component, suggesting the beginning of a secondary process such as partial membrane penetration, or a gradual stiffening of the membrane by introducing asymmetric tension. By increasing peptide concentration, the binding step becomes shorter (from -5 Hz to -3 Hz for 3 μ M and 10 μ M peptide concentration, respectively). This is followed by an abrupt shift to (0, -D) trend that is consistent with a major structural change that eliminates dissipative

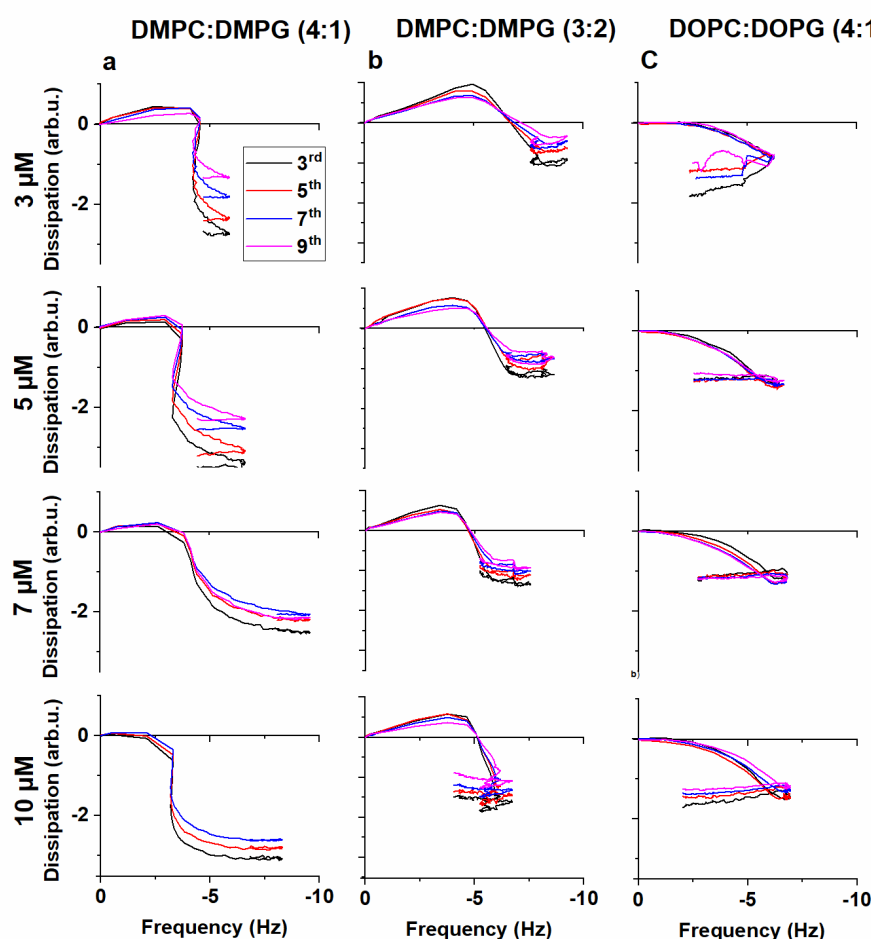


Figure 3. Viscoelastic fingerprint of 3, 5, 7, 10 μ M magainin 2 on; DMP:DMPG (4:1), DMPC:DMPG (3:2), DOPC:DOPG (4:1)

processes in the membrane. The trend quickly turns towards (-f) that can be the sign of further mass uptake or a purely elastic component of the structural change. There is some degree of material removal upon flushing the cells with buffer.

For DMPC: DMPG (3:2), the overall trend is same as DMPC: DMPG (4:1) with minor differences. The binding stage is longer, reaching -5 Hz for 3 μ M, although it becomes slightly shorter with increasing peptide concentration; and the trendline lacks the increasing (-f) component.

The DOPC:DOPG (4:1) membrane yields a notably different fingerprint. The viscoelastic binding trend is replaced by a short (-f,0) line that gains an increasing -D component, suggesting an immediate structural change from initial peptide binding. This fingerprint also shows a significant (+f, 0) trend, that is consistent with material removal from the already stiffened membrane, therefore missing the -D component of the typical material removal trendlines [46, 52].

It is notable that the relatively shallow slope of stage 2 is present in most fingerprints, which is a unique feature of magainin 2, suggesting a specific membrane modulating pathway not seen in QCM fingerprints of other peptides thus far.

AFM Imaging

AFM imaging was attempted to identify the morphological effect of the peptide. The results were inconclusive on most membranes, showing increased fluidity and a small degree of dissolution, detected by smearing of the edges of the membrane patches. It is a

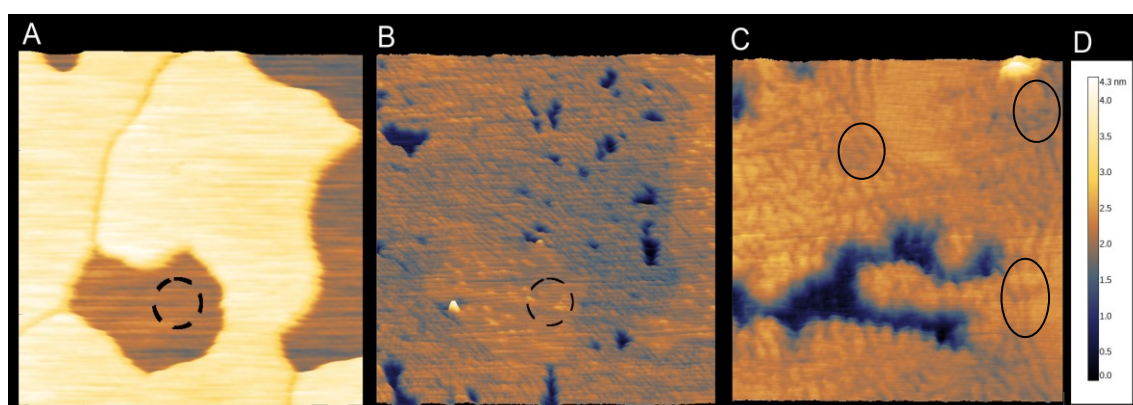


Figure 4. AFM images of DMPC:DMPG (4:1) membrane: (A), before the addition of magainin 2; (B), after the addition of magainin 2; (C) a high resolution zoom at the collapsed membrane area. Images are 3D rendered. Image sizes: 1.14 μ m (A, B) and 400 nm (C). Circles show some of the cylindrical structures resulting from membrane collapse. The colour bar for the height scale (total height: 4.3 nm for all frames) is provided in (D). the noise level is below the ADC step height (0.1 nm)

sign that the AFM probe can penetrate the membrane deeper and drag the membrane along. In case of DMPC: DMPG 4:1 membrane, however, the effect of the peptide was successfully imaged. Due to the unique structural features that it reveals the images are included here.

Figure 4 A shows a typical domain-separated DMPC:DMPG membrane as reported before [46]. The height difference between the domains is approximately 1 nm. When exposed to the peptide, the two domains respond differently: what was the higher domain appears to collapse (Figure 4 B) however the originally lower domain (indicated with a dash circle in Figure 4 A and B) appears intact, with some indication of peptide accumulation on the surface, appearing as small grains. High resolution image of the collapsed domain (Figure 4 C) reveals regular, cylindrical structures, consistent with mixed micelles. The appearance of linear fissure-like structures as opposed to circular pores has been observed before for melittin, another well-known membrane disruptor AMP, however the morphologies obtained in each case are markedly different [54].

Discussions

The data are consistent with the well-documented membrane disrupting activity of magainin 2, however further clues to the mechanism of action were revealed. Magainin 2 acted as a cell-lysing agent in all lipid mixtures but with some specific differences in the mechanism as revealed in the viscoelastic fingerprints. The peptide caused almost immediate structural change on saturated lipids, while it remained in a surface associated, highly dissipating state on unsaturated lipid. Thus the different packing of the unsaturated acyl chains prevents the immediate insertion of the peptide into the membrane.

On the other hand, the effect of cholesterol content was not straightforward. The presence of cholesterol did not inhibit the membrane disrupting effect of the peptide. It was shown before that cholesterol containing membranes form domains, but the membrane becomes saturated over ~25% cholesterol content, therefore the 20% cholesterol containing membrane is likely nearly homogeneous. The peculiar behaviour on the domain separated DMPC:cholesterol 9:1 membrane thus suggests that the peptide has a unique interaction to domain boundaries. Similar outlier behaviour is seen in the – also domain separated – DMPC:DMPG 4:1 membrane.

In the case of negatively charged saturated lipid membrane, magainin 2 shows higher binding affinity than neutral lipids that is usually attributed to stronger electrostatic attractions between positively charged peptide and negative charge of membrane, as it was reported before [35].

Yet, in the case of unsaturated lipids, adding DOPG to the mixture did not achieve the same outcome, yielding instead a fingerprint that was highly similar to the neat DMPC membrane. Thus, charge interaction does not appear to be the cause of the different interaction of magainin 2 with the PG-containing saturated membranes. While it is unclear what is the basis of this difference, we can hypothesize based on the documented tendency of DMPC:DMPG membranes to form distinct domains [46] that either the peptide is attached to the domain boundaries, or the packing of the lipids that leads to the formation of domains inhibits the insertion of the peptide to the headgroup region. This is consistent with the AFM results that show peptides remaining on top of one of the membrane domains, likely the DMPG-rich domain, while penetrate and break up the other, likely DMPC rich domain. The effect is negated likely by the different chain packing and potentially the resulting larger inter-headgroup distance in the unsaturated membrane. The fact that 20% cholesterol also did not have a major inhibitory effect corroborates the importance of the inter-lipid spacing in the headgroup zone, without much influence from membrane fluidity. Thus, the mechanism of magainin 2 action appears to be non-specific to the extent by which the peptide can sink into the headgroup zone to modulate membrane tension.

The data allows for assessing the validity of the existing models of magainin 2 action. The dye leakage results are consistent with an initial, transient dye release followed by a re-seal of the membrane, as described in the transient pore model [27, 35, 38]. The initial burst-like release is consistent with increasing peptide concentrations, without a disintegration threshold within the studied concentration range. The morphologies observed via AFM imaging suggest, however, that the membrane is not distorted into regular, circular pores, rather into a regular array of cylindrical mixed micelle-like structures. However, given that this is the equilibrium structure at high peptide concentration, the formation of more localized transient pores cannot be ruled out at the beginning of the process. The observed cylindrical (sausage-like) structures in the AFM images would yield similar membrane orientation loss that was reported by Nguyen et al. based on SFG study [18].

Furthermore, QCM results show at least three and in some cases four stages. In case of non-linear trendlines the number of underlying processes can be more than that. Thus, the simple two or three stage models (REF) do not capture the entire mechanism. The clue to the missing stages is in the AFM data: the presence of the peptides modulates the membrane into the observed structures, which likely form after the transfer of a substantial population of the peptides to the inner leaflet. This is analogous to, but structurally different than the membrane fissure model described before for melittin mechanism of action [54]. Thus the proposed stages for magainin 2-membrane interaction are 1) peptide binding to head group surface immediately folding to α -helix and modulation of the membrane tension, 2) asymmetric tension forces pore formation leading to peptide flip-flop to the inner leaflet, 3) balancing membrane tension by building a population of peptides in the inner leaflet, 4) membrane collapse into cylindrical structures (appearing sausage-like on the images) of mixed micelles. While it appears that membrane integrity is still retained at this stage, removal of some material cannot be ruled out. There is no clear distinction between the stages inasmuch as further material binding is possible during the flip-flop process etc. hence the curved trendlines observed in QCM.).

Conclusions

QCM nano-viscosimetry analysis with the support of dye leakage and AFM imaging revealed that magainin 2 acts as a non-specific membrane-lysing agent following a mechanism that mainly depend on the ability of the peptide to enter the headgroup zone. It was not sensitive, however, to the presence of cholesterol or the degree of lipid saturation. Importantly, the effect of charged lipids appeared to manifest through lipid-lipid packing and not charge interaction with the peptide.

The data points at a complex membrane disrupting mechanism that includes an initial transient pore stage allowing peptide flip-flop between the leaflets but leads to membrane modulation and collapse once equilibrium is achieved. The ability of the peptide to transfer between the leaflets suggests that the limit of membrane recovery, detailed in previous works, is the limit of membrane collapse into the cylindrical mixed micelle-like structures observed with AFM.

References

- [1] Shai Y, Oren Z. From “carpet” mechanism to de-novo designed diastereomeric cell-selective antimicrobial peptides. *Peptides* 2001;22:1629-41.
- [2] Wimley WC, Hristova K. Antimicrobial peptides: successes, challenges and unanswered questions. *J Membr Biol* 2011;239:27-34.
- [3] Pan H, Soman NR, Schlesinger PH, Lanza GM, Wickline SA. Cytolytic peptide nanoparticles (‘NanoBees’) for cancer therapy. *Wiley Interdiscip Rev Nanomed Nanobiotechnol* 2011;3:318-27.
- [4] Shai Y. Mode of action of membrane active antimicrobial peptides. *J Pept Sci* 2002;66:236-48.
- [5] Kauffman WB, Fuselier T, He J, Wimley WC. Mechanism matters: a taxonomy of cell penetrating peptides. *Trends Biochem Sci* 2015;40:749-64.
- [6] Liu S, Yang H, Wan L, Cai H-w, Li S-f, Li Y-p, et al. Enhancement of cytotoxicity of antimicrobial peptide magainin II in tumor cells by bombesin-targeted delivery. *Acta Pharmacol Sin* 2011;32:79.
- [7] Lehmann J, Retz M, Sidhu SS, Suttman H, Sell M, Paulsen F, et al. Antitumor activity of the antimicrobial peptide magainin II against bladder cancer cell lines. *Eur Urol* 2006;50:141-7.
- [8] Raaymakers C, Verbrugghe E, Hernot S, Hellebuyck T, Betti C, Peleman C, et al. Antimicrobial peptides in frog poisons constitute a molecular toxin delivery system against predators. *Nat commun* 2017;8:1495.
- [9] Gerlach SL, Rathinakumar R, Chakravarty G, Göransson U, Wimley WC, Darwin SP, et al. Anticancer and chemosensitizing abilities of cycloviolacin O2 from *Viola odorata* and psyle cyclotides from *Psychotria leptothyrsa*. *J Pept Sci* 2010;94:617-25.
- [10] Guha S, Ghimire J, Wu E, Wimley WC. Mechanistic Landscape of Membrane-Permeabilizing Peptides. *Chem Rev* 2019;119:6040-85.
- [11] Zasloff M. Magainins, a class of antimicrobial peptides from *Xenopus* skin: isolation, characterization of two active forms, and partial cDNA sequence of a precursor. *PNAS* 1987;84:5449-53.
- [12] Zasloff M, Martin B, Chen H-C. Antimicrobial activity of synthetic magainin peptides and several analogues. *PNAS* 1988;85:910-3.
- [13] Yang L, Harroun TA, Weiss TM, Ding L, Huang HW. Barrel-stave model or toroidal model? A case study on melittin pores. *Biophys J* 2001;81:1475-85.
- [14] Bechinger B, Zasloff M, Opella SJ. Structure and orientation of the antibiotic peptide magainin in membranes by solid-state nuclear magnetic resonance spectroscopy. *Protein Sci* 1993;2:2077-84.
- [15] Matsuzaki K, Harada M, Funakoshi S, Fujii N, Miyajima K. Physicochemical determinants for the interactions of magainins 1 and 2 with acidic lipid bilayers. *BBA-Biomembranes* 1991;1063:162-70.
- [16] Matsuzaki K, Murase O, Miyajima K. Kinetics of pore formation by an antimicrobial peptide, magainin 2, in phospholipid bilayers. *Biochemistry* 1995;34:12553-9.
- [17] Karal MAS, Alam JM, Takahashi T, Levadny V, Yamazaki M. Stretch-activated pore of the antimicrobial peptide, magainin 2. *Langmuir* 2015;31:3391-401.
- [18] Nguyen KT, Le Clair SV, Ye S, Chen Z. Molecular interactions between magainin 2 and model membranes in situ. *J Phys Chem B* 2009;113:12358-63.
- [19] Duclohier H, Molle G, Spach G. Antimicrobial peptide magainin I from *Xenopus* skin forms anion-permeable channels in planar lipid bilayers. *Biophys J* 1989;56:1017-21.
- [20] Hirsh DJ, Hammer J, Maloy WL, Blazys J, Schaefer J. Secondary structure and location of a magainin analogue in synthetic phospholipid bilayers. *Biochemistry* 1996;35:12733-41.
- [21] Ludtke SJ, He K, Heller WT, Harroun TA, Yang L, Huang HW. Membrane pores induced by magainin. *Biochemistry* 1996;35:13723-8.
- [22] Leontiadou H, Mark AE, Marrink SJ. Antimicrobial peptides in action. *J Am Chem Soc* 2006;128:12156-61.

- [23] Murzyn K, Pasenkiewicz-Gierula M. Construction of a toroidal model for the magainin pore. *J Mol Model* 2003;9:217-24.
- [24] Matsuzaki K, Sugishita K-i, Ishibe N, Ueha M, Nakata S, Miyajima K, et al. Relationship of membrane curvature to the formation of pores by magainin 2. *Biochemistry* 1998;37:11856-63.
- [25] Zasloff M. Antimicrobial peptides of multicellular organisms. *Nature* 2002;415:389.
- [26] Steiner H, Hultmark D, Engström Å, Bennich H, Boman HG. Sequence and specificity of two antibacterial proteins involved in insect immunity. *Nature* 1981;292:246.
- [27] Matsuzaki K. Why and how are peptide–lipid interactions utilized for self-defense? Magainins and tachyplesins as archetypes. *BBA-Biomembranes* 1999;1462:1-10.
- [28] Ge Y, MacDonald DL, Holroyd KJ, Thornsberry C, Wexler H, Zasloff M. In vitro antibacterial properties of pexiganan, an analog of magainin. *Antimicrob Agents Chemother* 1999;43:782-8.
- [29] Bush K, Courvalin P, Dantas G, Davies J, Eisenstein B, Huovinen P, et al. Tackling antibiotic resistance. *Nat Rev Microbiol* 2011;9:894.
- [30] Segrest JP, De Loof H, Dohlman JG, Brouillette CG, Anantharamaiah G. Amphipathic helix motif: classes and properties. *Protein* 1990;8:103-17.
- [31] Tamba Y, Yamazaki M. Magainin 2-induced pore formation in the lipid membranes depends on its concentration in the membrane interface. *J Phys Chem B* 2009;113:4846-52.
- [32] Tamba Y, Yamazaki M. Single giant unilamellar vesicle method reveals effect of antimicrobial peptide magainin 2 on membrane permeability. *Biochemistry* 2005;44:15823-33.
- [33] Tamba Y, Masum SM, Yamazaki M. Effects of Surface Charge Density of Lipid Membranes on the Pore Formation Induced by Magainin 2. *International Symposium on Micro-NanoMechatronics and Human Science: IEEE; 2007. p. 96-101.*
- [34] He K, Ludtke SJ, Huang HW, Worcester DL. Antimicrobial peptide pores in membranes detected by neutron in-plane scattering. *Biochemistry* 1995;34:15614-8.
- [35] Matsuzaki K. Magainins as paradigm for the mode of action of pore forming polypeptides. *Biochim Biophys Acta, Rev Biomembr* 1998;1376:391-400.
- [36] Bechinger B, Gierasch L, Montal M, Zasloff M, Opella S. Orientations of helical peptides in membrane bilayers by solid state NMR spectroscopy. *Solid State Nucl Magn Reson* 1996;7:185-91.
- [37] Papo N, Shai Y. Exploring peptide membrane interaction using surface plasmon resonance: differentiation between pore formation versus membrane disruption by lytic peptides. *Biochemistry* 2003;42:458-66.
- [38] Matsuzaki K, Murase O, Fujii N, Miyajima K. Translocation of a channel-forming antimicrobial peptide, magainin 2, across lipid bilayers by forming a pore. *Biochemistry* 1995;34:6521-6.
- [39] Zakharov SD, Kotova EA, Antonenko YN, Cramer WA. On the role of lipid in colicin pore formation. *BBA-Biomembranes* 2004;1666:239-49.
- [40] Murata N, Los DA. Membrane fluidity and temperature perception. *Plant Physiology* 1997;115:875.
- [41] Ludtke S, He K, Huang H. Membrane thinning caused by magainin 2. *Biochemistry* 1995;34:16764-9.
- [42] Yang L, Weiss TM, Harroun TA, Heller WT, Huang HW. Supramolecular structures of peptide assemblies in membranes by neutron off-plane scattering: method of analysis. *Biophys J* 1999;77:2648-56.
- [43] Yang L, Weiss TM, Lehrer RI, Huang HW. Crystallization of antimicrobial pores in membranes: magainin and protegrin. *Biophys J* 2000;79:2002-9.
- [44] Kim C, Spano J, Park E-K, Wi S. Evidence of pores and thinned lipid bilayers induced in oriented lipid membranes interacting with the antimicrobial peptides, magainin-2 and aurein-3.3. *BBA-Biomembranes* 2009;1788:1482-96.
- [45] Hall K, Lee T-H, Mechler AI, Swann MJ, Aguilar M-I. Real-time measurement of membrane conformational states induced by antimicrobial peptides: balance between recovery and lysis. *Sci Rep* 2014;4:5479.

- [46] Mechler A, Praporski S, Piantavigna S, Heaton SM, Hall KN, Aguilar M-I, et al. Structure and homogeneity of pseudo-physiological phospholipid bilayers and their deposition characteristics on carboxylic acid terminated self-assembled monolayers. *Biomaterials* 2009;30:682-9.
- [47] Chan Y-HM, Boxer SG. Model membrane systems and their applications. *Curr Opin Chem Biol* 2007;11:581-7.
- [48] Yoshina-Ishii C, Boxer SG. Arrays of mobile tethered vesicles on supported lipid bilayers. *J Am Chem Soc* 2003;125:3696-7.
- [49] Richter RP, Brisson AR. Following the formation of supported lipid bilayers on mica: a study combining AFM, QCM-D, and ellipsometry. *Biophys J* 2005;88:3422-33.
- [50] Feigenson GW. Phase boundaries and biological membranes. *Annu Rev Biophys Biomol Struct* 2007;36:63-77.
- [51] Kokavecz J, Mechler A. Investigation of fluid cell resonances in intermittent contact mode atomic force microscopy. *Appl Phys Lett* 2007;91:023113.
- [52] Shahmiri M, Enciso M, Mechler A. Controls and constrains of the membrane disrupting action of Aurein 1.2. *Sci Rep* 2015;5:16378.
- [53] Tate C. Overexpression of mammalian integral membrane proteins for structural studies. *FEBS Lett* 2001;504:94-8.
- [54] Pandidan S, Mechler A. Nano-viscosimetry analysis of the membrane disrupting action of the bee venom peptide melittin. *Sci Rep* 2019;9:1-12.

Chapter Five

**Further biophysical
characteristics of
AMP-membrane interactions**

Preamble

As it was demonstrated in previous chapters in order to understand the mechanism of peptide-membrane interaction, biophysical properties of the whole interaction process should be thoroughly investigated. The results that revealed different transmembrane states in the interaction of melittin and magainin 2 AMPs with model membranes, while they stand up to scrutiny on their own, prompted me to search for alternative ways to support and re-confirm the data. This directed me to deliberate over their influence on lipid phase transition temperatures. There are only limited studies in this area in the literature, mainly based on calorimetry measurements on different AMPs [1-6]. Studies on α -helical peptides stated that the presence of peptides would decrease the main transition temperature of lipids [5, 6], whereas studies on melittin suggested that the peptide can only shift the pre-transition temperature without changing main transition temperature of DPPC membrane [1]. There was a report of a stiffening effect on DMPC membrane [2]. Generally, these studies suggested that the presence of peptide in the membrane may have influence on phase transition temperature and/or viscoelastic properties of the membrane.

In the first part of chapter five I intend to find the distinct thermodynamic states of the transmembrane mechanism of action of melittin and magainin 2 AMPs by using QCM nano-viscosimetry measurement which was shown to provide a proper alternative to calorimetry measurements by determining the viscosity changes of membrane upon any phase transitions [7-10]. For this purpose, I used QCM temperature sweeping on DMPC membrane with different concentrations of melittin and magainin 2 and correlate the data to QCM fingerprinting results described in Chapters three and four.

In the second part of this chapter I embark on neutron reflectometry measurements to confirm the location of the peptides throughout the specific mechanism of action; the states can be separated by stepwise increase of the bulk peptide concentration as shown in the previous chapters. The limitations posed by neutron source access and the time-consuming nature of the experiments required a compromise in terms of which peptides to study. I chose melittin (which was introduced in the previous chapters) and, as a reference peptide that is known to remain on the membrane surface throughout its mechanism, aurein 1.2 from *Litoria aurea*, and Australian tree frog. The nano-

viscosimetry based analysis of the molecular stages of the interaction of both peptides was reported in detail before [11, 12], providing a solid basis for these experiments.

References

- [1] Lohner K, Latal A, Lehrer RI, Ganz T. Differential scanning microcalorimetry indicates that human defensin, HNP-2, interacts specifically with biomembrane mimetic systems. *Biochemistry* 1997;36:1525-31.
- [2] Sharma VK, Mamontov E, Anunciado DB, O'Neill H, Urban VS. Effect of antimicrobial peptide on the dynamics of phosphocholine membrane: role of cholesterol and physical state of bilayer. *Soft Matter* 2015;11:6755-67.
- [3] Prenner EJ, Lewis RN, Kondejewski LH, Hodges RS, McElhaney RN. Differential scanning calorimetric study of the effect of the antimicrobial peptide gramicidin S on the thermotropic phase behavior of phosphatidylcholine, phosphatidylethanolamine and phosphatidylglycerol lipid bilayer membranes. *BBA-Biomembranes* 1999;1417:211-23.
- [4] Aroui A, Dathe M, Blume A. Peptide induced demixing in PG/PE lipid mixtures: a mechanism for the specificity of antimicrobial peptides towards bacterial membranes? *BBA-Biomembranes* 2009;1788:650-9.
- [5] Liu F, Lewis RN, Hodges RS, McElhaney RN. A differential scanning calorimetric and ³¹P NMR spectroscopic study of the effect of transmembrane α -helical peptides on the lamellar– reversed hexagonal phase transition of phosphatidylethanolamine model membranes. *Biochemistry* 2001;40:760-8.
- [6] Seto GW, Marwaha S, Kobewka DM, Lewis RN, Separovic F, McElhaney RN. Interactions of the Australian tree frog antimicrobial peptides aurein 1.2, citropin 1.1 and maculatin 1.1 with lipid model membranes: differential scanning calorimetric and Fourier transform infrared spectroscopic studies. *BBA-Biomembranes* 2007;1768:2787-800.
- [7] Hasan IY, Mechler A. Analytical approaches to study domain formation in biomimetic membranes. *Analyst* 2017;142:3062-78.
- [8] Hasan IY, Mechler A. Viscoelastic changes measured in partially suspended single bilayer membranes. *Soft Matter* 2015;11:5571-9.
- [9] Le CTM, Hourai AJ, Balage NS, Smith BJ, Mechler A. Interaction of small ionic species with phospholipid membranes: the role of metal coordination. *Front Mater* 2018;5:80.
- [10] Mechler A, Praporski S, Atmuri K, Boland M, Separovic F, Martin LL. Specific and selective peptide-membrane interactions revealed using quartz crystal microbalance. *Biophys J* 2007;93:3907-16.
- [11] Shahmiri M, Enciso M, Mechler A. Controls and constraints of the membrane disrupting action of Aurein 1.2. *Sci Rep* 2015;5:16378.
- [12] Pandidan S, Mechler A. Nano-viscosimetry analysis of the membrane disrupting action of the bee venom peptide melittin. *Sci Rep* 2019;9:10841.

Part 1:

Membrane disrupting antimicrobial peptides form distinct domains in single bilayer membranes: a nano-viscosimetry study

Membrane disrupting antimicrobial peptides form distinct domains in single bilayer membranes: a nano-viscosimetry study

Sara Pandidan and Adam Mechler

La Trobe Institute for Molecular Science, La Trobe University, Melbourne, Australia

Abstract

Antimicrobial peptides (AMPs) are essential components of host defence against infections, which serve as the first line of innate immunity against bacterial and fungal infections in a wide range of organisms. These peptides exhibit potent and broad-spectrum antibacterial activity, offering a novel pathway to the development of novel therapeutic agents. Consistently AMPs were investigated for design motifs to design alternative antibiotic classes against multi-drug-resistant bacterial strains. However, despite the wide-ranging studies, in most cases the molecular process that leads to membrane disruption is not well understood. It is believed that the mechanism of action follows a series of thermodynamic equilibria, involving several distinct states. In this study nano-viscosimetry based phase transition measurements were used to identify domains formed by specific lipid-peptide structures, corresponding to distinct thermodynamic states. Two well known membrane disruptor AMPs were chosen for this study: melittin (from honeybee venom) and magainin 2 (from the skin of African clawed frog). It was found that membranes exposed to either of these pore former peptides have distinct domains, characterized by different phase transition temperatures. The number of the distinct domains correlate well to the previously described states of the mechanism of action of each peptide: four states of the fissure-forming mechanism of melittin and three states for magainin 2 that forms transient pores in the membrane. The phase transition data confirms these hitherto hypothetic stages as actual thermodynamic states, characterized by specific peptide-membrane interactions that lead to the formation of domains of different phase transition temperatures.

Introduction

Antimicrobial peptides (AMPs) provide immediate immune response at the site of infection with wide ranging activity [13]. Since AMPs evolved to target bacteria the most efficient way, they are less likely to give rise to resistant bacterial strains [14]. While AMPs can act via several pathways, pore forming membrane disruptor AMPs are the most studied category because of their relatively simple structure and mechanism of action, as well as broad spectrum activity that makes these AMPs potentially suitable antibiotics, and also for applications from anti-cancer therapeutics to drug delivery agents [15-24]. However, realising these applications was inhibited by the lack of understanding the way they exert their activity: the physicochemical properties that provide specificity and selectivity during the molecular mechanism of their action [25-28]. For most AMPs there is still no consensus on their dominant mechanism of action and even less information about the parameters and molecular interactions that define this mechanism.

Melittin and magainin 2 serve as typical examples. Melittin, the main component of bee (*Apis mellifera*) venom, is an extensively studied yet enigmatic AMP of a sequence of 26 amino acids [28, 29]. In apolar environment melittin is described as mostly α -helical, exhibiting two folded segments intersecting at an angle of 120° due to a proline residue [30, 31]. However, in a membrane environment, i.e. at the interface of polar aqueous and lipid media the N-terminal charged region is most likely unstructured, hence models describing melittin as an α -helical peptide are approximations. The mechanism of melittin action is debated. In early studies it was suggested that melittin induced barrel-stave pore-formation, that is, assemble into a small oligomeric transmembrane channel [32, 33]. This was revised upon further experimental and molecular dynamic simulation studies to toroidal pore formation [34-37]. However there is evidence that in anionic membranes the mechanism switches to detergent-like action [38], and that the peptide does not form pores at all, instead opening linear fissures in the membrane [39, 40]. Based on the model described in melittin action proceeds through the following steps on DMPC model membranes: unstructured peptide in solution \leftrightarrow surface adsorbed unstructured peptide \leftrightarrow surface adsorbed helical peptide \leftrightarrow membrane inserted monomeric peptide (top leaflet) \leftrightarrow membrane inserted linear aggregate (top leaflet) \leftrightarrow transmembrane fissure (opposing linear aggregates in both leaflets) \leftrightarrow pore/micelle formation [40].

Magainin 2 is another well-studied α -helical, cationic AMP, which was isolated from the skin of the African clawed frog (*Xenopus laevis*) [41]. Magainin 2 is mainly described as a toroidal pore former membrane disruptor AMP [42-50], albeit with a transient action: the pore size is reported to be larger at the beginning of interaction, decreasing gradually until reaching a steady state [27]. It was suggested that initially the peptide is oriented parallel to the membrane, associated to the head group region [51, 52]. By increasing the concentration, the peptide triggers local distortion in lipid packing leading to a transient transmembrane state that in turn allows translocation from the outer to the inner leaflet, forming pores in the process [46, 52]. The steady-state binding to the surface can alter the membrane curvature and form toroidal pores [45]. Consistently the magainin-membrane interaction is described as a two-state transition that includes a binding state transforming into insertion/pore state [48, 53] although logically it has to include another transition from the pore state to the inner leaflet [54-56]. As with melittin, the pore has never been observed directly, and there is surprisingly little data in support of the hypothetical mechanism. It is desirable to find new means of characterization of peptide-membrane interactions to detect the thermodynamic states of the system.

Calorimetry is the basic method to measure thermodynamic properties. In case of a peptide-membrane system, the phase transitions of model membranes are well described and may serve as a basis for calorimetric measurements of the effect of the peptides on the membrane. Model membranes are typically neat or binary mixtures of serving as a simple model of the 'fluid mosaic' of the biological membrane structure [57-59]. However, the simplicity of the model membrane allows for complex temperature-dependent changes in packing and viscosity. At characteristic temperatures the membrane undergoes reversible, cooperative phase transitions identified from a well-defined change in packing and viscoelastic properties [60]. During these phase transitions, the bilayer membrane remains intact [61]. DMPC (phosphocholine lipid of 14 carbon atom long saturated acyl chains) shows two phase transitions at the so called pre-transition and main transition temperatures [62]. At low temperature DMPC exists in the L_c crystalline dehydrated state where all molecular motions are restricted resulting in a water-impermeable structure [61]. By increasing the temperature the lipid molecules gain higher freedom of motion, lose alignment, which causes a decrease in bilayer thickness and a change in packing leading to the so called "rippled gel" (P_β) phase [63]. Upon further

heating the acyl chains “melt” at the so called main transition temperature, substantially increasing lipid mobility while reducing membrane thickness [64].

Given the profound effect they have on membrane structure it is expected that AMPs influence phase transitions. There is only scarce data in the literature, for a diverse group of peptides. A calorimetry study in 1996 suggested that melittin can shift pre-transition temperature of DPPC lipids, without noticeable change of main transition temperature [1]. In 1999, another study concluded that the presence of gramicidin did not have a significant effect on the phase transitions of zwitterionic bilayers, however it has a strong effect on the phase behaviour of anionic lipids [3]. Yet it was reported by others that interaction of melittin with lipid head groups lead to confined diffusion yielding a stiffening effect on DMPC membrane [2]. In a differential scanning calorimetry (DSC) and FT-IR study the synthetic peptide Ac-RRWWRF-NH₂ reduced the main phase transition temperature of 1,2-dipalmitoyl-sn-glycero-3-phosphoethanolamine (DPPG) vesicles [4]. Other studies by DSC on α -helical peptides with anionic and zwitterinic membranes [6] and 1,2-di-laidoylphosphatidylethanolamine (DEPE) [5] reported a reduction of the main transition temperature. Another DSC study suggested DPPC:DPPG phase transition appeared at lower temperatures in the presence of an analogue of the peptide Hyalina1 (from the skin secretion of the frog (*Hypsiboas albopunctatus*))[65].

Most recently a fluorescence study suggested that cecropin can increase the membrane rigidity without an effect on the phase transitions of DMPG membrane [66]. These studies suggest, with some ambiguity, that peptides can alter phase transition temperatures and/or viscoelastic properties of membranes.

We have shown before that QCM nano-viscosimetry can be used as an alternative to bulk calorimetry, identifying phase transitions from changes in viscosity of single bilayer membranes [7-10]. This led to identification of membrane domains [8, 39, 67]. Here this method is applied to detect the effect of peptide incorporation on membrane phase transitions, with an aim of identifying different membrane bound states, appearing as distinct membrane domains in their viscoelastic properties.

Materials and methods

Vesicle preparation

The phospholipid 1,2-dimyristoyl-sn-glycero-3-phosphocholine (DMPC) was purchased from Avanti Polar Lipids (Alabaster, AL, USA). Chloroform (ACS Reagent, 99.8%) was purchased from Sigma-Aldrich (Castle Hill, NSW, Australia). After preparing the stock solution by dissolving the precisely measured lyophilized lipids in chloroform, 100 μ M from DMPC stock solution was added in a clean test tube. The solvent was evaporated with moderate vortexing and gentle nitrogen gas flow to obtain a uniform layer on the wall of the test tube. The prepared tubes were placed in a desiccator to eliminate any remaining solvent residue. At the time of using, the dry lipid layers were hydrated in 1 ml PBS in 37°C incubator for 30 minutes, followed by one minute vortexing and brief sonication [39].

Buffer preparation

Fluka branded potassium hydrogen phosphate (K_2HPO_4) was purchased from Honeywell (Shanghai, China) and potassium dihydrogen phosphate (KH_2PO_4) was purchased from Sigma Aldrich (Castle Hill, NSW, Australia). Sodium chloride (NaCl) was purchased from Chem-Supply Pty Ltd, Gillman SA, Australia. The phosphate buffered saline (PBS) contained 20mM phosphate and 100mM NaCl at pH 7.2. Deionized water of 18.2 M Ω cm resistivity (from an Ultrapure instrument, Sartorius AG, Germany) was used for all samples.

Quartz Crystal Microbalance

All experiments were performed with a Q-SENSE E4 system (Q-SENSE, Sweden) using AT-cut gold-coated quartz QCM chips with a fundamental resonance frequency of 5 MHz. The QCM chips were cleaned with base piranha solution consisting of 1:1:3 mixture of hydrogen peroxide (aqueous solution, 30%) purchased from ChemSupply Pty Ltd, Australia, Gillman, SA; ammonia solution (28-30%) purchased from Merck, Darmstadt, Germany; and deionized water, at 70°C for 20 minutes. After cleaning and drying under a gentle stream of N_2 , the chips were modified in a solution of 2% 3-mercaptopropionic acid (MPA) (HPLC Grade, > 99%, Fluka branded product from Sigma Aldrich, Castle Hill, NSW, Australia) in propan-2-ol overnight. MPA promotes liposome fusion and the formation of a partially suspended bilayer [68]. Before use the modified chips were soaked in propan-2-ol to remove any excess thiol from the surface; after

subsequent drying, the chips were placed in deionized water for a few hours to hydrate the MPA self-assembled monolayer.

Lipid deposition

After the MPA modified chips were installed in to the QCM chambers, in order to confirm the stability of the sensor signals and to provide a reference, baselines were recorded first in deionized water and in PBS. Next, the DMPC lipid suspensions with flow rate of 50 $\mu\text{L}/\text{min}$ at 19°C were added into the chambers. When a stable baseline was reached, mild osmotic stress (20 mM phosphate buffer solution without salt) was used to rupture/remove liposome residues and form a uniform single bilayer based on previous study [69]. After obtaining a normal PBS baseline, melittin (GL Biochem Ltd., Shanghai) or magainin 2 (GL Biochem Ltd., Shanghai) solution were introduced at desired concentrations, following with a final stage of buffer wash. A temperature sweeping profile of 19°C to 37°C was programmed in QCM with a slope of 0.2 C/min while the flow of PBS was stopped. All experiments were repeated at least five times and the temperatures reported were the average obtained in each concentration for individual heating and cooling cycles.

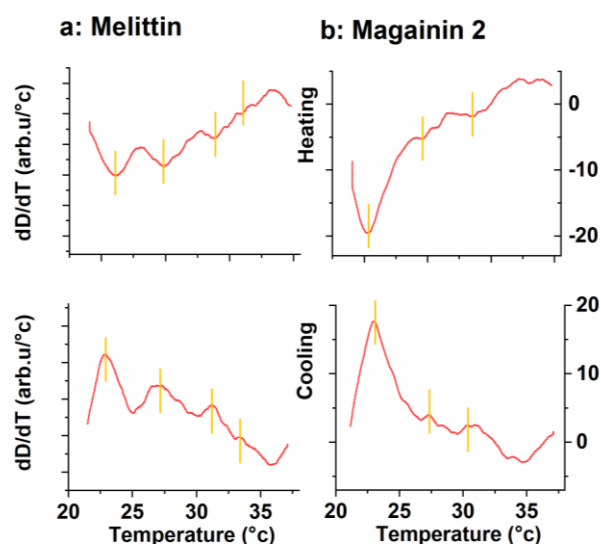


Figure 1. Heating and cooling versus temperature for third loop of temperature ramping after adding 15 μM a) melittin b) magainin 2

By using a partially suspended model membrane system, the membrane gains a high degree of freedom to dissipate energy by out-of-plane motion, hence the QCM dissipation signal becomes a useful measure of viscoelastic changes in the membrane upon various stimuli [8, 70].

The frequency (Δf) and energy dissipation (ΔD) were recorded simultaneously at five eigenmodes of the sensor (3, 5, 7, 9, 11 and 13th) corresponding to 15, 25, 35, 45, 55 and 65 MHz, respectively. However, the analysis was performed on the 5th eigenmode, 25MHz, as it was shown to provide the most reliable data on lipid membrane analysis [39].

To find the effect of membrane disrupting peptides on lipid phase transition, the temperature derivatives of the dissipation change signals [71] were plotted over temperature at each heating and cooling cycles at different concentrations of peptides. Melittin and magainin 2 were used as well-known models for membrane disrupting AMPs [48, 72-74]. As published previously, plotting first derivative of dissipation over temperature can clearly show the phase transitions at the fastest rate of viscosity changes [67].

Results and Discussions

After introducing the desired concentrations of peptide on the single bilayer membranes, temperature sweeping procedure was repeated three times, analogous to a calorimetry measurement. Figure 1 shows plots of dD/dT against temperature. The heating and cooling cycles show symmetrical patterns of different peaks in each cycle for both peptides. The magnitude of these peaks varies, which either reflect the size of, or the different magnitude of viscosity change upon phase transition in the corresponding domains.

There is an offset of $\sim 1^\circ\text{C}$ between heating and cooling cycles that is consistent in all cycles and is the result of a small heat gradient between the measurement chamber and the location of the thermometer; averaging the peak positions for the heating and the cooling cycles removes this systematic error.

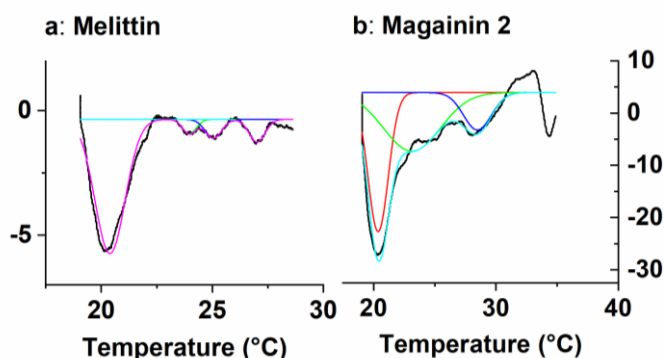


Figure 2. Gaussian fitting of dD/dT vs temperature for the heating cycle in the third loop of temperature sweeping for after adding a) $15\mu\text{M}$ melittin b) $15\mu\text{M}$ magainin 2 respectively

Figure 2 shows analysis of the phase transition information by Gaussian peak fitting for the case of $15\mu\text{M}$ peptide concentrations as an example. Gaussian fit to the multiple peaks results in envelopes that follow the raw data very well, and thus the phase transition temperatures can be determined with the accuracy of the QCM temperature sensor, that is, with approximately mK accuracy.

The average of heating and cooling phase transition temperatures for each individual peak with different concentrations of melittin and magainin 2 in all cycles were extracted and summarized in Figure 3. The distinct peaks reveal different domains that correlate to the membrane bound states of the peptides: in case of melittin, there are consistently four states whereas for magainin 2 there are three states.

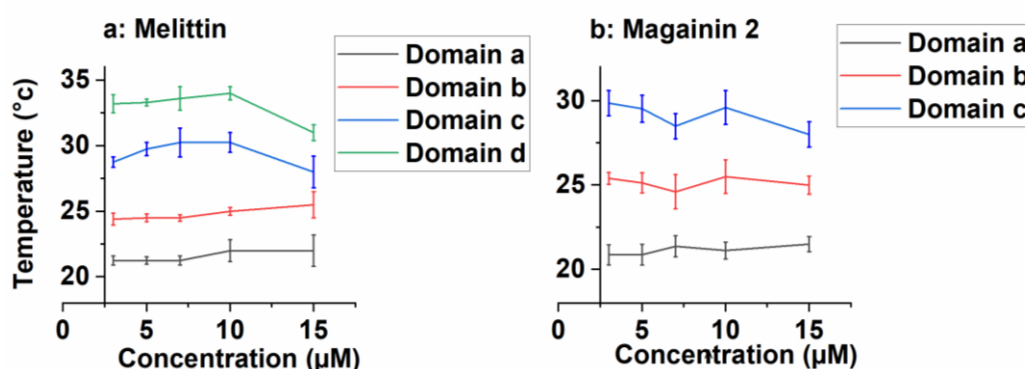


Figure 3. Average temperature achieved for each domain on different concentration of a) melittin and, b) magainin 2

The phase transition temperatures show some degree of peptide concentration dependence, following distinct trends. In the case of melittin, at low peptide concentrations up to $7\mu\text{M}$ the phase transition temperatures are not affected much, except

in domain c. By further increasing the concentration, for the first two domains the temperature shows a slight increase (0.75°C and 0.5°C, respectively). For domains c and d there are distinct gradual temperature increases of 1°C to 0.5°C to straight line and 0.1°C following by 0.3°C to 0.4°C, respectively. However, the temperature dependence terminates with a slight temperature drop of 2.25°C for domain c and 3°C for domain d at 15 μ M.

For magainin 2, there is a fluctuation at 5 μ M for domain c, however the nearly straight trends at ~21°C and ~25°C continue up to 15 μ M for domain a and b, respectively. For domain c, after a slight decrease up to 7 μ M the trend shows 1°C increase followed by a sharp drop at 15 μ M.

The distinct domains are the result of different peptide-membrane interactions, that perturb the main transition of DMPC [67], reflecting the different thermodynamic states and the equilibria between them throughout the membrane disrupting mechanism of the peptide, characterized by different intermolecular interactions. The system can be described from the point of the peptides as a series of states characterized by different free energies, while the membrane provides a platform offering these specific states for occupancy to the peptide. The phase transition of membrane domains representing these different thermodynamic states will be changing with peptide concentration due to changes in occupancy at each of the discrete energy states. The different phase transition temperatures are resulted from perturbations to membrane packing, related to the different insertion geometry of peptide. The occupancy of each state is governed by the Boltzmann distribution, balancing higher free energy with mixing entropy. Equilibria between multiple states can be described as constant chemical potential of any individual peptide irrespective of which state does it occupy. Thus, increasing concentration of the lowest energy state increases occupancy in the higher energy states. This is the thermodynamic basis of threshold behaviour of membrane disruption.

In a generic mechanism of action of membrane penetrating AMPs initially the peptide monomers would adsorb to the membrane surface (equilibrium 1) and form helical structure (equilibrium 2). The helical state might lead to immediate membrane penetration as in case of melittin, or a deeper insertion to the core-headgroup interface of the membrane. It is expected that in calorimetric measurements the key observable difference is between surface bound state and membrane penetrated state, as in the first case the peptide interacts mostly with the headgroups and in the latter case with the alkyl chains.

Hence if the membrane adsorbed helical state is distinct, the two initial states are indistinguishable; however if the folding takes place continuously (as a process) during membrane penetration, it is expected to yield a different membrane domain in calorimetry. Neither of melittin or magainin 2 are known to aggregate on the membrane surface [75, 76]. Hence the two key states we expect for both peptides are i) a surface bound and ii) a membrane inserted monomeric state.

The third observable state is markedly different between melittin and magainin 2. In the hypothesis presented in [40] the next state for melittin is a linear aggregate that opens superficial fissures in the membrane that is in equilibrium with the monomeric state (equilibrium 3) that leads to flip-flopping and matching linear aggregates from the inner leaflet, leading to transmembrane cracks (equilibrium 4). These two are characterized by distinct changes in lipid-peptide interaction, therefore expected to form two separate domains. Breaking up the membrane into disc-like aggregates, while geometrically speaking is a different stage, it is not a different state since the peptide-membrane interaction is not changing in the process. Consistently, in the fissure pathway melittin would be expected to form a total of four membrane domains that is consistent with the calorimetric data.

For magainin 2, the membrane insertion is achieved by membrane modulation, effectuating transient pore opening, from which the peptide might return to either (inner or outer) membrane leaflet, leading to an eventual equilibrium between the surface densities of the peptide between the two leaflets and reduction in pore activity. The two surface bound states might be equivalent in the thermodynamic sense, if membrane curvature and solvent effects (cytoplasm has different ionic environment) are disregarded. They are distinctly different, however, in the nano-viscometry experiments: the membrane tension and lipid mobility are substantially different between the leaflets in the initial state, whereas close to even in the final equilibrium state. Hence, for magainin 2, three distinct states are expected: outer surface populated, transmembrane state and both surfaces populated. This is also consistent with the QCM data.

We can attempt to identify these states from the calorimetry data. Surface adsorption leads to direct peptide interactions with the lipid headgroups and replacing water, hence reducing headgroup repulsion. This could lead to a small increase in phase transition temperature. Consistently, one of the domains exhibited phase transitions close to, but slightly above the neat membrane (the average of 24.78 for melittin and 25.12 for

magainin 2). The phase transition temperature showed weak dependence on the peptide concentration, suggesting that the occupancy of this state is nearly complete at low concentrations.

The next detectable state is the membrane penetrated monomeric state, which for melittin is likely limited to the top leaflet as described before [40]. In this state the polar side of the helix is surrounded by aliphatic chains, that is energetically unfavourable and is expected to lead to a decrease in phase transition temperature. Thus the $\sim 21^\circ\text{C}$ phase transition can be assigned to the domain containing the membrane inserted monomeric state. Similarly, in case of magainin 2 the transmembrane state eventuates from the disruption of lipid order, hence the transition at $\sim 21^\circ\text{C}$ is the likely domain corresponding to this state. Notably, a very similar phase transition temperature but very different geometric effects: in the first case, the membrane is intact; in the second, that is the actual pore formation.

The remaining two states for melittin are both characterized by increased membrane phase transition temperature, suggesting increased lateral (binding) interactions. This is consistent with an aggregated state of the peptide that restrains membrane mobility. For melittin, the linear aggregates and the transmembrane fissures as described in [40] would be able to impose such constraints; likely the latter is the domain with the highest phase transition temperature, as it shows a major change towards high peptide concentration when the membrane finally breaks up and thus the constraints are relaxed [39, 40].

For magainin 2, the third state is characterized by increased phase transition temperature that is consistent with the increased lipid-peptide-lipid interaction in the two adjacent leaflets, and the collapse of the membrane into linear micelles as described before [Chapter four] [37, 48].

The data confirms the coexistence of these distinct states in the membrane, suggesting a chain of interdependent equilibria in which the individual peptide monomer has the same chemical potential irrespective of which state it is in, and therefore it can move reversibly between the states as described by equation 1[77]:

$$\mu = \mu_n^i + kT \log(X_n) = \text{Constant} \quad \text{for all states } n = 1, 2, 3, \dots$$

Equation 1. Chemical potential

The chemical potential gives the total energy of each molecule, including the free energy μ and the entropic effect of the ensemble through the $kT \ln(X_n)$ term [77]. The free energy

term is dominated by binding energy, which in this case is a sum of intermolecular interactions between lipid and peptide molecules, that is seen indirectly in the way the presence of the peptide disrupts lipid-lipid interactions (replaced by lipid-peptide interactions between neighbours), and therefore the phase transition temperatures. As an approximation, acknowledging that the peptide-peptide interactions are not measured, the free energies of each state can be therefore correlated to the change in membrane phase transition temperature. Considering that the phase transition temperature changes were both positive and negative, entropy factors must play a role in the process, explaining the existence of threshold concentration(s) in the membrane disruption. In simple terms, the occupancy of the higher energy states is only noticeable when the concentration of the lowest energy (and most dispersed) state is increased, in a process similar to aggregation of surfactants at critical micelle concentration.

Importantly the chain of dynamic equilibria between all membrane bound states as described here is consistent with a model proposed before that described AMP action in terms of effect on membrane and recoverability of the induced changes [78].

Conclusions

In this work a new method was presented to study the mechanism of membrane disrupting antimicrobial peptides based on phase transitions of the target membranes, measured as viscosity changes as the function of temperature changes. The existence of domains of different phase transition temperatures proves the existence of distinct thermodynamic states in terms of peptide-membrane interactions. The four distinct thermodynamic states detected for melittin correlate well to hypothetical model mechanism described before; similarly, the three states detected for magainin 2 are consistent with the accepted model of the mechanism of action. Thus, data is presented here that indicated, albeit qualitatively, the thermodynamic states occupied by the peptides in the membrane, opening new avenues for future physicochemical studies of antimicrobial peptides.

References

- [1] Lohner K, Latal A, Lehrer RI, Ganz T. Differential scanning microcalorimetry indicates that human defensin, HNP-2, interacts specifically with biomembrane mimetic systems. *Biochemistry* 1997;36:1525-31.
- [2] Sharma VK, Mamontov E, Anunciado DB, O'Neill H, Urban VS. Effect of antimicrobial peptide on the dynamics of phosphocholine membrane: role of cholesterol and physical state of bilayer. *Soft Matter* 2015;11:6755-67.
- [3] Prenner EJ, Lewis RN, Kondejewski LH, Hodges RS, McElhaney RN. Differential scanning calorimetric study of the effect of the antimicrobial peptide gramicidin S on the thermotropic phase behavior of phosphatidylcholine, phosphatidylethanolamine and phosphatidylglycerol lipid bilayer membranes. *BBA-Biomembranes* 1999;1417:211-23.
- [4] Aroui A, Dathe M, Blume A. Peptide induced demixing in PG/PE lipid mixtures: a mechanism for the specificity of antimicrobial peptides towards bacterial membranes? *BBA-Biomembranes* 2009;1788:650-9.
- [5] Liu F, Lewis RN, Hodges RS, McElhaney RN. A differential scanning calorimetric and ³¹P NMR spectroscopic study of the effect of transmembrane α -helical peptides on the lamellar– reversed hexagonal phase transition of phosphatidylethanolamine model membranes. *Biochemistry* 2001;40:760-8.
- [6] Seto GW, Marwaha S, Kobewka DM, Lewis RN, Separovic F, McElhaney RN. Interactions of the Australian tree frog antimicrobial peptides aurein 1.2, citropin 1.1 and maculatin 1.1 with lipid model membranes: differential scanning calorimetric and Fourier transform infrared spectroscopic studies. *BBA-Biomembranes* 2007;1768:2787-800.
- [7] Hasan IY, Mechler A. Analytical approaches to study domain formation in biomimetic membranes. *Analyst* 2017;142:3062-78.
- [8] Hasan IY, Mechler A. Viscoelastic changes measured in partially suspended single bilayer membranes. *Soft Matter* 2015;11:5571-9.
- [9] Le CTM, Hourri AJ, Balage NS, Smith BJ, Mechler A. Interaction of small ionic species with phospholipid membranes: the role of metal coordination. *Front Mater* 2018;5:80.
- [10] Mechler A, Praporski S, Atmuri K, Boland M, Separovic F, Martin LL. Specific and selective peptide-membrane interactions revealed using quartz crystal microbalance. *Biophys J* 2007;93:3907-16.
- [11] Shahmiri M, Enciso M, Mechler A. Controls and constraints of the membrane disrupting action of Aurein 1.2. *Sci Rep* 2015;5:16378.
- [12] Pandidan S, Mechler A. Nano-viscosimetry analysis of the membrane disrupting action of the bee venom peptide melittin. *Sci Rep* 2019;9:10841.
- [13] Hancock RE, Sahl H-G. Antimicrobial and host-defense peptides as new anti-infective therapeutic strategies. *Nat. Biotechnol.* 2006;24:1551-7.
- [14] O'Connell KM, Hodgkinson JT, Sore HF, Welch M, Salmond GP, Spring DR. Combating multidrug-resistant bacteria: current strategies for the discovery of novel antibacterials. *Angew. Chem. Int. Ed.* 2013;52:10706-33.
- [15] Shai Y, Oren Z. From “carpet” mechanism to de-novo designed diastereomeric cell-selective antimicrobial peptides. *Peptides* 2001;22:1629-41.
- [16] Wimley WC, Hristova K. Antimicrobial peptides: successes, challenges and unanswered questions. *J Membr Biol* 2011;239:27-34.
- [17] Pan H, Soman NR, Schlesinger PH, Lanza GM, Wickline SA. Cytolytic peptide nanoparticles ('NanoBees') for cancer therapy. *Wiley Interdiscip Rev Nanomed Nanobiotechnol* 2011;3:318-27.

- [18] Shai Y. Mode of action of membrane active antimicrobial peptides. *Pept Sci* 2002;66:236-48.
- [19] Kauffman WB, Fuselier T, He J, Wimley WC. Mechanism matters: a taxonomy of cell penetrating peptides. *Trends Biochem. Sci* 2015;40:749-64.
- [20] Liu S, Yang H, Wan L, Cai H-w, Li S-f, Li Y-p, et al. Enhancement of cytotoxicity of antimicrobial peptide magainin II in tumor cells by bombesin-targeted delivery. *Acta Pharmacol. Sin.* 2011;32:79.
- [21] Lehmann J, Retz M, Sidhu SS, Suttman H, Sell M, Paulsen F, et al. Antitumor activity of the antimicrobial peptide magainin II against bladder cancer cell lines. *Eur Urol* 2006;50:141-7.
- [22] Raaymakers C, Verbrugghe E, Hernot S, Hellebuyck T, Betti C, Peleman C, et al. Antimicrobial peptides in frog poisons constitute a molecular toxin delivery system against predators. *Nat Commun* 2017;8:1495.
- [23] Gerlach SL, Rathinakumar R, Chakravarty G, Göransson U, Wimley WC, Darwin SP, et al. Anticancer and chemosensitizing abilities of cycloviolacin O2 from *Viola odorata* and psyle cyclotides from *Psychotria leptothyrsa*. *Pept Sci* 2010;94:617-25.
- [24] Guha S, Ghimire J, Wu E, Wimley WC. Mechanistic Landscape of Membrane-Permeabilizing Peptides. *Chem Rev* 2019;119:6040-85.
- [25] Brogden KA. Antimicrobial peptides: pore formers or metabolic inhibitors in bacteria? *Nat Rev Microbiol* 2005;3:238-50.
- [26] Melo MN, Ferre R, Castanho MA. Antimicrobial peptides: linking partition, activity and high membrane-bound concentrations. *Nat Rev Microbio* 2009;7:245.
- [27] Tamba Y, Ariyama H, Levadny V, Yamazaki M. Kinetic pathway of antimicrobial peptide magainin 2-induced pore formation in lipid membranes. *J Phys Chem B* 2010;114:12018-26.
- [28] Sun D, Forsman J, E Woodward C. Current understanding of the mechanisms by which membrane-active peptides permeate and disrupt model lipid membranes. *Curr Top Med Chem* 2016;16:170-86.
- [29] Raghuraman H, Chattopadhyay A. Melittin: a membrane-active peptide with diverse functions. *Biosci Rep* 2007;27:189-223.
- [30] Terwilliger TC, Eisenberg D. The structure of melittin. I. Structure determination and partial refinement. *J Biol Chem* 1982;257:6010-5.
- [31] Bazzo R, Tappin MJ, Pastore A, Harvey TS, Carver JA, Campbell ID. The structure of melittin: A 1H-NMR study in methanol. *Eur J Biochem* 1988;173:139-46.
- [32] Vogel H, Jähnig F. The structure of melittin in membranes. *Biophys J* 1986;50:573.
- [33] Sansom MS. The biophysics of peptide models of ion channels. **Prog Biophys Mol Biol** 1991;55:139-235.
- [34] Yang L, Harroun TA, Weiss TM, Ding L, Huang HW. Barrel-stave model or toroidal model? A case study on melittin pores. *Biophys J* 2001;81:1475-85.
- [35] Lin J-H, Baumgaertner A. Stability of a melittin pore in a lipid bilayer: a molecular dynamics study. *Biophys J* 2000;78:1714-24.
- [36] Irudayam SJ, Berkowitz ML. Influence of the arrangement and secondary structure of melittin peptides on the formation and stability of toroidal pores. *BBA-Biomembranes* 2011;1808:2258-66.
- [37] Sengupta D, Leontiadou H, Mark AE, Marrink S-J. Toroidal pores formed by antimicrobial peptides show significant disorder. *BBA-Biomembranes* 2008;1778:2308-17.
- [38] Papo N, Shai Y. Exploring peptide membrane interaction using surface plasmon resonance: differentiation between pore formation versus membrane disruption by lytic peptides. *Biochemistry* 2003;42:458-66.

- [39] Lee T-H, Hall K, Mechler A, Martin L, Popplewell J, Ronan G, et al. Molecular imaging and orientational changes of antimicrobial peptides in membranes. *Peptides for Youth*: Springer; 2009. p. 313-5.
- [40] Pandidan S, Mechler A. Nano-viscosimetry analysis of the membrane disrupting action of the bee venom peptide melittin. *Sci Rep* 2019;9:1-12.
- [41] Zasloff M. Magainins, a class of antimicrobial peptides from *Xenopus* skin: isolation, characterization of two active forms, and partial cDNA sequence of a precursor. *PNAS* 1987;84:5449-53.
- [42] Nguyen KT, Le Clair SV, Ye S, Chen Z. Molecular interactions between magainin 2 and model membranes in situ. *Journal Phys Chem B* 2009;113:12358-63.
- [43] Kim C, Spano J, Park E-K, Wi S. Evidence of pores and thinned lipid bilayers induced in oriented lipid membranes interacting with the antimicrobial peptides, magainin-2 and aurein-3.3. *BBA-Biomembranes* 2009;1788:1482-96.
- [44] Tamba Y, Masum SM, Yamazaki M. Effects of Surface Charge Density of Lipid Membranes on the Pore Formation Induced by Magainin 2. *International Symposium on Micro-NanoMechatronics and Human Science: IEEE*; 2007. p. 96-101.
- [45] Karal MAS, Alam JM, Takahashi T, Levadny V, Yamazaki M. Stretch-activated pore of the antimicrobial peptide, magainin 2. *Langmuir* 2015;31:3391-401.
- [46] Yang L, Weiss TM, Harroun TA, Heller WT, Huang HW. Supramolecular structures of peptide assemblies in membranes by neutron off-plane scattering: method of analysis. *Biophys J* 1999;77:2648-56.
- [47] Murzyn K, Pasenkiewicz-Gierula M. Construction of a toroidal model for the magainin pore. *J Mol Model* 2003;9:217-24.
- [48] Ludtke SJ, He K, Heller WT, Harroun TA, Yang L, Huang HW. Membrane pores induced by magainin. *Biochemistry* 1996;35:13723-8.
- [49] Hallock KJ, Lee D-K, Ramamoorthy A. MSI-78, an analogue of the magainin antimicrobial peptides, disrupts lipid bilayer structure via positive curvature strain. *Biophys J* 2003;84:3052-60.
- [50] Yang L, Weiss TM, Lehrer RI, Huang HW. Crystallization of antimicrobial pores in membranes: magainin and protegrin. *Biophys J* 2000;79:2002-9.
- [51] Hirsh DJ, Hammer J, Maloy WL, Blazyk J, Schaefer J. Secondary structure and location of a magainin analogue in synthetic phospholipid bilayers. *Biochemistry* 1996;35:12733-41.
- [52] Bechinger B, Zasloff M, Opella SJ. Structure and orientation of the antibiotic peptide magainin in membranes by solid-state nuclear magnetic resonance spectroscopy. *Protein Sci* 1993;2:2077-84.
- [53] Tamba Y, Yamazaki M. Magainin 2-induced pore formation in the lipid membranes depends on its concentration in the membrane interface. *J Phys Chem B* 2009;113:4846-52.
- [54] Tamba Y, Yamazaki M. Single giant unilamellar vesicle method reveals effect of antimicrobial peptide magainin 2 on membrane permeability. *Biochemistry* 2005;44:15823-33.
- [55] Matsuzaki K, Murase O, Fujii N, Miyajima K. Translocation of a channel-forming antimicrobial peptide, magainin 2, across lipid bilayers by forming a pore. *Biochemistry* 1995;34:6521-6.
- [56] Matsuzaki K, Sugishita K-i, Ishibe N, Ueha M, Nakata S, Miyajima K, et al. Relationship of membrane curvature to the formation of pores by magainin 2. *Biochemistry* 1998;37:11856-63.
- [57] Van Meer G, Voelker DR, Feigenson GW. Membrane lipids: where they are and how they behave. *Nat Rev Mol Cell Biol* 2008;9:112-24.

- [58] Vereb G, Szöllösi J, Matko J, Nagy P, Farkas T, Vigh L, et al. Dynamic, yet structured: the cell membrane three decades after the Singer–Nicolson model. *PNAS* 2003;100:8053-8.
- [59] Nicolson GL. The Fluid—Mosaic Model of Membrane Structure: Still relevant to understanding the structure, function and dynamics of biological membranes after more than 40 years. *BBA-Biomembranes* 2014;1838:1451-66.
- [60] Eze MO. Phase transitions in phospholipid bilayers: Lateral phase separations play vital roles in biomembranes. *Biochem. Educ* 1991;19:204-8.
- [61] McElhaney RN, Souza KA. The relationship between environmental temperature, cell growth and the fluidity and physical state of the membrane lipids in *Bacillus stearothermophilus*. *BBA-Biomembranes* 1976;443:348-59.
- [62] Caffrey M, Hogan J. LIPIDAT: A database of lipid phase transition temperatures and enthalpy changes. DMPC data subset analysis. *Chem phys lipid* 1992;61:1-109.
- [63] Engelman DM. Lipid bilayer structure in the membrane of *Mycoplasma laidlawii*. *J Mol Biol* 1971;58:153-65.
- [64] Lewis RN, McElhaney RN. Calorimetric and spectroscopic studies of the thermotropic phase behavior of lipid bilayer model membranes composed of a homologous series of linear saturated phosphatidylserines. *Biophys J* 2000;79:2043-55.
- [65] Enoki TA, Moreira-Silva I, Lorenzon EN, Cilli EM, Perez KR, Riske KA, et al. Antimicrobial peptide K0-W6-Hyal induces stable structurally modified lipid domains in anionic membranes. *Langmuir* 2018;34:2014-25.
- [66] Onate-Garzon J, Manrique-Moreno M, Trier S, Leidy C, Torres R, Patino E. Antimicrobial activity and interactions of cationic peptides derived from *Galleria mellonella* cecropin D-like peptide with model membranes. *J Antibiot (Tokyo)* 2017;70:238-45.
- [67] Hasan IY, Mechler A. Cholesterol Rich Domains Identified in Unilamellar Supported Biomimetic Membranes via Nano-Viscosity Measurements. *Anal Chem* 2016;88:5037-41.
- [68] Steinem C, Janshoff A, Ulrich W-P, Sieber M, Galla H-J. Impedance analysis of supported lipid bilayer membranes: a scrutiny of different preparation techniques. *BBA-Biomembranes* 1996;1279:169-80.
- [69] Hasan IY, Mechler A. Formation of planar unilamellar phospholipid membranes on oxidized gold substrate. *Biointerphases* 2016;11:031017.
- [70] Shahmiri M, Enciso M, Adda CG, Smith BJ, Perugini MA, Mechler A. Membrane Core-Specific Antimicrobial Action of Cathelicidin LL-37 Peptide Switches Between Pore and Nanofibre Formation. *Sci Rep* 2016;6:38184.
- [71] Voinova MV, Rodahl M, Jonson M, Kasemo B. Viscoelastic acoustic response of layered polymer films at fluid-solid interfaces: continuum mechanics approach. *Phys Scr* 1999;59:391.
- [72] Dufourcq EJ, Smith IC, Dufourcq J. Molecular details of melittin-induced lysis of phospholipid membranes as revealed by deuterium and phosphorus NMR. *Biochemistry* 1986;25:6448-55.
- [73] Dempsey CE, Sternberg B. Reversible disc-micellization of dimyristoylphosphatidylcholine bilayers induced by melittin and [Ala-14] melittin. *BBA-Biomembranes* 1991;1061:175-84.
- [74] Haimovich B, Tanaka JC. Magainin-induced cytotoxicity in eukaryotic cells: kinetics, dose-response and channel characteristics. *BBA-Biomembranes* 1995;1240:149-58.

- [75] Matsuzaki K, Murase O, Tokuda H, Funakoshi S, Fujii N, Miyajima K. Orientational and aggregational states of magainin 2 in phospholipid bilayers. *Biochemistry* 1994;33:3342-9.
- [76] Altenbach C, Hubbell WL. The aggregation state of spin-labeled melittin in solution and bound to phospholipid membranes: Evidence that membrane-bound melittin is monomeric. *Proteins* 1988;3:230-42.
- [77] Israelachvili JN. *Intermolecular and surface forces*: Academic press; 2015.
- [78] Hall K, Lee T-H, Mechler AI, Swann MJ, Aguilar M-I. Real-time measurement of membrane conformational states induced by antimicrobial peptides: balance between recovery and lysis. *Sci Rep* 2014;4:5479.

Part 2:

Neutron reflectometry study of the
mechanism of membrane disrupting
antimicrobial peptide action

Neutron reflectometry study of the mechanism of membrane disrupting antimicrobial peptide action

Sara Pandidan and Adam Mechler

La Trobe Institute for Molecular Science, La Trobe University, Melbourne, Australia

Abstract

Antimicrobial peptides (AMPs) kill bacteria by disrupting their plasma membrane. While the ability of AMPs to breach the membrane is well documented, still there are many uncertainties about their mechanistic pathways leading to cell lysis. Melittin (from bee venom) and aurein 1.2 (secreted by Australian tree frog *Litoria aurea*) are two well-known AMPs with substantive data on their mechanism of action, exhibiting transmembrane and surface acting mechanism, respectively. The mechanism of action of these two AMPs with model membranes have been widely studied though there are still uncertainties about their orientation throughout the interaction. In this study neutron reflectometry was used to determine and compare the location of these typical model AMPs during their interaction with DMPC (dimyristoylphosphatidylcholine) membrane. The results reveal the peptide position in the membrane at different stages of the disruption mechanism. As expected at low concentrations the peptides are mainly located in the head group region of the top leaflet. In the case of melittin the analysis shows that by increasing the concentration, the peptide first penetrates the tail region of the upper membrane leaflet, and only upon further increase in concentration can it reach the bottom leaflet. This is consistent with a multi-state equilibrium process where the peptide is driven into higher energy states by excess bulk concentration. For the case of aurein 1.2 swelling of the top leaflet and potential blistering of the membrane is detected, consistent with a surface tension-driven carpet-like mechanism.

Introduction

Antimicrobial peptides (AMPs) deliver innate immunity in practically all complex organisms [1, 2]. A subclass of these peptides acts via disrupting the plasma membrane of the pathogens. The membrane disrupting mechanism of action is classified into roughly two main groups: surface acting peptides that dissolve the membranes and transmembrane peptides that open pores through membranes [3]. It is challenging to characterize these

processes due to the small size and high mobility of the peptides, therefore the molecular mechanism of action that leads to these outcomes is still not well understood, and the hypothetic models are based on indirect measurements [4, 5].

Perhaps one of the best known transmembrane pore former peptides is melittin, the main component of honey bee (*Apis mellifera*) venom of 26 residues [6, 7]. Aurein 1.2 is a surface acting AMP that is secreted by various species of Australian tree frog (*Litoria aurea*), a short 13 residues long peptide [8-10]. Melittin and aurein 1.2 are both cationic, amphiphilic and (in apolar media) α -helical peptides that have shown to be active against numerous micro-organisms [10-13] and show anticancer activity as well [8, 14, 15]. The nano-viscosimetry based analysis of the stages of the molecular mechanism of melittin and aurein 1.2 was reported in detail before [16, 17].

The proposed model for melittin action in zwitterionic membranes includes four steps: after peptide binding to the head group region and obtaining α -helix fold the peptide can insert into the top leaflet of the membrane. Aggregation leads to the formation of linear fissures, locally destabilizing the bottom leaflet and thus the peptides access the bottom leaflet by flip-flopping; this leads to the opening of transmembrane “cracks” [17]. The surface acting aurein 1.2 follows a simpler mechanism: it was proposed that the first step is largely identical, the linear peptides can bind to the surface and become helical; after reaching a threshold concentration, the peptides aggregate on the top leaflet surface and as a loose bundle they can partially penetrate into the top leaflet, leading to asymmetric tension and thus distortion and blistering of the membrane; these blisters can eventually detach as mixed micelles, hence dissolving the membrane [16].

The models have been proposed based largely on QCM data. QCM can infer but cannot prove the localization and orientation of the peptide in the membrane during the stages of the interaction. This information would clarify many features about each specific mechanistic model. In this study the location and orientation of different concentrations of these two different AMPs during the membrane disruption process was studied by using neutron reflectometry.

Materials and Methods

Buffer preparation

Potassium dihydrogen phosphate (KH_2PO_4) and Fluka branded potassium hydrogen phosphate (K_2HPO_4) were purchased from Sigma Aldrich (Castle Hill, NSW, Australia) and Honeywell (Shanghai, China), respectively. Sodium chloride (NaCl) was purchased from Chem-Supply Pty Ltd, Gillman SA, Australia. The phosphate buffered saline (PBS) assay buffer contained 20mM phosphate and 100mM NaCl at pH 7.2. Deionized water of 18.2 M Ω cm resistivity (purified using an Ultrapure system, Sartorius AG, Germany) was used for all solutions.

Vesicle preparation

Deuterated 1,2-dimyristoyl-sn-glycero-3-phosphocholine (d_{54} -DMPC) were purchased from Avanti Polar Lipids (Alabaster, AL, USA) and chloroform (ACS Reagent, 99.8%) was purchased from Sigma-Aldrich (Castle Hill, NSW, Australia). Lyophilized lipids were dissolved in chloroform to a 100 μ M concentration and aliquoted into clean round bottom test tubes. The chloroform was evaporated with a gentle flow of nitrogen gas during continuous vortexing to obtain a uniform lipid layer at the bottom of the test tube; the prepared tubes were stored in a desiccator. Before use the lipid aliquots were hydrated in 1 ml PBS in a 37°C incubator for 30 minutes, followed by one-minute vortexing and brief sonication. This method was shown before to yield a broad distribution of mostly unilamellar liposomes [18]. The prepared lipid suspensions were used immediately. The lipid bilayers were deposited on to silica wafers by in-situ vesicle deposition [19]. Aurein 1.2 and melittin were purchased from GL Biochem Ltd., Shanghai.

Neutron reflectometry

Circular silicon wafers with diameter of 100 mm and 10 mm thick were cleaned in acidic piranha solution ($\text{H}_2\text{O}/\text{H}_2\text{SO}_4/\text{H}_2\text{O}_2$ 4:3:1) for 30 minutes at 85°C. After cleaning, the wafers were rinsed with deionized water and propanol. Neutron reflectometry data were collected using the Platypus time-of-flight neutron reflectometer and a cold neutron spectrum ($2.8 \text{ \AA} \leq \lambda \leq 18.0 \text{ \AA}$) at the OPAL 20 MW research reactor (Sydney, Australia) [20-23]. Neutron pulses of 20 Hz were generated using a disc-chopper system (EADS Astrium, Germany) in low-resolution mode ($\Delta\lambda/\lambda = 8\%$) and recorded on a 2-dimensional

helium-3 neutron detector (Denex, Germany). Reflected beam spectra were collected for each of the surfaces at 0.8° for 1 h (0.6 mm slits) and 3.0° for 3 h (2.25 mm slits), respectively, for a D₂O subphase and 0.6° (0.45 mm slits) for 1 h and 2.5° (1.875 mm slits) for 3 h for other subphase contrasts. Direct beam measurements were collected under the same collimation conditions for 1 h each. The data were reduced using the SLIM reduction package which stitches the two data sets together in the appropriate overlap region, re-bins the data at instrument resolution, and corrects for background and detector efficiency [24].

Data was refined using the MOTOFIT reflectivity analysis software [25] with presenting the reflectivity data as a function of the momentum transfer vector, Q :

$$Q = \frac{4\pi \sin \Theta}{\lambda}$$

Where Θ and λ are the angle of incidence and the neutron wavelength, respectively.

The neutron scattering length density ρ , can be considered as a neutron refractive index which is a function of the chemical composition of the material according to:

$$\rho = N_A \sum \left(\frac{P_i}{A_i} \right) b_i$$

Where N_A is Avogadro's number, P_i and A_i the mass density and the atomic mass, respectively, and b_i the nuclear scattering length of component i . By using deuterated molecules and choosing a suitable solvent contrast different parts of the lipid bilayer can be explored. Here the deuterated phospholipid hydrocarbon tails used and the solvents were either a pure D₂O ($\rho = 6.35 \times 10^{-6} \text{ \AA}^{-2}$) to highlight the protonated peptide, or a mixture of D₂O and H₂O where the nSLD is matched to silicon ($\rho = 2.07 \times 10^{-6} \text{ \AA}^{-2}$, 38% D₂O/62% H₂O) and a pure H₂O ($\rho = -0.55 \times 10^{-6} \text{ \AA}^{-2}$) to highlight the deuterated tails.

Lipid bilayer data were fitted using a four discrete layers model consisting of silicon oxide, head group 1 (closest to the silica surface), tail region, head group 2 being the head groups in contact with the bulk solution. The ρ of each layer can be estimated by sum of the scattering length density of each component in the layer.

$$\rho_{\text{layer}} = \phi_{\text{lipid}} \rho_{\text{lipid}} + \phi_{\text{peptide}} \rho_{\text{peptide}} + \phi_{\text{solvent}} \rho_{\text{solvent}}$$

Where ϕ is the volume fraction of component. When changing between different subphase contrasts, the physical structure of the system is assumed not to change. This

means that the thickness and roughness in the models are constrained to be the same between each subphase whilst only letting the scattering length density vary.

Results and discussions

The silica layer was reported to have an interfacial roughness of 4 Å [26], which was used for all subsequent fits to the bilayers. Hydrocarbon deuterated chain lipids were used to enable contrast against the protonated peptide. Three subphase contrasts of D₂O, H₂O and CMSI were used for bilayer measurement. For each layer, we started fitting from known values for the parameters based on the literature [26, 27].

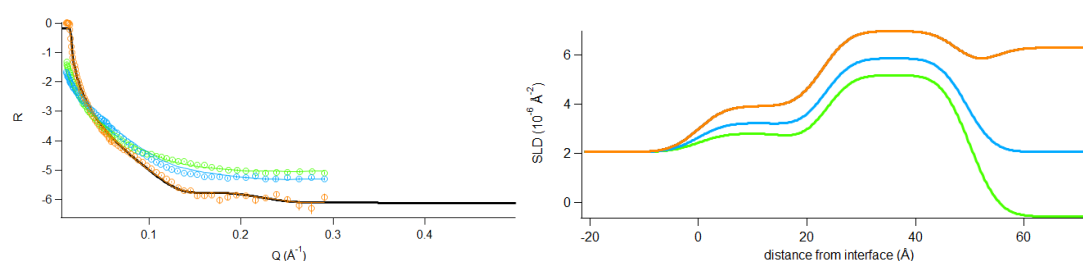


Figure 1. SLD graph and reflectivity graph for the fitted lipid on three contrasts as D₂O amber, CMSI blue and H₂O green

For the analysis first the neat deuterated DMPC membrane at each position was fitted on three different contrasts at the same time to obtain the thickness, SLD and solvent penetration for each layer [25]. To account for any holes or discontinuity in the membrane, we trained the fit by applying sensible boundaries and head group to tail proportion but still allowing some variations depending on each individual fit. As shown in figure 1, the lipid data were fitted for three different contrasts (solvent backgrounds) simultaneously.

In this study aurein 1.2 and melittin were used as typical surface acting and transmembrane model AMPs, respectively. Afterward, for each position the NR profile of each concentrations of peptides recorded with three different contrasts were fitted by using the fitted lipid data for the same position as the starting point. As an example, the fitted model for adding 10 µM melittin on fitted lipid data is presented in figure 2 with the representative schematic figure referring to each layer.

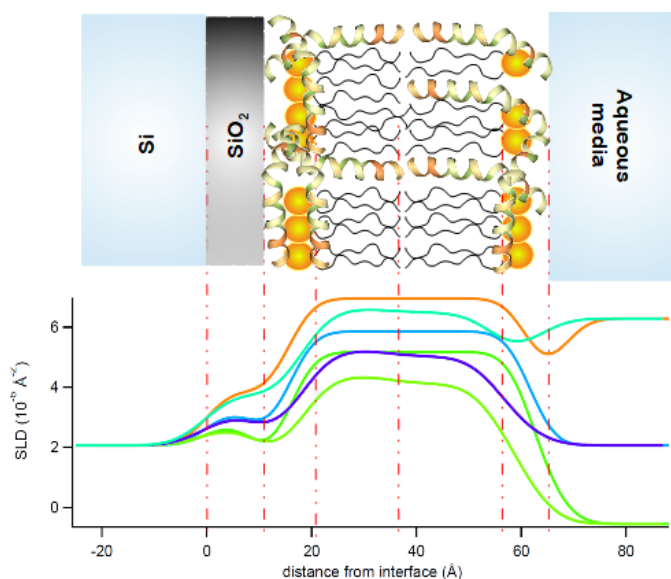


Figure 2. SLD graph of fitted 10 μM melittin on fitted lipid data for the same position on three contrasts as D_2O amber, CMSI blue and H_2O green

In the case of melittin based on the literature we know that at lower concentrations the peptide mainly affects the top leaflet [17] so in order to separate the two leaflets the peptide data were fitted using a five-layer model by dividing the core region into two distinct layers. In each fitting all three parameters of top head group (H.G I) and core region were varied individually while other layers were fixed, and by increasing the concentration from 7 μM even bottom head group (H.G II) was allowed to change to

Table 1. Changes of different parameters for fitted melittin with different concentrations on different positions starting from the neat fitted lipid parameters

Melittin Conc.	Thickness (Å)				SLD (ρ / 10 ⁻⁶ Å ⁻²)						Solvent (% v/v)				
	SiO ₂	H.G I	Core		H.G II	SiO ₂	H.G I	Core		H.G II	SiO ₂	H.G I	Core		H.G II
Lipid	10	5.16	36.75		5.16	3.47	1.88	7.21		1.88	15.8	76.2	49.78		56.5
1μM	10	5.16	18.37	10.54	7.17	3.47	1.88	7.21	9.01	2.31	15.8	76.2	49.78	25.48	42.8
Lipid	10	5.16	36.75		5.16	3.47	1.88	7.21		1.88	15.8	76.2	49.78		56.5
3μM	10	5.16	18.37	20.62	6.76	3.47	1.88	7.21	7.86	2.99	15.8	76.2	49.78	74.38	89.7
Lipid	16.1 5	4.24	33.15		4.24	3.47	1.88	7.21		1.88	16.206	38.88	26.05		39.9
7μM	16.1 5	7.16	10	19.92	5.96	3.47	1.10	9.8	5.75	1.96	16.209	14.81	35.30	23.20	51.8
Lipid	10.0 8	5.4	46.27		5.4	3.47	1.88	7.21		1.88	16.209	38.88	26.05		39.9
10μM	10.0 8	7.73	16.97	20.74	6.45	3.47	2.13	6.78	6.60	3.4	16.209	31.01	32.5	34.64	42.3

obtain the best fit. As summarized in Table 1, at lower concentrations the scattering length density (SLD) values for the top head group and the core region of the top leaflet are increasing due to the presence of the dense peptide in those layers.

Presence of peptide in the top leaflet initially decreases the thicknesses of these layers, likely by introducing disorder in the orientation. However, increasing the concentration to 3 μM leads to swelling in the same layers, with concomitant higher solvent penetration. This suggests that the insertion and potential aggregation of the amphiphilic peptide allows water to enter the membrane core.

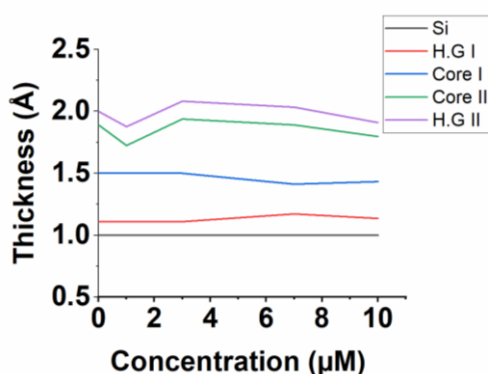


Figure 3. Membrane thickness changes in each layer by adding different concentrations of melittin

By further increase of the peptide concentration to 7 μM and 10 μM there is a slight change: some peptides transfer to the lower leaflet of the membrane, seen from the increased SLD as well as the swelling of both head group zones. This is associated with shrinking of core regions (figure 3); this is likely an artefact due to increased water penetration. This is consistent with neutron scattering results reported for another transmembrane peptide, magainin from African clawed frog; there it was explained with lateral membrane expansion caused by peptide adsorption in the head group region and thus decrease of the core region thickness [28, 29].

For the case of the surface acting aurein 1.2 it was proven before that converging the core

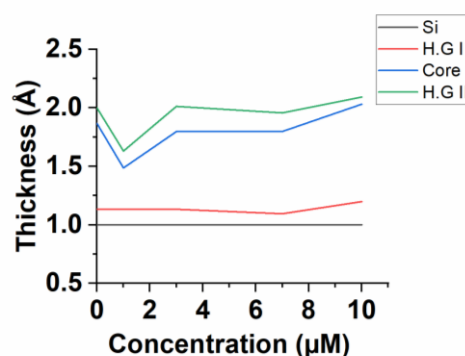


Figure 4. Membrane thickness changes in each layer by adding different concentrations of aurein 1.2

region as a single layer could result in more reliable fits [22] so the data were fitted using

the common four-layer model used for neat lipid. As expected from literature [16, 22], the results show that for aurein 1.2 at lower concentrations the change is mostly in the top headgroup zone, as expected for surface effect (carpet-like mechanism). In each fitting all parameters of H.G II and core region were varied individually, and by increasing the concentration from 10 μM , H.G I was allowed to change as well. The intrusion to the headgroup region also perturbs the membrane packing that causes a slight decrease in the thickness. The SLD increase for top head group indicates the presence of peptide. However, we do not expect the peptide to cover the whole surface at this concentration. With increasing concentration, the addition of more peptides compensates for the membrane thickening effect. By increasing the concentration up to 7 μM , it appears that the peptide enters the core region of the membrane and causes membrane collapse as well, indicated by increasing in SLD while the thickness decreases, showing that dense material enters the core region.

Table 2. Changes of different parameters for fitted aurein 1.2 with different concentrations on different positions

Aurein Conc.	Thickness (\AA)				SLD ($\rho / 10^{-6} \text{\AA}^{-2}$)				Solvent (% v/v)			
	SiO ₂	H.G I	Core	H.G II	SiO ₂	H.G I	Core	H.G II	SiO ₂	H.G I	Core	H.G II
Lipid	16.85	5.39	29.71	5.39	3.47	1.88	7.21	1.88	20.32	71.64	51.98	51.66
1 μM	16.85	5.39	14.13	5.83	3.47	1.88	9.86	2.79	20.32	71.64	40.05	45.47
Lipid	16.85	5.39	29.71	5.39	3.47	1.88	7.21	1.88	20.32	71.64	51.98	51.66
3 μM	16.85	5.39	26.88	8.72	3.47	1.88	7.6	2.25	20.32	71.64	46.66	68.69
Lipid	10.08	5.4	46.27	5.4	3.47	1.88	7.21	1.88	16.209	38.88	26.05	39.89
7 μM	10.08	5.4	40.13	9.07	3.47	1.88	9.93	1.89	16.209	38.88	23.98	30.33
Lipid	16.15	4.24	33.15	4.24	3.47	1.88	7.21	1.88	16.206	38.88	26.05	39.89
10 μM	16.15	8.27	34.65	2.53	3.47	1.1	7.9	1.55	16.206	10.19	10.14	22.80

This behaviour is consistent with the mechanism hypothetically proposed in [17] where the peptide penetration into the membrane was described as a 4 stage process: surface binding, penetration, aggregation in the top leaflet to form fissures, flip-flopping and completing the fissures in the bottom leaflet to break up the membrane into islands. On the other hand, as can be seen in table 2 the solvent penetration shows a slight decrease in this case, which suggests that the presence of the inserted α -helical aurein 1.2 increases membrane density without opening any partial pockets for water penetration. Further peptide aggregation can be seen as thickness increase at 10 μM . This could also show the beginning of asymmetric tension-induced blistering of the membrane as suggested before [16] which is the only pathway for the membrane to expand, eventually leading to break

up of the membrane and the individual “blisters” forming mixed micelles. That is indicated by the greatly increased bottom leaflet thickness at this stage.

This data is consistent with the mechanism proposed in [16], where aurein1.2 binding has the following distinct stages: surface binding, aggregation induced partial penetration to the top leaflet, increased lateral pressure and hence asymmetric membrane tension induced blistering of the membrane, which will eventually lead to breaking up of the membrane to mixed micelles.

Conclusions

NR measurements were able to reveal the position of the peptides in the bilayer membranes at different stages of disruption due to the highly concentration-dependent mechanism. At lower concentrations, peptides are mainly on the top leaflet bound to the head group region. Regarding aurein 1.2 the analysis of neutron results shows disruption of the outer leaflet, consistent with surface action known as carpet mechanism, revealed by SLD increase of top leaflet layers. Melittin model fitting confirms initial interaction of peptide with top leaflet and insertion to bottom leaflet at higher concentrations. These data confirm the hypothetical mechanism of each peptide as described before.

References

- [1] Brogden KA. Antimicrobial peptides: pore formers or metabolic inhibitors in bacteria? *Nat Rev Microbiol* 2005;3:238-50.
- [2] Shai Y. Mechanism of the binding, insertion and destabilization of phospholipid bilayer membranes by α -helical antimicrobial and cell non-selective membrane-lytic peptides. *BBA-Biomembranes* 1999;1462:55-70.
- [3] Sato H, Feix JB. Peptide-membrane interactions and mechanisms of membrane destruction by amphipathic α -helical antimicrobial peptides. *BBA-Biomembranes* 2006;1758:1245-56.
- [4] Nguyen KT, Le Clair SV, Ye S, Chen Z. Molecular interactions between magainin 2 and model membranes in situ. *J Phys Chem B* 2009;113:12358-63.
- [5] Karal MAS, Alam JM, Takahashi T, Levadny V, Yamazaki M. Stretch-activated pore of the antimicrobial peptide, magainin 2. *Langmuir* 2015;31:3391-401.
- [6] Son DJ, Lee JW, Lee YH, Song HS, Lee CK, Hong JT. Therapeutic application of anti-arthritis, pain-releasing, and anti-cancer effects of bee venom and its constituent compounds. *Pharmacol Therapeut* 2007;115:246-70.
- [7] Terwilliger TC, Weissman L, Eisenberg D. The structure of melittin in the form I crystals and its implication for melittin's lytic and surface activities. *Biophys J* 1982;37:353-61.
- [8] Apponyi MA, Pukala TL, Brinkworth CS, Maselli VM, Bowie JH, Tyler MJ, et al. Host-defence peptides of Australian anurans: structure, mechanism of action and evolutionary significance. *Peptides* 2004;25:1035-54.
- [9] Rozek T, Wegener KL, Bowie JH, Olver IN, Carver JA, Wallace JC, et al. The antibiotic and anticancer active aurein peptides from the Australian bell frogs *Litoria aurea* and *Litoria raniformis*: the solution structure of aurein 1.2. *Eur J Biochem* 2000;267:5330-41.
- [10] Fernandez DI, Gehman JD, Separovic F. Membrane interactions of antimicrobial peptides from Australian frogs. *BBA-Biomembranes* 2009;1788:1630-8.
- [11] Sharma VK, Mamontov E, Anunciado DB, O'Neill H, Urban VS. Effect of antimicrobial peptide on the dynamics of phosphocholine membrane: role of cholesterol and physical state of bilayer. *Soft Matter* 2015;11:6755-67.
- [12] Tossi A, Sandri L, Giangaspero A. Amphipathic, α -helical antimicrobial peptides. *Peptide Sci* 2000;55:4-30.
- [13] Wang G, Watson KM, Peterkofsky A, Buckheit RW. Identification of novel human immunodeficiency virus type 1-inhibitory peptides based on the antimicrobial peptide database. *Antimicrob. Agents Chemother.* 2010;54:1343-6.
- [14] Hancock RE, Diamond G. The role of cationic antimicrobial peptides in innate host defences. *Trends Microbiol* 2000;8:402-10.
- [15] Dennison SR, Harris F, Phoenix DA. The interactions of aurein 1.2 with cancer cell membranes. *Biophys Chem* 2007;127:78-83.
- [16] Shahmiri M, Enciso M, Mechler A. Controls and constraints of the membrane disrupting action of Aurein 1.2. *Scientific Rep* 2015;5:16378.
- [17] Pandidan S, Mechler A. Nano-viscosimetry analysis of the membrane disrupting action of the bee venom peptide melittin. *Scientific Rep* 2019;9:10841.
- [18] Mechler A, Praporski S, Piantavigna S, Heaton SM, Hall KN, Aguilar M-I, et al. Structure and homogeneity of pseudo-physiological phospholipid bilayers and their deposition characteristics on carboxylic acid terminated self-assembled monolayers. *Biomaterials* 2009;30:682-9.
- [19] Kalb E, Frey S, Tamm LK. Formation of supported planar bilayers by fusion of vesicles to supported phospholipid monolayers. *BBA-Biomembranes* 1992;1103:307-16.
- [20] James M, Nelson A, Brule A, Schulz J. Platypus: a time-of-flight neutron reflectometer at Australia's new research reactor. *J. Neutron Res.* 2006;14:91-108.
- [21] James M, Nelson A, Holt S, Saerbeck T, Hamilton W, Klose F. The multipurpose time-of-flight neutron reflectometer "Platypus" at Australia's OPAL reactor. *Nuclear Instruments and Methods*

in Physics Research Section A: Accelerators, Spectrometers, Detectors and Associated Equipment 2011;632:112-23.

[22] Fernandez DI, Le Brun AP, Whitwell TC, Sani M-A, James M, Separovic F. The antimicrobial peptide aurein 1.2 disrupts model membranes via the carpet mechanism. *Phys Chem Chem Phys* 2012;14:15739-51.

[23] Le Brun AP, Haigh CL, Drew SC, James M, Boland MP, Collins SJ. Neutron reflectometry studies define prion protein N-terminal peptide membrane binding. *Biophys J* 2014;107:2313-24.

[24] Nelson A. Motofit—integrating neutron reflectometry acquisition, reduction and analysis into one, easy to use, package. *Journal of Physics: Conference Series: IOP Publishing*; 2010. p. 012094.

[25] Nelson A. Co-refinement of multiple-contrast neutron/X-ray reflectivity data using MOTOFIT. *J App Crystallogr* 2006;39:273-6.

[26] Fernandez DI, Le Brun AP, Lee T-H, Bansal P, Aguilar M-I, James M, et al. Structural effects of the antimicrobial peptide maculatin 1.1 on supported lipid bilayers. *Eur Biophys J* 2013;42:47-59.

[27] Hazell G, Arnold T, Barker RD, Clifton LA, Steinke N-J, Tognoloni C, et al. Evidence of lipid exchange in styrene maleic acid lipid particle (SMALP) nanodisc systems. *Langmuir* 2016;32:11845-53.

[28] Huang HW. Elasticity of lipid bilayer interacting with amphiphilic helical peptides. *J Phys II* 1995;5:1427-31.

[29] Ludtke SJ, He K, Heller WT, Harroun TA, Yang L, Huang HW. Membrane pores induced by magainin. *Biochemistry* 1996;35:13723-8.

Conclusions

The central aim of my thesis was to conduct a systematic study of the interaction between transmembrane AMPs with biomimetic membranes of different structures, in order to understand the steps in their molecular mechanism of action. I have undertaken this study by using QCM-D nanoviscosimetry measurements as the principal technique. First, I studied melittin from *Apis mellifera* venom. Melittin was chosen as it is probably the most studied membrane disruptor AMP and yet there are persistent controversies concerning its mechanism of action. After confirming the membrane disrupting effect of the peptide by dye leakage method, I used QCM-D fingerprinting measurements to identify the viscoelastic characteristics of the stages of the mechanism of action of the peptide on different model membranes selected to emphasize on the fundamental differences between mammalian and bacterial membranes. The initial results suggested that melittin is a non-specific cell-lysing peptide regardless of membrane composition, including presence or absence of cholesterol. However, the data allowed me to propose two main disrupting pathways, both of these novel, to describe activity against the model membranes used in the study. Thus, for zwitterionic membranes I suggested that the peptide follows the fissure-forming pathway whereas in phosphatidylglycerol containing membrane the main pathway is asymmetric tension, leading to membrane breach and eventually to the formation of toroidal type pores.

Following on from the many controversies in the literature about melittin even when the same model membranes were used, I have turned my attention specifically to the effect of different membrane morphologies on the peptide mechanism of action. I thus compared melittin interaction on liposome containing deposits and multiple bilayer membrane stacks with activity against single bilayer membranes, which I have described in the previous section. By using QCM viscosimetry measurements it was clear that membrane morphology differences lead to considerable variances in the fingerprints and thus the apparent peptide-membrane interaction. While I have identified the characteristic features of the liposome containing and multilamellar membranes, it was also revealed that melittin shows stranger activity, including full membrane dissolution, against membranes with edges and/or sharp curvatures, such as a multi bilayer and liposome containing deposits. In these cases, melittin can almost entirely remove the bilayers on top of the initial single bilayer.

Next in the hope of suggesting a common model for transmembrane disruptor AMPs, I used QCM-D fingerprinting method with the support of dye leakage and AFM imaging to identify any hitherto hidden stages in magainin 2 mechanism of action. I found that magainin 2 also acts as a non-specific membrane-lysing peptide not sensitive to membrane composition or the presence of cholesterol, at least in the model membrane systems used in this study. I found that the mechanism of action is also very different. Based on the results the mechanism follows the model proposed in the literature, which includes an initial binding stage followed by transient pore stage and eventually leading to peptide flip-flop from outer to inner leaflet and ensuing equilibrium with cessation/reduction of pore activity. It should be noted that the presence of the peptide leads to extensive membrane modulation and AFM image shows the final collapse of membrane into cylindrical mixed micelle structures.

Based on the multi-stage mechanism of action uncovered for these transmembrane AMPs, I endeavoured to find the thermodynamic states involved in those stages. I used QCM to measure the viscosity changes as the function of temperature changes to study the mechanism of membrane disrupting AMPs, based on DMPC phase transition temperature. Presence of different phase transition temperatures demonstrates the existence of distinct domains, characterized by specific peptide-membrane interactions and thus specific thermodynamic states of the peptide within the membrane. The presence of four distinct domains was identified for melittin-DMPC interaction and three thermodynamic states shown for magainin 2. These results well correlated to their hypothetical model mechanism described thoroughly previously.

In order to find the peptide position in the bilayer membrane throughout the mechanism of action I attempted neutron reflectometry measurements on DMPC membrane with different concentrations of melittin. Because of the lack of a well-established methodology I required a reference peptide, for which I chose aurein 1.2 a well-known surface acting peptide. It was shown that in low concentrations, both peptides are mainly associated with the head group region of top leaflet of the membrane. However, by increasing the concentration the top leaflet SLD increased for aurein 1.2 suggesting surface action which is in agreement with its carpet mechanism. On the other hand, increasing concentration pushed melittin into the top leaflet of the membrane, and eventually from top leaflet to the bottom leaflet, confirming the previously proposed model.

My results open a new perspective on the mechanism of transmembrane AMPs, by identifying distinct molecular mechanistic stages and revealing distinct thermodynamic states involved in the mechanism of action. I believe that my results will contribute to developing membrane disrupting AMPs into actual pharmaceutical application by overcoming the challenges of specificity and selectivity that hitherto thwarted all efforts to design AMP based therapeutic agents.

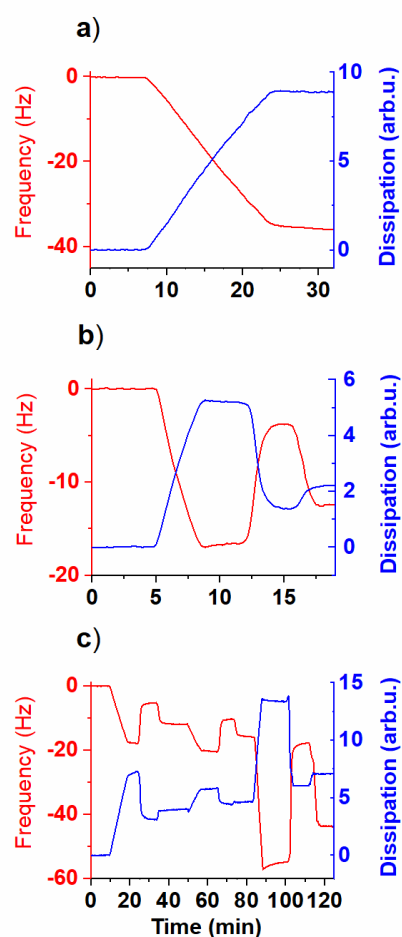
Supplementary Information

Membrane morphology effects in quartz crystal microbalance characterization of antimicrobial peptide activity

Sara Pandidan and Adam Mechler*

La Trobe Institute for Molecular Science, La Trobe University, Melbourne, Australia

*a.mechler@latrobe.edu.au



S1. Representative sensograms of QCM experiment (shown from buffer baseline) for a) liposome containing deposit b) single bilayer membrane c) multiple bilayer stack. b) and c) show the osmotic stress treatment to remove any residual liposomes.

Supplementary Information

Nano-viscosimetry analysis of the membrane disrupting action of the bee venom peptide melittin

Sara Pandidan and Adam Mechler

La Trobe Institute for Molecular Science, La Trobe University, Melbourne, Australia

Dynamic Light Scattering (DLS) experiments

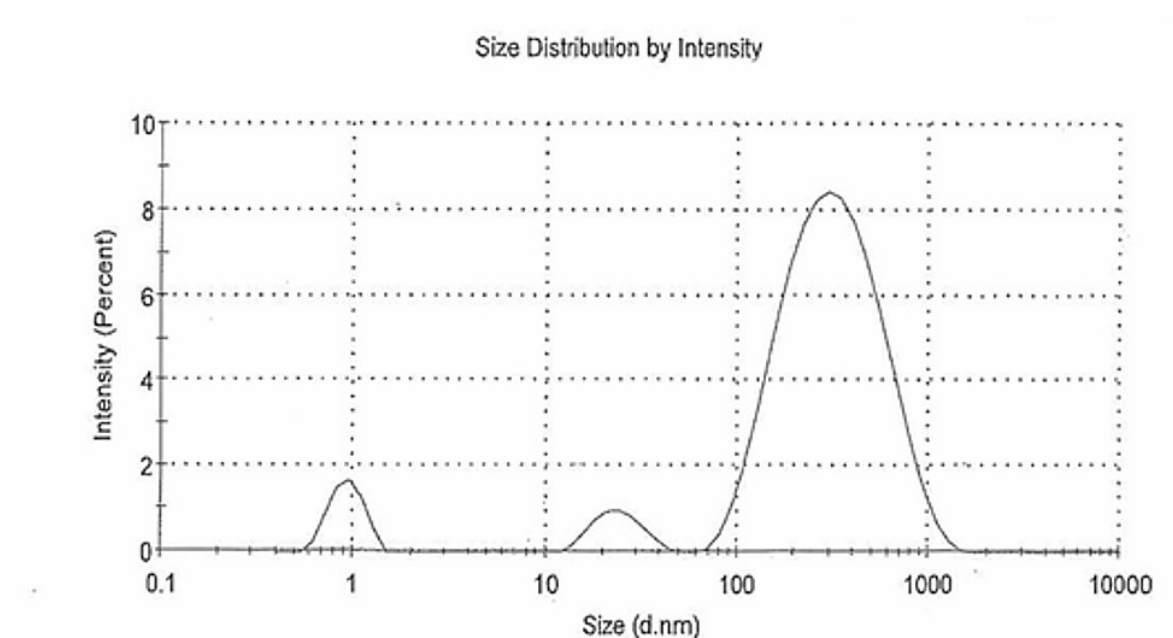


Figure S1. Representative DLS size distribution graph of the product of melittin membrane disruption at high peptide concentration.